A NOVEL FUNCTION FOR FIBULIN-5 IN CONTROLLING INTEGRIN-INDUCED ROS PRODUCTION: IMPLICATIONS ON ANGIOGENESIS AND CANCER

APPROVED BY SUPERVISORY COMMITTEE

Mentor: Rolf A. Brekken, Ph.D. _____

Chairperson: James Amatruda, M.D., Ph.D. _____

Hiromi Yanagisawa, M.D. _____

Eric Olson, Ph.D. _____

To my mother and father, for their constant love and support through all my life's endeavors. To my husband Lyle, for his enthusiasm, encouragement and friendship.

A NOVEL FUNCTION FOR FIBULIN-5 IN CONTROLLING INTEGRIN-INDUCED ROS PRODUCTION: IMPLICATIONS ON ANGIOGENESIS AND CANCER

by

MARIE KAY SCHLUTERMAN

DISSERTATION

Presented to the Faculty of the Graduate School of Biomedical Sciences

The University of Texas Southwestern Medical Center at Dallas

In Partial Fulfillment of the Requirements

For the Degree of

DOCTOR OF PHILOSOPHY

The University of Texas Southwestern Medical Center at Dallas

Dallas, Texas

August, 2009

A NOVEL FUNCTION FOR FIBULIN-5 IN CONTROLLING INTEGRIN-INDUCED ROS PRODUCTION: IMPLICATIONS ON ANGIOGENESIS AND CANCER

Marie Kay Schluterman, Ph.D.

The University of Texas Southwestern Medical Center at Dallas, 2009

Supervising Professor: Rolf A. Brekken, Ph.D.

Tumor survival depends in part on the ability of tumor cells to transform the surrounding extracellular matrix (ECM) into an environment conducive to tumor progression. Matricellular proteins are secreted into the ECM and impact signaling pathways required for pro-tumorgenic activities such as angiogenesis. Fibulin-5 (Fbln5) is a matricellular protein recently shown to regulate angiogenesis, however its effect on tumor angiogenesis and thus tumor growth is currently unknown. We report that the growth of pancreatic tumors and tumor angiogenesis was suppressed in *Fbln5 null* (*Fbln5*$^{-/-}$) mice compared to *wild-type* (*WT*) littermates. Furthermore, we observed an increase in the level of reactive

oxygen species (ROS) in tumors grown in *Fbln5*$^{-/-}$ animals. Increased ROS resulted in elevated DNA damage, increased apoptosis of endothelial cells within the tumor and represented the underlying cause for the reduction in angiogenesis and tumor growth. *In vitro*, we identified a novel pathway by which Fbln5 controls ROS production through a mechanism dependent on β1 integrins. These results were validated in *Fbln5*$^{RGE/RGE}$ mice, which harbor a point mutation in the integrin-binding RGD motif of Fbln5 preventing its interaction with integrins. Tumor growth and angiogenesis was reduced in *Fbln5*$^{RGE/RGE}$ mice, however treatment with an antioxidant rescued angiogenesis and elevated tumor growth to *WT* levels. These findings introduce a novel function for Fbln5 in the regulation of integrin-induced ROS production and establish a rationale for future studies to examine whether blocking Fbln5 function could be an effective anti-tumor strategy, alone or in combination with other therapies.

TABLE OF CONTENTS

PRIOR PUBLICATIONS

Garg V, Kathiriya IS, Barnes R**, Schluterman MK**, King IN, Butler CA, Rothrock CR, Eapen RS, Hirayama-Yamada K, Joo K, Matsuoka R, Cohen JC, and Srivastava D. (2003) GATA4 mutations cause human congenital heart defects and reveal an interaction with TBX5. Nature 24, 443-447.

Garg V, Muth AN, Ransom JF, **Schluterman MK,** Barnes R, King IN, Grossfeld PD, Srivastava D. (2005). Mutations in NOTCH1 cause aortic valve disease. Nature 437, 270-274.

Schluterman, MK., Krysiak, AE**.,** Kathiriya, IS., Abate N., Chandalia, M., Srivastava, D., Garg, V. (2007), Screening and Biochemical Analysis of GATA4 Sequence Variations Identified in Patients With Congenital Heart Disease. AJMG Part A 143A: 817-823.

Maitra M, **Schluterman MK**, Nichols HA, Richardson JA, Lo CW, Srivastava D, Garg V. (2008), Interaction of Gata4 and Gata6 with Tbx5 is critical for normal cardiac development. Dev Biol 326(2):368-77.

LIST OF FIGURES

LIST OF ABBREVIATIONS

ECM - Extracellular matrix

PDGF - Platelet derived growth factor

VEGF - Vascular endothelial growth factor

TGFβ - Transforming growth factor β

MMP - Matrix metalloproteinase

TME - Tumor microenvironment

SPARC - Secreted protein acidic and rich in cysteine

TSP-1 - Thrombospondin-1

OPN - Osteopontin

Fbln5 - Fibulin-5

***Fbln5*$^{-/-}$** - Mice deficient in Fbln5

WT - Wild-type

VSMCs - Vascular smooth muscle cells

SMA - Smooth muscle actin

ROS - Reactive oxygen species

H_2O_2 - Hydrogen peroxide

SOD - Superoxide dismutase

DOX - Doxycycline

DHE - Dihydroethidium

NOS - Nitric oxide synthase

MEFs - Mouse embryonic fibroblasts

DCF-DA - 2'-7'-dicholordihydrofluorescein diacetate

NAC - N-acetyl cysteine

***Fbln5*$^{RGE/RGE}$** - Mice containing a point mutation in the RGD motif of Fbln5

INTRODUCTION

Defining the Extracellular Matrix

Within tissues, cells are surrounded by a meshwork of proteins collectively called the extracellular matrix (ECM). The ECM fills the gaps between cells compartmentalizing tissues and providing shape and flexibility. It consists of numerous fibrous proteins that bind to one another building a grid upon which cells adhere. Collagen, the most abundant structural protein found in the ECM is secreted predominantly by fibroblasts into the ECM as single polypeptide chains. Once secreted, the single chains are crosslinked to other collagen molecules to form collagen fibrils.[1] These fibrils arrange in specific patterns forming the foundation of the ECM upon which other structural proteins such as fibronectin and elastin bind. Similar to collagen, fibronectin is produced and secreted by fibroblasts. Fibronectin fibrillogenesis is an integrin-dependent process where short fibronectin fibrils are formed as fibronectin dimers bind to each other creating an insoluble fibular network.[2] By binding to collagen and cells, fibronectin facilitates the movement of cells through the ECM. Elastic fibers are the largest structure found in the ECM and provide tissues with elasticity. The two main components of elastic fibers are: 1) elastin, which is secreted in a precursor form as tropoelastin and 2) microfibrils, which serve as a backbone for elastic fiber assembly. Assembly begins by the coacervation of tropoelastin molecules, which are then modified and crosslinked by lysyl oxidase like-1 (LOXL-1). The elastin "bundle" forms the core of elastic fibers, which are then wrapped by microfibrils forming mature elastic fibers.[3] These proteins, along with other structural proteins including laminin and vitronectin, intertwine with collagen fibrils generating a platform upon which cells bind to and migrate through.

Cells adhere to the ECM through cell surface adhesion molecules known as integrins. Integrins are a family of heterodimeric transmembrane proteins that contain α and β subunits. The particular ECM protein an integrin binds to depends on the combination of subunits. For example, $\alpha_1\beta_1$ and $\alpha_2\beta_1$ interact with collagen while $\alpha_5\beta_1$ serves as the primary fibronectin receptor.[4] Adherence to the ECM is also critical for cell survival and loss of cell-ECM contact can result in a form of apoptosis termed anoikis.[5] Integrin-binding also mediates outside-in stimuli that activate signaling pathways, which influence cellular activities such as survival, proliferation, apoptosis and migration.[4] The exact pathway initiated and the extent of activation is related directly to the specific combination of integrin and ECM protein involved.

The ECM not only serves a structural role in tissues but also functions as a reservoir for proteins required for proper tissue function and repair. This includes a plethora of growth factors and proteases. Growth factors such as basic fibroblast growth factor (bFGF), platelet derived growth factor (PDGF), vascular endothelial growth factor (VEGF), and transforming growth factor β (TGFβ) are involved intricately in development and continued expression of these factors is required to maintain tissue homeostasis during adulthood. These pleiotropic molecules have been shown to robustly effect proliferation, survival and migration in numerous cell types. VEGF, for example, is one of the most potent inducers of angiogenesis, the sprouting of new blood vessels from pre-existing ones. Treatment with VEGF stimulates proliferation and migration of endothelial cells by binding to tyrosine kinase receptors on the cell surface.[6] Once growth factors are secreted from cells, they often become embedded within the ECM and require ECM degradation by proteases such as elastase to release the active protein allowing it to interact with surrounding cells and transduce downstream signaling. For instance, the ECM serves as a VEGF “sink” where high levels of

VEGF are found incorporated within the ECM. Matrix metalloproteinases (MMP), a family of proteases, which degrade structural proteins within the ECM, can liberate VEGF from the ECM and therefore control VEGF induced angiogenesis.[7] Also, TGFβ is deposited within the ECM in a latent form, which requires proteolytic processing to generate active TGFβ. The latent form binds to microfibrils of elastic fibers, which prevents cleavage by shielding the protein from proteases. Break down of microfibrils by elastase releases latent TGFβ freeing it for proper cleavage into its active form, which can then participate in signal transduction.[8] The ability of the ECM to control the bioavailability of growth factors provides another means of regulating cellular activities and further explains how alterations in the makeup of the ECM can affect cell response during disease such as cancer.

Matricellular proteins also reside in the ECM. They are a unique family of proteins that do not function as structural proteins. Matricellular proteins orchestrate the deposition of the ECM and mediate cell:cell and cell:ECM interactions.To do this, matricellular proteins interact directly with cell surface receptors, structural proteins, growth factors and proteases found within the ECM.[9] Their expression is found in every tissue, begins early in development, persists throughout adulthood and is increased during any tissue remodeling event. Matricellular proteins are critical regulators of many aspects of cell function including differentiation, survival, proliferation, and migration making them necessary for proper tissue function. Given their affect on signaling pathways initiated within the ECM, matricellular proteins have been shown to strongly influence tumor growth. The focus of this chapter, therefore, will be on reviewing present data concerning the function of matricellular proteins in the context of tumor development.

Manipulation of the ECM during tumor development

Tumor formation requires remodeling of the local ECM and the initiation of angiogenesis, which facilitates nutrient delivery as well as metastasis to distant organs. Successful completion of these steps requires that tumor cells take advantage of the host response to tumor development. The host response encompasses production and deposition of ECM and the recruitment of inflammatory cells such as macrophages, neutrophils and NK cells to invade the tumor microenvironment (TME). To survive, tumor cells must adapt to the TME and manipulate proteins within the TME to activate signaling pathways (i.e. survival, proliferation) that promote progression. For example, to promote invasion into the surrounding host tissue, tumor cells will increase the expression of matrix-degrading proteases such as MMPs within the TME. MMPs degrade the surrounding ECM enabling tumor cells to escape the primary tumor, invade the surrounding tissue and metastasize to secondary sites.[10] MMPs degrade proteins such as collagen and fibronectin. Increased protease expression also assists in the release of growth factors bound within the ECM that aid in tumor cell survival and promote angiogenesis. Numerous tumor studies performed in the presence of synthetic MMP inhibitors or in MMP deficient mice highlight the positive correlation between MMP activity and tumor progression to a metastatic phenotype.[11-13] However, recent data suggests that the increase in MMP expression may also have adverse affects on tumor development. Cleavage of type IV and type XVIII collagen by MMP-9 releases hidden protein fragments with anti-angiogenic properties such as α3NC1 and endostatin respectively.[14] These endogenous angiogenic inhibitors have been shown to have a negative impact on tumor angiogenesis and growth *in vivo*.[15, 16] It is still unclear how the effects of MMP activity are regulated within the TME but it appears that the source of MMP expression (host or tumor derived) contributes to the diverse response.

The TME is often hypoxic. Therefore, the development of a functioning blood vessel network within the TME to provide tumor cells with oxygen and nutrients is critical for tumor survival. Angiogenesis is required during embryonic development, wound healing and tumor progression. It is a multi-step process that begins with the activation of endothelial cells by cell-ECM stimuli or hypoxia-induced cytokines released by surrounding cells (macrophages, fibroblasts and tumor cells). Endothelial cells are activated by pro-angiogenic growth factors such as VEGF or bFGF that promote the sprouting and migration of endothelial cells and supporting cells such as pericytes from the existing blood vessel. MMPs released by endothelial cells degrade the basement membrane of the existing vessel freeing cells to migrate out into the surrounding tissue. MMPs expressed at the leading edge of activated endothelial cells degrade the ECM forming a tunnel through which cells travel to surrounding tissues where they proliferate and undergo tubulogenesis to establish a new vessel.[17] To facilitate this process within the TME, tumor cells modify the host ECM to increase expression of matrix proteins, growth factors and cytokines that aid in endothelial cell activation. Large amounts of VEGF are found within the TME and blocking VEGF activity has profound effects on tumor angiogenesis. Multiple antibodies designed to block VEGF binding to receptors can diminish vessel formation within tumors and inhibit tumor progression.[18, 19]

Integrins are critical determinants of how a cell responds to its environment. Integrins physically anchor cells to the ECM and integrin signaling influences the makeup of the ECM by stimulating deposition of certain proteins (structural proteins, growth factors, proteases). Integrins are pivotal in promoting cell survival, proliferation and migration therefore, a growing tumor will alter its integrin expression profile to encourage activation of these pathways. [4] Integrin expression patterns have been examined exhaustively in various tumor types with the hopes of developing cell surface signatures that may denote tumor stage

and/or drug sensitivity. These studies[4] have revealed stark differences in not only the expression level but also in the distribution pattern of integrins on the cell surface between normal and tumor-derived human tissue samples. Numerous integrins have been coined "vascular integrins" because they have been implicated in tumor-induced angiogenesis. $\alpha_V\beta_3$, the most well studied vascular integrin, promotes survival and proliferation and initiates migration of endothelial cells.[20] Its expression on endothelial cells is enhanced within the TME and has been shown to be critical for tumor angiogenesis in multiple tumor types including breast cancer and melanoma. In these studies,[21, 22] treatment with monoclonal antibodies to $\alpha_V\beta_3$ (LM609 and Mab 17E6) inhibited tumor angiogenesis and promoted regression of $\alpha_V\beta_3$-positve tumors. Given these results, several clinical trials have been initiated targeting vascular integrins. Promising results keep anti-integrin therapy as an interesting therapeutic prospect.

The presence of a growing tumor also leads to dramatic changes in the expression of matricellular proteins. The altered expression of matricellular proteins suggests a possible function for these proteins during tumor growth and metastasis. Therefore, elucidating the function matricellular proteins serve in tumor progression has become a focal point of intense research.

Matricellular proteins and their complex effects on tumor development

Matricellular proteins are expressed at sites of tissue remodeling where they coordinate cell-ECM interaction. As such this unique class of proteins is well-suited to influence the TME and tumor progression. Much of our understanding about the function of matricellular proteins in tumorigenesis is a result of studies in mice engineered to lack the expression of specific matricellular proteins including SPARC, thrombospondin-1 (TSP-1), osteopontin (OPN) and fibulin-5 (Fbln5). Although it is clear that these proteins influence tumor growth,

the exact effect appears to be dependent on the origin of the protein, whether it is produced by host cells or tumor cells and on the particular type of tumor. These obstacles make understanding the function of matricellular proteins complex and contextually dependent. The rest of this chapter will discuss the best-characterized matricellular proteins with a specific emphasis on fibulin-5.

SPARC

SPARC (Secreted Protein Acidic and Rich in Cysteine), a founding member of the matricellular protein family, has been shown to modulate multiple cellular functions. It has deadhesive and antiproliferative effects and is critical for proper ECM (collagen) deposition.[9] These effects are attributed to SPARC's ability to bind to ECM proteins such as collagen and vitronectin and to growth factors such as PDGF and bFGF.[23-25] SPARC has also been shown to bind to VEGF resulting in the inhibition of endothelial cell proliferation and migration. The effect of SPARC on the development of cancer is dependent on the context of its expression. For example, in relation to breast cancer, forced expression of SPARC by human breast cancer cells, MDA-MB-231 inhibited their invasiveness *in vitro,* indicating a negative relationship between SPARC and breast cancer progression.[26] However, recent reports identified a positive correlation between increased expression of SPARC in the stroma of human breast cancer samples and disease-free survival indicating that SPARC maybe used by the host to control tumor growth.[27, 28] In addition, the SPARC promoter was found to be hyper-methylated in multiple colorectal cancer cell lines as well as pancreatic, lung, and prostate cancer lines.[29] Overexpressing SPARC in these colorectal cancer cell lines enhanced cell death after treatment with chemotherapeutics indicating a function for SPARC in the initiation of apoptosis.[30] This effect was further validated when it was shown that SPARC could turn on apoptosis by increasing gene expression of several members of the caspase family including 8 and 10.[31]

These results coincide with expression analysis of SPARC in human colorectal cancer. SPARC was found to be highly expressed in the tumor stroma but not expressed in the epithelium of these cancers and patients with higher-expressing SPARC colorectal tumors had better clinical outcome than those with tumors that did not express SPARC.[32, 33] It appears from these studies that host-derived SPARC functions within the TME to inhibit tumor growth while tumor cells attempt to block these effects by reducing the level of SPARC expression.

Thrombospondin-1

Similar findings have been observed with the matricellular protein, thrombospondin-1 (TSP-1). TSP-1 has been well characterized as an anti-angiogenic protein that functions via multiple mechanisms. For example, TSP-1 can inhibit the release ofVEGF from the tumor stroma by directly binding VEGF of inhibiting MMP-9 mediated release of VEGF from the ECM. [34, 35] TSP-1 has also been shown to directly induce apoptosis of endothelial cells by decreasing expression of Bcl-2 and increasing expression of Bax.[36, 37] Given its effect on angiogenesis, it is not surprising that various groups have shown TSP-1 expression to be highly regulated by oncogenes as well as tumor suppressor genes. For example, the RAS-oncoprotein modifies TSP-1 expression via a mechanism dependent on Myc-phosphorylation. Tumor cells with high RAS expression express low levels of TSP-1 and have a more aggressive nature when grown *in vivo* than cells with elevated TSP-1 expression.[38] It has also been reported that tumor suppressor genes such as p53 turn on expression of TSP-1 to control tumor growth in mice by reducing the level of VEGF present in the TME.[39] Human tumor samples with a loss in p53 expression also exhibited a decrease in TSP-1 expression confirming the existence of this relationship in human disease.[40] Much like SPARC, TSP-1 was found expressed highly in the stroma of various tumor types, such as invasive breast carcinoma, but not by the

tumor cells suggesting that the host uses TSP-1 as a tool to control tumor growth.[40] This was further supported by tumor studies performed in *TSP-1-null* mice where tumors grew significantly faster than in *wild-type* (*WT*) mice.[41]

Although TSP-1 as an angiogenic inhibitor has been well documented, a second function for TSP-1 has been identified that labels TSP-1 as a pro-tumorgenic protein making its effect on tumor growth even more complex. The primary goal of a developing tumor is to invade surrounding tissue and spread beyond the initial site. To accomplish this, two important steps must occur. The surrounding ECM must be degraded to allow tumor cell invasion and tumor cells must be able to bind to components of the TME to migrate through the ECM. Recent reports have identified functions of TSP-1 that promote both of these steps. First, TSP-1 increases the expression of the proteolytic enzyme plasmin, which functions to degrade the ECM providing tumor cells with clear avenues to blood vessels where they are then able to metastasize to secondary sites. [42] Secondly, TSP-1 directly anchors tumor cells to structural proteins of the ECM including type IV collagen enabling them to invade and migrate through the TME.[43] These characteristics help explain why TSP-1 has reportedly been found highly expressed by tumor cells in late stage, highly aggressive breast cancers.[44] It has been hypothesized that in the early stages of tumor development TSP-1 expression is turned off by tumor cells to help create a pro-angiogenic environment, but turned on by host cells to limit tumor angiogenesis. However, once the tumor adapts to this environment and becomes vascularized, tumors begin to express TSP-1 for it's pro-metastatic functions. Further research is needed to better understand TSP-1 and its effect on cancer. It is yet to be determined how best to target TSP-1 for therapeutic purposes.

Osteopontin

The effects of osteopontin (OPN) on tumor development appear to be more straightforward than the aforementioned matricellular proteins. It is a multi-

functional protein implicated in promoting a metastatic phenotype in numerous tumor types. OPN affects cell adhesion, survival, proliferation and migration. It serves as an adhesion molecule by binding to various integrins thus anchoring cells to the ECM. Its interaction with cell surface integrins induces survival and evasion of apoptosis in various tumor cell lines.[45] By inducing migration and the expression of MMPs, OPN expression correlates with a more metastatic tumor phenotype. For example, transformed NIH 3T3 fibroblasts develop a highly invasive, malignant phenotype. This phenotype corresponds with a higher level of OPN expression.[46] OPN has also been shown to promote tumor angiogenesis by binding to integrin $\alpha_V\beta_3$. This interaction induces migration of endothelial cells and allows OPN to protect endothelial cells from apoptosis *in vitro*.[47] *In vivo*, forced overexpression of OPN in SBC-3 lung cancer cells increased tumor growth by augmenting angiogenesis.[48] This effect was ameliorated by abrogation of the interaction between OPN and $\alpha_V\beta_3$.[48] OPN expression has been analyzed in multiple different human carcinomas to determine its relevancy in human disease. OPN mRNA was expressed highly in cancers of the stomach, breast, bladder, pancreas and prostate compared to normal tissues.[49] In addition, increased expression of OPN correlated with advancing stages of colon cancer. This work was supported by *in vitro* data showing treatment of human colon cancer cells with OPN resulted in increased invasiveness.[50] OPN now serves as a prognostic marker for several different cancer types including ovarian, and malignant glioblastomas.[45] Inhibition of OPN as a therapeutic approach is intriguing but to date has not been well established. Pre-clinical trials using antibodies against OPN showed decreased prostate cancer growth in mice however no strategies have advanced to clinical trials.[51]

Fibulin-5

Fibulin-5 (Fbln5) is a matricellular protein required for maturation of elastic fibers, which provide elasticity to the blood vessel wall. Therefore, Fbln5 has a direct effect on the efficiency of the vasculature. But it is its unique ability to alter cell-ECM signaling via integrin binding and the downstream affects this has on angiogenesis that make it an interesting protein for cancer research.

Fbln5 (Dance, EVEC) is a member of the fibulin family of ECM proteins which all contain a string of calcium-binding epidermal growth factor-like (cbEGF) repeats at the N-terminus followed by the defining globular COOH-terminal fibulin-type module. cbEGF motifs have been shown to be important for proper protein folding and structure stabilization and act as signaling sequences for protein interaction. To date, the function for the fibulin-type module is unknown. Unique to Fbln5 is the insertion of an RGD motif in the first cbEGF repeat. This sequence facilitates binding to RGD-dependent integrins such as $\alpha_5\beta_1$ and the $\alpha_v\beta$ integrins (**Figure I.1**).

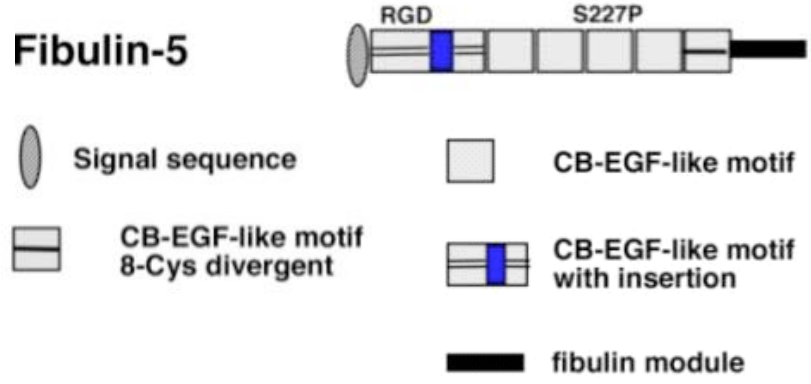

Figure I.1 Schematic presentation of Fbln5. Blue line indicates location of RGD motif.

Originally, fibulins were identified for their involvement in the formation and stabilization of structural components such as collagen and elastic fibers.[52, 53] However, more recently, an increasingly interesting function for fibulins has been

identified as mediators of cell-cell or cell-ECM interactions. This function allows them to directly regulate processes such as proliferation, survival and migration.

A main function for Fbln5 was first identified with the generation of *Fbln5*-deficient (*Fbln5*$^{-/-}$) mice. *Fbln5*$^{-/-}$ mice are born at Mendelian ratios, are fertile, and appear relatively normal. However, closer examination revealed that *Fbln5*$^{-/-}$ mice exhibit fragmented and disorganized elastic fibers, indicating Fbln5's function in the proper assembly of elastic fibers.[54] It was shown to bind to tropoelastin, the precursor protein of elastin, but not polymerized elastin. Fbln5 is believed to facilitate the coacervation of tropoelastin molecules preparing them for crosslinking by LOXL1. Furthermore, Fbln5 was shown to interact with fibrillin-1, a molecule expressed highly within microfibrils.[55] This interaction assists in the tethering of tropoelastin to microfibrils to form mature elastic fibers.[53, 56] The disruption in elastic fiber deposition in *Fbln5*$^{-/-}$ mice resulted in loose skin and led to the identification of mutations in human FBLN5 that result in cutis laxa, a genetic skin disease.[57] *Fbln5*$^{-/-}$ mice also present with alveolar defects. Lungs of mutant mice were expanded due to dilated alveoli. By 6 months of age, the lung defect progressed to severe emphysema. *Fbln5*$^{-/-}$ mice also exhibited vascular anomalies. Aortas of *Fbln5*$^{-/-}$ mice were distended and tortuous compared to aortas from *WT* mice. The defect in vessel development was also observed in subcutaneous vessels from *Fbln5*$^{-/-}$ mice. These vessels developed in a disorganized, sinuous pattern and had an increase in vessel sprouting (**Figure I.2**). The defect in blood vessel development was contributed to fragmented elastic fibers within the elastic laminae decreasing the integrity of the blood vessel wall.[54]

Within tissues, Fbln5 co-localizes with elastin, the main protein of elastic fibers. It is expressed predominantly in tissues containing high levels of elastic

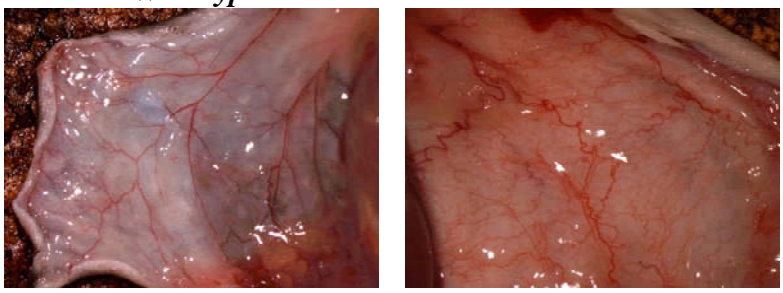

Figure I.2 Defect in subcutaneous blood vessels observed in *Fbln5*$^{-/-}$ mice. WT mice exhibit normal blood vessel patterning while blood vessels in *Fbln5*$^{-/-}$ mice appear tortuous with irregular patterning. Courtesy of H.Yanagisawa, unpublished data

fibers particularly blood vessels including the great vessels and the aorta. Fbln5 is also present in lungs, skin and uterus, and it is interesting to note that within these tissues, expression is mostly localized to blood vessels.[54] The level of Fbln5 protein expression is reduced in adult vessels compared to neonatal blood vessels but is elevated in adult mice in response to vascular insult or atherosclerotic plaques and in interstitial fibroblasts during lung injury repair. This suggests a possible function for Fbln5 in the remodeling process that occurs after vascular injury.[58-60]

Fbln5 is secreted by fibroblasts, vascular smooth muscle cells (VSMCs) and endothelial cells. Within the ECM, Fbln5 binds to structural proteins such as collagen allowing it to assist in cell adhesion by acting as a bridge between cells and the ECM via its interaction with integrins through its RGD motif.[52, 61] Fbln5 serves as a substrate for cells through interaction with integrins $\alpha_V\beta_3$, $\alpha_V\beta_5$, and $\alpha_9\beta_1$.[62] Fbln5 was also shown to bind to smooth muscle cells by interacting with $\alpha_5\beta_1$ and $\alpha_4\beta_1$, the primary fibronectin receptors. The ability of Fbln5 to bind to integrins allows it to directly influence signals transduced by cell-ECM interactions. However, the effect is cell type dependent. For example, over-

expression of Fbln5 by retroviral infection in 3T3-L1 fibroblasts increased DNA synthesis and proliferation through a mechanism involving TFGβ. In the same study, researchers showed that increased expression of Fbln5 in an epithelial cell line (Mv1Lu) curtailed proliferation by suppressing cyclin A expression.[63]

Convincing evidence suggests that Fbln5 may function as a blocking peptide by binding to integrins and preventing their interaction with growth factors and other ECM proteins. For example, VSMCs harvested from *Fbln5*$^{-/-}$ mice exhibit no difference in proliferation rates compared to *WT* VSMCs. However, when treated with PDGF, *Fbln5*$^{-/-}$ VSMCs exhibit a two fold increase in proliferation compared to PDGF-treated *WT* cells. This effect was curtailed by treatment with recombinant Fbln5 protein.[64] In addition, Fbln5 binding to $\alpha_5\beta_1$ and $\alpha_4\beta_1$ does not result in integrin activation and cells plated on fibronectin in the presence of Fbln5 do not undergo fibronectin-mediated spreading, migration or proliferation.[61] These results support the hypothesis that Fbln5 functions as a blocking peptide to control integrin-mediated cell signaling.

Fibulin-5 and angiogenesis

The high level of Fbln5 expression by endothelial cells and the aberrant vessel defect in *Fbln5*$^{-/-}$ mice indicates a critical function for Fbln5 in the vascular environment. Initial *in vitro* studies denoted Fbln5 as an inhibitor of angiogenesis. Treatment with recombinant Fbln5 inhibited the proliferation and invasion of murine brain microvascular endothelial cells through matrigel by antagonizing VEGF activation of the ERK1/ERK2 signaling pathway. Furthermore, Fbln5 was shown to be a target of TGFβ and induced the expression of the anti-angiogenic protein TSP-1. In addition, activated endothelial cells undergoing tubulogenesis downregulated expression of Fbln5.[65]

In vivo studies using *Fbln5*$^{-/-}$ mice also support that Fbln5 regulates

angiogenesis. *Fbln5*$^{-/-}$ mice bearing implanted PVA sponges showed an increase in vascular invasion compared to *WT* animals. [66] Expression of pro-angiogenic proteins such as VEGF and angiopoietin -1, -2, and -3 were increased in sponges removed from *Fbln5*$^{-/-}$ mice compared to those from *WT* mice. *Fbln5*$^{-/-}$ mice also exhibited an increase in vessel branching off the long thoracic artery.[66] Furthermore, studies addressing Fbln5's function during wound repair, a process that requires angiogenesis, revealed increased neovascularization in the skin of *Fbln5*$^{-/-}$ mice before and during wound repair. However, this study did not observe a difference in wound repair rates between *Fbln5*$^{-/-}$ and *WT* mice despite the increase in vessel formation.[67, 68] These studies suggest that in certain physiological circumstances Fbln5 can inhibit angiogenesis. However, the mechanism behind Fbln5's negative impact on angiogenesis is still unclear.

Fibulin-5 and tumor development

Investigation into the effect of Fbln5 on tumor development and progression are still in the early stages and little is currently known. However, the expression of Fbln5 in human cancers has recently been examined in a small subset of tumor types including kidney, breast, lung, ovary and some gastrointestinal cancers. In this study, Fbln5 mRNA was evaluated using a cDNA microarray coated with matched normal/tumor cDNA from 68 patients with varying cancers. Fbln5 expression was altered in 44 of 68 samples and of those 44 cases, expression was down-regulated in 42 and up-regulated in only two. [63] It is important to note, however, that the samples examined in this study were derived from whole tumors. Therefore, the source of Fbln5 expression was not determined, whether from the stromal/host comparment or tumor cells. As mentioned previously, studies of SPARC and TSP-1 have shown that proteins expressed by stromal cells can have vastly different effects on tumor growth than proteins secreted from tumor cells. A closer look at the expression level of Fbln5

by these two compartments is needed to fully determine how human tumor development effects Fbln5 expression. In a related study[69], analysis of prostate cancer identified an increase in Fbln5 expression compared to benign tissue. Expression did not correlate with advancing stages but instead remained consistent throughout prostate cancer progression. Interestingly, staining of tumor tissue with a Fbln5-specific antibody found Fbln5 expression to be present in the nuclei of tumor cells.[69] A function for Fbln5 in the nucleus has not been investigated but might explain how Fbln5 affects gene expression.

As seen with other matricellular proteins, *in vitro* and *in vivo* studies have shown the effect of Fbln5 on tumor growth to be complex and context-dependent. Given that forced expression of Fbln5 in 3T3-L1 fibroblasts enhanced DNA synthesis and proliferation, experiments were performed to determine the effect of Fbln5 on the tumorigencity of fibrosarcoma cells. Although forced expression of Fbln1, a closely related family member, in fibrosarcoma cells inhibited proliferation, expression of Fbln5 increased proliferation and improved invasion.[63] Fbln1 does not contain an RGD domain, therefore it is possible that the different effects observed in these cells was do to Fbln5's ability to modify integrin signaling. In stark contrast to the *in vitro* findings, fibrosarcoma cells modified to increase expression of Fbln5 and injected into genetically normal mice developed smaller, slower tumors. Tumors overexpressing Fbln5 had impaired angiogenesis, which is believed to be the cause for decreased tumor growth.[70] Furthermore, histamine, an inflammatory molecule, was shown to heighten B16-F10 melanoma growth in mice. A study exploring this effect identified Fbln5 as an indirect target for histamine. Melanomas secreting high levels of histamine had significantly reduced expression of Fbln5 compared to tumors not expressing histamine. Histamine secretion also decreased insulin-like growth factor II receptor (IGF-IIR) expression, which is required for activation of TGF-β. Since Fbln5

expression had previously been shown to be induced by TGF-β, it was hypothesized that histamine indirectly regulates the level of Fbln5 expression by reducing IGF-IIR expression thus aiding in the promotion of tumor growth.[71] Unfortunately, angiogenesis was not evaluated in these tumors.

Although, these results have provided useful information regarding Fbln5's effect on tumor development, a large piece of data is missing from the literature, the effect of endogenous Fbln5 on tumor growth. The aforementioned data have been developed through the use of exogenously added or forced overexpression of Fbln5, which has historically provided vastly different effects than that of the endogenous protein. Therefore, the goal of my project was to investigate the effect of endogenous Fbln5 on tumor progression by performing tumor studies in *Fbln5*$^{-/-}$ mice. In doing so, we have identified a novel function for Fbln5 in controlling integrin-induced ROS production and have shown this function to be critical for tumor angiogenesis and growth.

REFERENCES

1. Kadler KE, Hill A, Canty-Laird EG. Collagen fibrillogenesis: fibronectin, integrins, and minor collagens as organizers and nucleators. Curr Opin Cell Biol 2008;20(5):495-501.
2. Mao Y, Schwarzbauer JE. Fibronectin fibrillogenesis, a cell-mediated matrix assembly process. Matrix Biol 2005;24(6):389-99.
3. Wagenseil JE, Mecham RP. New insights into elastic fiber assembly. Birth Defects Res C Embryo Today 2007;81(4):229-40.
4. Mizejewski GJ. Role of integrins in cancer: survey of expression patterns. Proc Soc Exp Biol Med 1999;222(2):124-38.
5. Giannoni E, Buricchi F, Grimaldi G, et al. Redox regulation of anoikis: reactive oxygen species as essential mediators of cell survival. Cell Death Differ 2008;15(5):867-78.
6. Pourgholami MH, Morris DL. Inhibitors of vascular endothelial growth factor in cancer. Cardiovasc Hematol Agents Med Chem 2008;6(4):343-7.
7. Lee S, Jilani SM, Nikolova GV, Carpizo D, Iruela-Arispe ML. Processing of VEGF-A by matrix metalloproteinases regulates bioavailability and vascular patterning in tumors. J Cell Biol 2005;169(4):681-91.
8. ten Dijke P, Arthur HM. Extracellular control of TGFbeta signalling in vascular development and disease. Nat Rev Mol Cell Biol 2007;8(11):857-69.
9. Framson PE, Sage EH. SPARC and tumor growth: where the seed meets the soil? J Cell Biochem 2004;92(4):679-90.
10. Liaw L, Crawford HC. Functions of the extracellular matrix and matrix degrading proteases during tumor progression. Braz J Med Biol Res 1999;32(7):805-12.
11. Wojtowicz-Praga SM, Dickson RB, Hawkins MJ. Matrix metalloproteinase inhibitors. Invest New Drugs 1997;15(1):61-75.
12. Balbin M, Fueyo A, Tester AM, et al. Loss of collagenase-2 confers increased skin tumor susceptibility to male mice. Nat Genet 2003;35(3):252-7.
13. McCawley LJ, Crawford HC, King LE, Jr., Mudgett J, Matrisian LM. A protective role for matrix metalloproteinase-3 in squamous cell carcinoma. Cancer Res 2004;64(19):6965-72.
14. Deryugina EI, Quigley JP. Matrix metalloproteinases and tumor metastasis. Cancer Metastasis Rev 2006;25(1):9-34.
15. Pasco S, Ramont L, Venteo L, Pluot M, Maquart FX, Monboisse JC. In vivo overexpression of tumstatin domains by tumor cells inhibits their invasive properties in a mouse melanoma model. Exp Cell Res 2004;301(2):251-65.
16. O'Reilly MS, Boehm T, Shing Y, et al. Endostatin: an endogenous inhibitor of angiogenesis and tumor growth. Cell 1997;88(2):277-85.

17. Bauer SM, Bauer RJ, Velazquez OC. Angiogenesis, vasculogenesis, and induction of healing in chronic wounds. Vasc Endovascular Surg 2005;39(4):293-306.
18. Brekken RA, Overholser JP, Stastny VA, Waltenberger J, Minna JD, Thorpe PE. Selective inhibition of vascular endothelial growth factor (VEGF) receptor 2 (KDR/Flk-1) activity by a monoclonal anti-VEGF antibody blocks tumor growth in mice. Cancer Res 2000;60(18):5117-24.
19. Ferrara N, Hillan KJ, Gerber HP, Novotny W. Discovery and development of bevacizumab, an anti-VEGF antibody for treating cancer. Nat Rev Drug Discov 2004;3(5):391-400.
20. Silva R, D'Amico G, Hodivala-Dilke KM, Reynolds LE. Integrins: the keys to unlocking angiogenesis. Arterioscler Thromb Vasc Biol 2008;28(10):1703-13.
21. Brooks PC, Stromblad S, Klemke R, Visscher D, Sarkar FH, Cheresh DA. Antiintegrin alpha v beta 3 blocks human breast cancer growth and angiogenesis in human skin. J Clin Invest 1995;96(4):1815-22.
22. Mitjans F, Meyer T, Fittschen C, et al. In vivo therapy of malignant melanoma by means of antagonists of alphav integrins. Int J Cancer 2000;87(5):716-23.
23. Hasselaar P, Sage EH. SPARC antagonizes the effect of basic fibroblast growth factor on the migration of bovine aortic endothelial cells. J Cell Biochem 1992;49(3):272-83.
24. Raines EW, Lane TF, Iruela-Arispe ML, Ross R, Sage EH. The extracellular glycoprotein SPARC interacts with platelet-derived growth factor (PDGF)-AB and -BB and inhibits the binding of PDGF to its receptors. Proc Natl Acad Sci U S A 1992;89(4):1281-5.
25. Yan Q, Sage EH. SPARC, a matricellular glycoprotein with important biological functions. J Histochem Cytochem 1999;47(12):1495-506.
26. Koblinski JE, Kaplan-Singer BR, VanOsdol SJ, et al. Endogenous osteonectin/SPARC/BM-40 expression inhibits MDA-MB-231 breast cancer cell metastasis. Cancer Res 2005;65(16):7370-7.
27. Beck AH, Espinosa I, Gilks CB, van de Rijn M, West RB. The fibromatosis signature defines a robust stromal response in breast carcinoma. Lab Invest 2008;88(6):591-601.
28. Bergamaschi A, Tagliabue E, Sorlie T, et al. Extracellular matrix signature identifies breast cancer subgroups with different clinical outcome. J Pathol 2008;214(3):357-67.
29. Tai IT, Tang MJ. SPARC in cancer biology: Its role in cancer progression and potential for therapy. Drug Resist Updat 2008.

30. Tai IT, Dai M, Owen DA, Chen LB. Genome-wide expression analysis of therapy-resistant tumors reveals SPARC as a novel target for cancer therapy. J Clin Invest 2005;115(6):1492-502.
31. Tang MJ, Tai IT. A novel interaction between procaspase 8 and SPARC enhances apoptosis and potentiates chemotherapy sensitivity in colorectal cancers. J Biol Chem 2007;282(47):34457-67.
32. Lussier C, Sodek J, Beaulieu JF. Expression of SPARC/osteonectin/BM4O in the human gut: predominance in the stroma of the remodeling distal intestine. J Cell Biochem 2001;81(3):463-76.
33. Yang E, Kang HJ, Koh KH, Rhee H, Kim NK, Kim H. Frequent inactivation of SPARC by promoter hypermethylation in colon cancers. Int J Cancer 2007;121(3):567-75.
34. Wang-Rodriguez J, Urquidi V, Rivard A, Goodison S. Elevated osteopontin and thrombospondin expression identifies malignant human breast carcinoma but is not indicative of metastatic status. Breast Cancer Res 2003;5(5):R136-43.
35. Greenaway J, Lawler J, Moorehead R, Bornstein P, Lamarre J, Petrik J. Thrombospondin-1 inhibits VEGF levels in the ovary directly by binding and internalization via the low density lipoprotein receptor-related protein-1 (LRP-1). J Cell Physiol 2007;210(3):807-18.
36. Jimenez B, Volpert OV, Crawford SE, Febbraio M, Silverstein RL, Bouck N. Signals leading to apoptosis-dependent inhibition of neovascularization by thrombospondin-1. Nat Med 2000;6(1):41-8.
37. Nor JE, Mitra RS, Sutorik MM, Mooney DJ, Castle VP, Polverini PJ. Thrombospondin-1 induces endothelial cell apoptosis and inhibits angiogenesis by activating the caspase death pathway. J Vasc Res 2000;37(3):209-18.
38. Watnick RS, Cheng YN, Rangarajan A, Ince TA, Weinberg RA. Ras modulates Myc activity to repress thrombospondin-1 expression and increase tumor angiogenesis. Cancer Cell 2003;3(3):219-31.
39. Gautam A, Densmore CL, Melton S, Golunski E, Waldrep JC. Aerosol delivery of PEI-p53 complexes inhibits B16-F10 lung metastases through regulation of angiogenesis. Cancer Gene Ther 2002;9(1):28-36.
40. Kazerounian S, Yee KO, Lawler J. Thrombospondins in cancer. Cell Mol Life Sci 2008;65(5):700-12.
41. Lawler J, Miao WM, Duquette M, Bouck N, Bronson RT, Hynes RO. Thrombospondin-1 gene expression affects survival and tumor spectrum of p53-deficient mice. Am J Pathol 2001;159(5):1949-56.
42. Albo D, Berger DH, Vogel J, Tuszynski GP. Thrombospondin-1 and transforming growth factor beta-1 upregulate plasminogen activator inhibitor type 1 in pancreatic cancer. J Gastrointest Surg 1999;3(4):411-7.

43. Wang TN, Qian X, Granick MS, et al. Thrombospondin-1 (TSP-1) promotes the invasive properties of human breast cancer. J Surg Res 1996;63(1):39-43.
44. Clezardin P, Frappart L, Clerget M, Pechoux C, Delmas PD. Expression of thrombospondin (TSP1) and its receptors (CD36 and CD51) in normal, hyperplastic, and neoplastic human breast. Cancer Res 1993;53(6):1421-30.
45. Johnston NI, Gunasekharan VK, Ravindranath A, O'Connell C, Johnston PG, El-Tanani MK. Osteopontin as a target for cancer therapy. Front Biosci 2008;13:4361-72.
46. Chambers AF, Behrend EI, Wilson SM, Denhardt DT. Induction of expression of osteopontin (OPN; secreted phosphoprotein) in metastatic, ras-transformed NIH 3T3 cells. Anticancer Res 1992;12(1):43-7.
47. Standal T, Borset M, Sundan A. Role of osteopontin in adhesion, migration, cell survival and bone remodeling. Exp Oncol 2004;26(3):179-84.
48. Cui R, Takahashi F, Ohashi R, et al. Abrogation of the interaction between osteopontin and alphavbeta3 integrin reduces tumor growth of human lung cancer cells in mice. Lung Cancer 2007;57(3):302-10.
49. Brown LF, Papadopoulos-Sergiou A, Berse B, et al. Osteopontin expression and distribution in human carcinomas. Am J Pathol 1994;145(3):610-23.
50. Irby RB, McCarthy SM, Yeatman TJ. Osteopontin regulates multiple functions contributing to human colon cancer development and progression. Clin Exp Metastasis 2004;21(6):515-23.
51. Weber GF. The metastasis gene osteopontin: a candidate target for cancer therapy. Biochim Biophys Acta 2001;1552(2):61-85.
52. Timpl R, Sasaki T, Kostka G, Chu ML. Fibulins: a versatile family of extracellular matrix proteins. Nat Rev Mol Cell Biol 2003;4(6):479-89.
53. Zheng Q, Davis EC, Richardson JA, et al. Molecular analysis of fibulin-5 function during de novo synthesis of elastic fibers. Mol Cell Biol 2007;27(3):1083-95.
54. Yanagisawa H, Davis EC, Starcher BC, et al. Fibulin-5 is an elastin-binding protein essential for elastic fibre development in vivo. Nature 2002;415(6868):168-71.
55. Freeman LJ, Lomas A, Hodson N, et al. Fibulin-5 interacts with fibrillin-1 molecules and microfibrils. Biochem J 2005;388(Pt 1):1-5.
56. Liu X, Zhao Y, Gao J, et al. Elastic fiber homeostasis requires lysyl oxidase-like 1 protein. Nat Genet 2004;36(2):178-82.
57. Loeys B, Van Maldergem L, Mortier G, et al. Homozygosity for a missense mutation in fibulin-5 (FBLN5) results in a severe form of cutis laxa. Hum Mol Genet 2002;11(18):2113-8.

58. Kowal RC, Richardson JA, Miano JM, Olson EN. EVEC, a novel epidermal growth factor-like repeat-containing protein upregulated in embryonic and diseased adult vasculature. Circ Res 1999;84(10):1166-76.
59. Kuang PP, Goldstein RH, Liu Y, Rishikof DC, Jean JC, Joyce-Brady M. Coordinate expression of fibulin-5/DANCE and elastin during lung injury repair. Am J Physiol Lung Cell Mol Physiol 2003;285(5):L1147-52.
60. Nakamura T, Ruiz-Lozano P, Lindner V, et al. DANCE, a novel secreted RGD protein expressed in developing, atherosclerotic, and balloon-injured arteries. J Biol Chem 1999;274(32):22476-83.
61. Lomas AC, Mellody KT, Freeman LJ, Bax DV, Shuttleworth CA, Kielty CM. Fibulin-5 binds human smooth-muscle cells through alpha5beta1 and alpha4beta1 integrins, but does not support receptor activation. Biochem J 2007;405(3):417-28.
62. Nakamura T, Lozano PR, Ikeda Y, et al. Fibulin-5/DANCE is essential for elastogenesis in vivo. Nature 2002;415(6868):171-5.
63. Schiemann WP, Blobe GC, Kalume DE, Pandey A, Lodish HF. Context-specific effects of fibulin-5 (DANCE/EVEC) on cell proliferation, motility, and invasion. Fibulin-5 is induced by transforming growth factor-beta and affects protein kinase cascades. J Biol Chem 2002;277(30):27367-77.
64. Spencer JA, Hacker SL, Davis EC, et al. Altered vascular remodeling in fibulin-5-deficient mice reveals a role of fibulin-5 in smooth muscle cell proliferation and migration. Proc Natl Acad Sci U S A 2005;102(8):2946-51.
65. Albig AR, Schiemann WP. Fibulin-5 antagonizes vascular endothelial growth factor (VEGF) signaling and angiogenic sprouting by endothelial cells. DNA Cell Biol 2004;23(6):367-79.
66. Sullivan KM, Bissonnette R, Yanagisawa H, Hussain SN, Davis EC. Fibulin-5 functions as an endogenous angiogenesis inhibitor. Lab Invest 2007;87(8):818-27.
67. Lee MJ, Roy NK, Mogford JE, Schiemann WP, Mustoe TA. Fibulin-5 promotes wound healing in vivo. J Am Coll Surg 2004;199(3):403-10.
68. Zheng Q, Choi J, Rouleau L, et al. Normal wound healing in mice deficient for fibulin-5, an elastin binding protein essential for dermal elastic fiber assembly. J Invest Dermatol 2006;126(12):2707-14.
69. Wlazlinski A, Engers R, Hoffmann MJ, et al. Downregulation of several fibulin genes in prostate cancer. Prostate 2007;67(16):1770-80.
70. Albig AR, Neil JR, Schiemann WP. Fibulins 3 and 5 antagonize tumor angiogenesis in vivo. Cancer Res 2006;66(5):2621-9.
71. Pos Z, Wiener Z, Pocza P, et al. Histamine suppresses fibulin-5 and insulin-like growth factor-II receptor expression in melanoma. Cancer Res 2008;68(6):1997-2005.

CHAPTER 1: Loss of endogenous Fibulin-5 reduces angiogenesis and abates pancreatic tumor growth.

INTRODUCTION

Pancreatic cancer is one of the deadliest types of cancer killing an estimated 35,000 Americans each year making it the fourth leading cause of cancer deaths in the United States (ACS, 2007). Pancreatic cancer often progresses with very little symptoms so by the time of diagnosis, the cancer is highly advanced and has often metastasized making the five-year survival rate for patients less than 5% (ACS, 2007). To date, our resources to fight pancreatic cancer are limited. Gemcitabine is the standard chemotherapy but unfortunately, most pancreatic cancers respond marginally or not at all. Given these grave statistics, the need for research focused on identifying molecular mechanisms involved in the development of pancreatic cancer to aid in the generation of more effective therapies is critical. The Brekken laboratory is focused on the host response to pancreatic cancer. The induction of pancreatic cancer elicits a unique desmoplastic response by the host. Desmoplasia describes a process by which the host initiates the deposition of large amounts of ECM generating a band of dense fibrous tissue that encapsulates the growing tumor in an attempt to contain it. This type of host response makes pancreatic cancer a perfect model for studying the effect ECM has on tumor development. Throughout our investigations, the Brekken laboratory have acquired valuable tools for studying the induction and progression of pancreatic cancer in mice including multiple pancreatic cancer cell lines and the development of an unique orthotopic pancreatic tumor mouse model. The work described herein, uses these tools along with *Fbln5*$^{-/-}$ mice from Hiromi Yanagisawa's laboratory to investigate the function of endogenous Fbln5 in pancreatic tumor growth.

RESULTS

Pancreatic tumor growth is reduced in *Fbln5*$^{-/-}$ mice

Given the effect of Fbln5 on angiogenesis and its reduced expression in a subset of human tumors, Fbln5 has been labeled a tumor suppressor. However, the effect of endogenous Fbln5 on tumor growth has not been evaluated. To investigate this effect, we collaborated with Hiromi Yanagisawa's laboratory to perform pancreatic tumor studies in *Fbln5*$^{-/-}$ mice. Dr. Grzegorz Korpanty, a former post-doctoral fellow in the Brekken laboratory, spearheaded the initial tumor studies performed in *Fbln5*$^{-/-}$ mice. Pan02 cells, a murine pancreatic carcinoma cell line, were injected subcutaneously into the right flank of *Fbln5*$^{-/-}$ and *WT* littermates. Tumor growth was monitored weekly and after four weeks, animals were sacrificed and tumors harvested for analysis. The initial tumor study revealed a surprising decrease in tumor growth in *Fbln5*$^{-/-}$ mice compared to tumors in *WT* mice (data not shown). To optimize tumor growth in the mixed background of *Fbln5*$^{-/-}$ mice (C57B1/6 X 129/SvEv), Dr. Korpanty derived a tumor cell line from a subcutaneous tumor grown in a *WT* animal from the same background. This cell line was labeled Pan02HY and was used in all subsequent experiments.

To confirm these results, a larger subcutaneous tumor study was performed. Throughout the four weeks of the study, tumors in *Fbln5*$^{-/-}$ mice grew significantly slower than tumors from *WT* mice (**Figure 1.1A**). At the time of sacrifice, tumors were removed and weighed. As observed in the initial study, final tumor weights were significantly smaller in *Fbln5*$^{-/-}$ mice compared to tumors grown in *WT* mice (**Figure 1.1B**).

There is accumulating evidence that the site of tumor growth greatly affects gene expression and physiologic characteristics of a tumor that can alter tumor survival. Therefore, to better assess pancreatic cancer growth, we have established an orthotopic pancreatic tumor model that mimics the

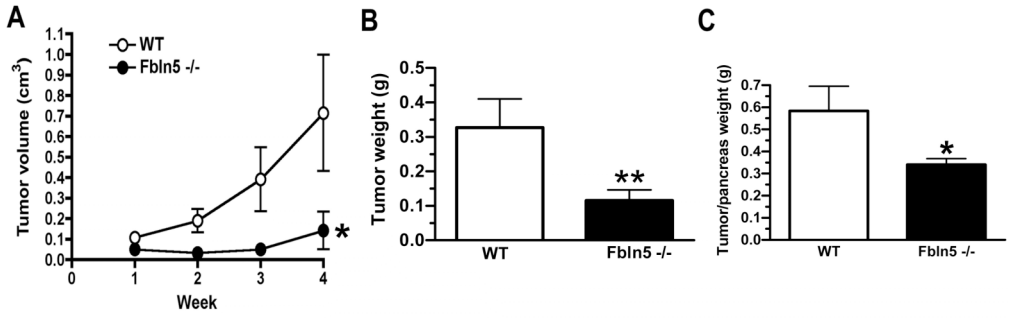

D

	Metastatic Incidence (%)						Total Metastatic Events				
Genotype	n=	Lymph	Peritoneal	Liver	Other	Total	Lymph	Peritoneal	Liver	Other	Total
WT	7	4(57.1)	4(57.1)	0	0	4(57.1)	25	26	0	0	51
Fbln5 -/-	6	1(16.7)	0	0	0	1(16.7)	2	0	0	0	2

Figure 1.1 Pancreatic tumor growth is reduced in *Fbln5*$^{-/-}$ mice. Murine pancreatic carcinoma cells (Pan02) were injected subcutaneously ($3x10^6$) (A, B) or orthotopically ($5x10^5$) (C, D) into *WT* and *Fbln5*$^{-/-}$ mice. A) Mean subcutaneous tumor volume +/- s.e.m. of a representative experiment (n=5 for *WT* and *Fbln5*$^{-/-}$). B) Mean +/- s.e.m. final subcutaneous tumor weight for three individual experiments (*WT*, n=18; *Fbln5*$^{-/-}$, n=19). C) Mean +/- s.e.m. tumor/pancreas weight (D) and the number of observed metastatic events of *WT* (n=7) and *Fbln5*$^{-/-}$ (n=6) animals injected orthotopically with Pan02 cells is shown. *, $p<0.05$; **, $p<0.01$

course of human disease similar to previously reported methods.[1] Briefly, tumor cells are implanted into the tail of the pancreas allowing tumors to develop in their natural environment. We used this procedure to further characterize pancreatic tumor growth in *Fbln5*$^{-/-}$ mice. Pan02HY cells were injected into the tail of the pancreas of *Fbln5*$^{-/-}$ and *WT* mice. Tumors were first palpable two weeks after tumor cell injection. At four weeks, animals were sacrificed and the pancreas with the tumor was harvested and weighed. Final orthotopic tumor weights in *Fbln5*$^{-/-}$ mice were smaller when compared to tumors grown in *WT* littermates (**Figure 1.1C**). Upon examination of *WT* animals, multiple metastases were identified in the surrounding peritoneum and lymph nodes however, we observed a significant decrease in the number of metastases in *Fbln5*$^{-/-}$ mice (**Figure 1.1D**). These surprising results distinguished the effect of endogenous Fbln5 from the

exogenous protein and indicated an unexpected function for Fbln5 that facilitates tumor progression.

Characterization of tumors grown in *Fbln5*$^{-/-}$ mice

To understand the mechanism(s) behind the decreased tumor growth in *Fbln5*$^{-/-}$ mice, we analyzed different characteristics of tumors from both WT and *Fbln5*$^{-/-}$ mice. These characteristics include alterations in ECM protein expression, survival rates of cells within the tumor and development of a vascular network. Our results are listed below:

Normal ECM deposition observed in tumors from *Fbln5*$^{-/-}$ mice

Matricellular proteins regulate the deposition and assembly of ECM proteins and alterations in their expression can impact tumor growth by disrupting proper ECM formation. Therefore, we performed histological analysis on orthotopic tumors from *WT* and *Fbln5*$^{-/-}$ animals to identify alterations in ECM protein expression. H&E stained tumor sections revealed no striking differences in morphology or tissue architecture in tumors from *Fbln5*$^{-/-}$ mice compared to *WT* animals. Collagen deposition was examined by trichrome staining and appeared normal in tumors from *Fbln5*$^{-/-}$ mice (**Figure 1.2A**). Laminin and fibronectin levels were analyzed by immunohistochemistry. Both ECM proteins were expressed at equal levels with no obvious structural defect in orthotopic tumors (data not shown). Analysis of fibronectin expression in subcutaneous tumors from *Fbln5*$^{-/-}$ mice did suggest an increase in expression, however these findings were not confirmed by reverse transcriptase PCR (RT-PCR). Overall, these results suggested that the decreased tumor growth observed in *Fbln5*$^{-/-}$ mice was not due to defects in ECM deposition or assembly.

As a control, we evaluated the expression of Fbln5 in Pan02 cells by RT-PCR and Western blot analysis and determined that Pan02 cells do not express

Fbln5. This was confirmed by immunohistochemistry staining showing that tumors from *WT* animals express high levels of Fbln5 while tumors from *Fbln5*$^{-/-}$ mice were devoid of any Fbln5 protein. These results indicated that only host cells found within the tumor expressed Fbln5 (**Figure 1.2B**). Importantly, a significant portion of Fbln5 present in tumors from *WT* mice was localized to blood vessels and perivascular areas (**Figure 1.2B**).

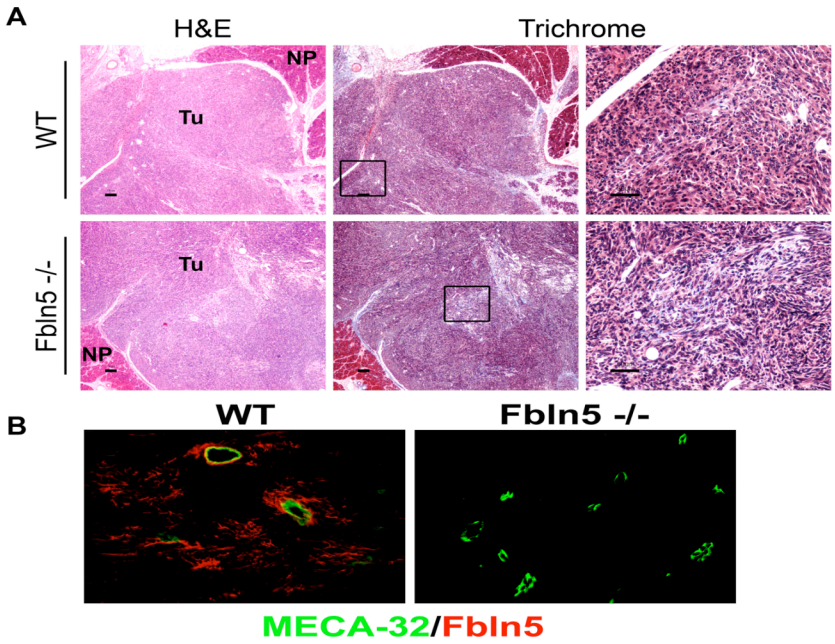

Figure 1.2 Histological analysis of tumors from *WT* and *Fbln5*$^{-/-}$ mice A) H&E and trichrome staining was performed on fixed tumor sections from *WT* and *Fbln5*$^{-/-}$ mice. Analysis revealed no difference in tissue architecture or fibrillar collagen (dark blue) deposition between the two genotypes. B) Fbln5 expression was analyzed in tumors from *WT* and *Fbln5*$^{-/-}$ mice to determine the location of Fbln5 and if Pan02 tumor cells expressed the protein. Immunohistochemistry was performed using a Fbln5 specific antibody (red) and MECA-32 (green) to identify blood vessels. A larger portion of Fbln5 was seen localized to blood vessels in tumors from *WT* animals while no expression was observed in tumors from *Fbln5*$^{-/-}$ mice indicating that Pan02 cells do not express Fbln5.

Proliferation decreased and apoptosis increased in tumors from *Fbln5*$^{-/-}$ mice

A disruption in tumor growth is often caused from a decrease in the proliferation rate of cells that make up a tumor along with an increase in the death of these cells. We examined these characteristics in Pan02 tumors from *WT* and *Fbln5*$^{-/-}$ animals. Immunohistochemistry with an antibody specific for phosphorylated histone H3, a marker of mitosis, revealed a significant decrease in the number of proliferating cells in tumors grown in the absence of Fbln5 (**Figure 1.3**). In contrast, TUNEL analysis showed a significant increase in the number of apoptotic cells in tumors grown in *Fbln5*$^{-/-}$ animals compared to *WT* mice (**Figure 1.3**). These results correlate with anticipated characteristics of smaller, slower growing tumors such as those seen in *Fbln5*$^{-/-}$ animals.

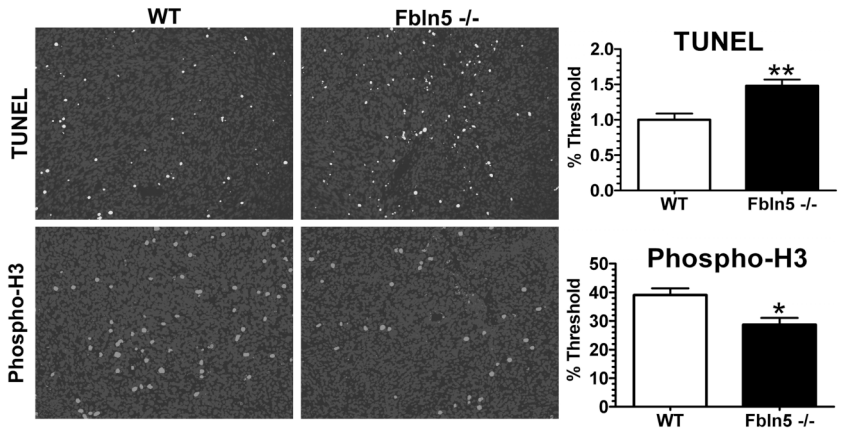

Figure 1.3 Absence of host Fbln5 results in increased apoptosis and decreased proliferation in Pan02 tumors. Formalin-fixed sections of subcutaneous tumors from *WT* (n=4) and *Fbln5*$^{-/-}$ (n=3) mice were evaluated for the level of apoptosis by TUNEL staining (TUNEL, top panels) and cell proliferation by immunohistochemistry for phosphorylated histone H3 (Phospho-H3, bottom panels). The number of TUNEL or Phospho-H3 positive cells was determined by fluorescence microscopy using tumor slides counterstained with DAPI. Metamorph imaging software was used to quantify the % signal above a threshold, which was set by evaluating sections that were treated with secondary alone. Ten pictures (total magnification, 200x) were taken from each tumor for quantification. The results shown are mean +/- s.e.m. *, $p<0.01$; **, $p<0.001$

Angiogenesis is decreased in tumors from *Fbln5*$^{-/-}$ mice

Sustained tumor growth requires angiogenesis to facilitate nutrient delivery to the tumor mass. Given this knowledge and the recent studies suggesting that Fbln5 is a regulator of angiogenesis, we evaluated vascular density in tumors from *Fbln5*$^{-/-}$ mice to determine if the decrease in tumor growth was due to an inadequate blood supply.[2] We examined blood vessel density in tumors by immunohistochemistry using the endothelial cell marker MECA-32 The number of blood vessels per mm^2 was significantly lower in subcutaneous and orthotopic tumors grown in *Fbln5*$^{-/-}$ mice compared to *WT* animals (**Figure 1.4A**). These results suggested that the increase in apoptosis observed in tumors from *Fbln5*$^{-/-}$ mice maybe caused in part by the inability of tumors to develop and maintain a sufficient blood vessel network resulting in reduced tumor growth.

Pericytes are supporting cells found wrapped around endothelial tubes. These cells protect the underlying endothelium and add strength and integrity to the blood vessel wall.[3] Pericyte-association indicates a mature, stable functioning blood vessel. To determine the nature of blood vessels present within tumors from *Fbln5*$^{-/-}$ mice, we evaluated pericyte-association in Pan02 tumors from both genotypes. The pericyte marker, smooth muscle actin (SMA), was co-localized with MECA-32 positive blood vessels to identify pericyte-associated blood vessels. Although total blood vessel density was decreased in tumors grown in *Fbln5*$^{-/-}$ mice, the percentage of blood vessels associated with pericytes was significantly higher in tumors from *Fbln5*$^{-/-}$ mice than tumors from *WT* mice (**Figure 1.4B**). These data suggest that the TME created in the absence of host Fbln5 is altered in such a way that only mature blood vessels are able to survive.

Previous results have reported an increase in vessel sprouting in *Fbln5*$^{-/-}$ animals.[2] Therefore, we next asked whether the reduction in angiogenesis we observed was specific to the tumor microenvironment. To answer this, we

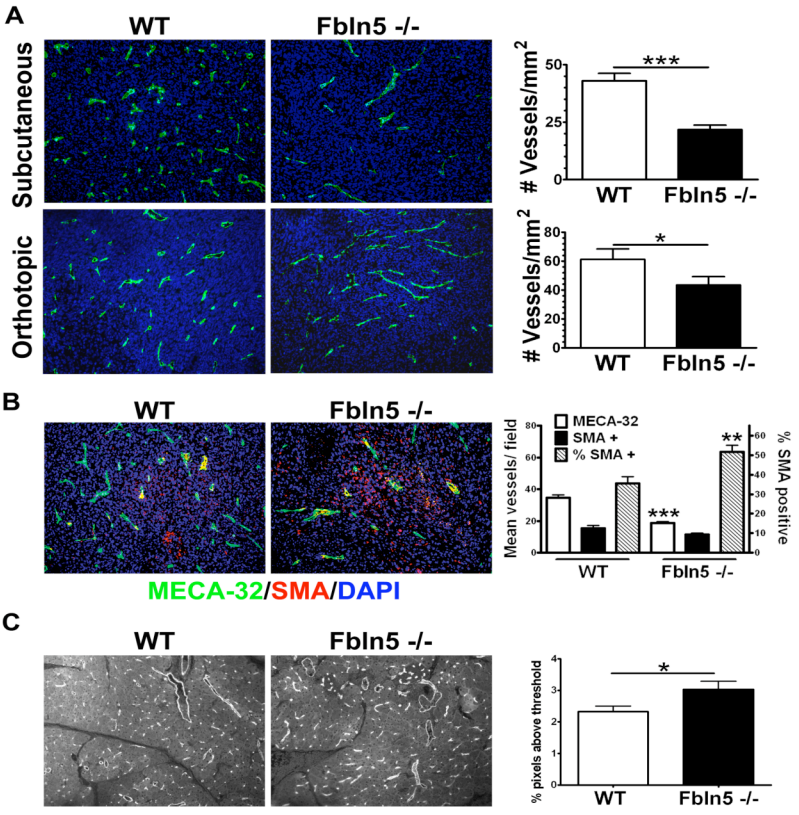

Figure 1.4 Vessel density is decreased in tumors grown in *Fbln5*$^{-/-}$ mice. A) Sections from subcutaneous and orthotopic tumors were stained with MECA-32 (green) and counter stained with DAPI (blue) to analyze blood vessel density. The number of MECA-32 positive structures were counted in a minimum of six microscopic fields (total magnification, 200x) from each tumor (at least 3 tumors/genotype) *, $p<0.05$; ***, $p<0.0001$ Mean blood vessel density +/- s.d. B) Mean vessel density +/- sd (open bars), MECA-32/SMA double positive vessels (filled in bars) per 200x field is shown. The % blood vessels associated with pericytes is shown in the hatched bar. MVD was reduced significantly in tumors grown in *Fbln5*$^{-/-}$ mice (***, $p<0.0001$) while the percentage of pericyte associated blood vessels was increased (**, $p<0.005$). C) MECA-32 positive blood vessel density in non-tumor bearing normal pancreas from *WT* and *Fbln5*$^{-/-}$ mice was determined by immunohistochemistry. Mean blood vessel density +/- s.e.m. is shown, *, $p<0.05$.

analyzed blood vessel density in the pancreas of non-tumor bearing *WT* and *Fbln5*$^{-/-}$ animals. Consistent with results described previously [2], we observed an increase in the number of vessels in the pancreas of non-tumor bearing *Fbln5*$^{-/-}$ animals compared to *WT* (**Figure 1.4C**). These results indicated that the reduction

in blood vessels observed in tumors grown in *Fbln5*$^{-/-}$ mice was due to a characteristic solely of the tumor microenvironment and not present under non-pathological conditions.

DISCUSSION

Given previous reports identifying Fbln5 as a tumor suppressor, we initially hypothesized that the absence of host Fbln5 would enhance tumor growth and metastasis. Surprisingly, however, we observed a decrease in subcutaneous pancreatic tumor growth in *Fbln5*$^{-/-}$ mice. Moreover, these results were recapitulated in our orthotopic model. This was reassuring because the organ environment greatly influences specific characteristics of the host response to a tumor including ECM deposition and growth factor expression. It also strongly affects tumor cell function and is, therefore, an important determinant of tumor growth. Orthotopic tumor cell implantation studies provide a more accurate analysis of tumor growth *in vivo* and have been shown to better mimic human tumor growth and metastasis.[4, 5]

Prior reports have shown that forced overexpression of Fbln5 by tumor cells impairs tumor growth. The contradictions observed in our studies most likely stem from the fact that we are studying the loss of endogenous host-derived Fbln5. Our findings suggest that, in the context of pancreatic cancer, host-derived Fbln5 functions to support tumor growth. Given the context-dependent nature of Fbln5, it possible that these results are unique to pancreatic cancer and further studies are needed to determine how the loss of endogenous Fbln5 affects the development of other types of cancer.

Once we had confirmed our findings, we began a thorough examination of tumors from *Fbln5*$^{-/-}$ mice to identify any abnormal characteristics that could account for the decrease in tumor growth. First, we performed histological analysis of tumors from *Fbln5*$^{-/-}$ and *WT* mice by evaluating the structure and

composition of the TME. Matricellular proteins, including Fbln5, regulate the deposition and assembly of ECM proteins, and a disruption in proper formation can alter tumor growth. For example, defects in collagen deposition and fibrillogenesis in *SPARC*$^{-/-}$ mice led to enhanced pancreatic tumor growth and metastasis [6, 7]. Since Fbln5 has been shown to augment collagen deposition in wound healing assays, which elicits a host response similar to that of a tumor, we analyzed collagen levels within the TME of tumors from *Fbln5*$^{-/-}$ and *WT* mice by H&E and trichrome staining [8]. However, we detected no differences in collagen expression or collagen assembly. We also examined laminin and fibronectin but again detected no significant alterations in their expression within tumors from *Fbln5*$^{-/-}$ mice tumors when compared to tumors from *WT*. We can conclude from these sets of experiments that in response to tumor formation, the lack of Fbln5 expression does not result in alterations in ECM deposition or defects in the architecture of the TME. However, it is important to note that we did not examine the status of elastic fibers within tumors from *Fbln5*$^{-/-}$ mice. The involvement of elastic fibers and their individual components in tumor development and progression have not been characterized, but since Fbln5 is critical to proper elastic fiber formation, it would be worthwhile to explore.

We observed a decrease in cell survival within tumors from *Fbln5*$^{-/-}$ mice. This suggests that in the absence of host derived Fbln5, the TME is altered in such a way that it can no longer support the survival or enhance the proliferation of cells. Although we did identify a portion of the dying cells to be endothelial cells (data that will be discussed in the following chapter), we did not attempt to determine other cell types undergoing apoptosis. However, given that Pan02 tumor cells do not express Fbln5, they may rely on host generated Fbln5 to perform specific functions required for survival. It is possible then that the decrease in tumor growth observed in *Fbln5*$^{-/-}$ mice is due to the increased death rate of both host-derived cells and tumor cells.

Loss of endogenous Fbln5 antagonizes tumor angiogenesis

In the literature, the adverse effects of Fbln5 on tumor growth have been attributed mostly to its function as an angiogenic inhibitor [8, 9]. Paradoxically, we observed a significant decrease in angiogenesis in pancreatic tumors from *Fbln5*$^{-/-}$ mice suggesting an unidentified function for Fbln5 in the regulation of angiogenesis. However, consistent with previous reports, we also observed increased blood vessel density in the pancreas of non-tumor bearing *Fbln5*$^{-/-}$ mice as compared to *WT* [2]. This was a pivotal observation because it proved that the decrease in angiogenesis within tumors from *Fbln5*$^{-/-}$ mice was due to a characteristic unique to the TME. From this, we hypothesized that the loss of Fbln5 expression modified the TME in such a way that reduced endothelial cell survival. Consistent with this idea, we observed an increase in pericyte-associated blood vessels. Anti-angiogenic therapies control tumor growth by inhibiting the function of pro-angiogenic molecules thereby reducing the level of angiogenesis within the TME. It has been shown that this type of therapy 'prunes' the vascular tree leaving only stabilized pericyte-associated blood vessels [10]. Our data would suggest then that the loss of host Fbln5 creates an anti-angiogenic environment similar to that observed with anti-angiogenic therapy where only pericyte-associated blood vessels are able to survive.

Here, we describe results from the first tumor experiments performed in *Fbln5*$^{-/-}$ mice. This work provides valuable information pertaining to the effect of endogenous Fbln5 on tumor growth that has been lacking from the literature. We showed that in the absence of endogenous Fbln5, tumor angiogenesis is diminished and pancreatic tumor growth is impaired. These data indicated an uncharacterized function for Fbln5 that may shed further light on how matricellular proteins regulate ECM signaling. The rest of my work, therefore, is focused on deciphering the mechanism by which the loss of Fbln5 leads to decreased tumor angiogenesis and growth.

METHODS

Cell Culture

The murine pancreatic carcinoma cell line (Pan02) was purchased from the Developmental Therapeutics Program, Division of Cancer Treatment and Diagnosis, National Cancer Institute (Frederick, MD), and grown in Dulbecco's Modified Eagles Medium (DMEM; Invitrogen, Carlsbad, CA) supplemented with L-glutamine (2 mM), penicillin G (100 units/ml), streptomycin sulfate (100 μg/ml), and 5% fetal bovine serum (FBS) (Life Technologies, Grand Island, NY). The Pan02 cell line was tested (Impact III PCR profiles; MU Research Animal Diagnostic Laboratory, Columbia, MO) and was found to be pathogen-free. Generation of the Pan02HY cell line was performed by harvesting a subcutaneous Pan02 tumor from a WT littermate with a background identical to *Fbln5*$^{-/-}$ mice. The tumor was removed from the mouse and cleared of any residual skin and hair. It was immediately immersed in DMEM supplemented with 5% FBS and streptomycin sulfate to reduce contamination then minced with a sterile razor blade in a tissue culture dish. Tumor pieces were then forced through a wire mesh plate to generate a single cell suspension. Cells were resuspended in fresh DMEM and grown under normal cell conditions.

Mice

Fbln5$^{-/-}$ mice and *WT* littermates (C57B1/6 X 129/SvEv hybrid background) age 4-6 months old were used for tumor studies. The phenotype was identical to that previously described [11].

In vivo tumor growth

Pan02HY cells were injected subcutaneously or orthotopically into *WT* and *Fbln5*$^{-/-}$ mice. Cells were harvested from subconfluent cultures by treatment with 0.25%

trypsin and 5 mM EDTA in PBS. After trypsinization, the cells were washed once in serum-free medium. Cells were pelleted, washed with PBS, counted and resuspended in PBS. Only single-cell suspensions with greater than 90% viability (as determined by trypan blue exclusion) were used for injections.

For subcutaneous injection, Pan02HY cells ($3x10^6$/100 μl) were injected (27 gauge needle) into the shaved flank region of *WT* and *Fbln5*$^{-/-}$ mice [7]. After tumor cell injection, the mice were monitored for weight, signs of discomfort or morbidity, and tumor size. Tumor volume was measured weekly by the use of digital calipers. Tumor volume was calculated using the formula: $(D \times d)^2 \times \pi/6$ (D, largest diameter, d, perpendicular to D). Four weeks after tumor cell injection, mice were euthanized. Subcutaneous tumors were excised, weighed and the tumor samples were frozen in liquid nitrogen or fixed in methyl Carnoy's fixative for histological analysis.

Orthotopic tumor cell injection was performed by Dr. Korpanty and carried out as described previously [12]. Briefly, the mice were anesthetized with isoflurane that was maintained throughout the time of surgery. A small left abdominal incision was made and the spleen exposed to access the pancreas. Tumor cells ($5x10^5$/50 μl) in PBS were injected into the tail of the pancreas. A successful subcapsular intrapancreatic injection of tumor cells was identified by the appearance of a fluid bleb without intraperitoneal leakage. The animals tolerated the surgical procedure well, and no anesthesia-related deaths occurred. Four weeks after injection, mice were euthanized and the peritoneal cavity (including liver and spleen), inguinal and axillary regions, kidneys, thoracic cavity (including lungs and heart), and brain were screened for metastases by visual inspection under a dissecting microscope and then confirmed by histology. The entire pancreas containing the tumor lesion was harvested and weighed. Once

removed, tumors were either frozen in liquid nitrogen or fixed in methyl Carnoy's fixative for histological analysis.

At the time of sacrifice for both subcutaneous and orthotopic experiments, mice were euthanized and the lungs, liver, spleen, pancreas and kidneys were removed, weighed, frozen in liquid nitrogen and stored at -80° for further analysis. The blood was also collected from each animal and immediately mixed with herapin to prevent clotting. Blood samples were spun down for twenty minutes at 4°C and the top aqueous layer (serum) was removed and stored at -20°C for further analysis.

The tumor weights were recorded in Prism Graphpad and average tumor weights were calculated for comparison.

Immunohistochemistry

Immunohistochemistry was performed on frozen and fixed tissue sections. Methyl Carnoy's or formalin-fixed tissues were embedded in paraffin and sectioned by the Molecular Histopathology Laboratory at UT Southwestern Medical Center (Dallas, TX). Sections were stained with hematoxylin and eosin (H&E) and Masson's trichrome according to standard protocols. For immunohistochemistry on fixed tissues, tissues were deparaffinized in xylene followed by a graded series of ethanol exchanges and rehydrated in PBS containing 0.2% Tween (PBST). Frozen tissues were sectioned on a cryostat (10 μm) and air-dried overnight. Frozen sections were rehydrated in PBS for five minutes and fixed with acetone for five minutes prior to staining. Both frozen and fixed sections were incubated for one hour at room temperature with a protein-blocking solution consisting of 20% AquaBlock and DMEM (East Coast Biologics, Inc., North Berwick, ME). Sections were incubated with primary antibodies diluted in 1% BSA/PBS for either one hour at room temperature or overnight at 4°C. Primary antibodies used

were: rabbit anti-human fibronectin (F3648 Sigma Aldrich, St. Louis, MO), rabbit anti-mouse laminin (AHP420, Serotec, Raleigh, NC), rabbit anti-mouse Fbln5 (10 μg/ml) (BSYN1923) [13], rabbit anti-phosphorylated histone H3 (phospho-H3) (Upstate Biotechnology, Inc., Lake Placid, NY), rat anti-mouse endothelial cell marker, MECA-32 [14] (Developmental Studies Hybridoma Bank, University of Iowa, Iowa City, IA), rabbit anti- mouse smooth muscle actin (SMA) (RB-9010-P, LabVision, Fremont, CA). Sections were washed three times in PBST for five minutes each and incubated for one hour at room temperature with fluorophore-conjugated (fluorescein FITC or Cy3) secondary antibodies in 1% BSA/PBS (1:1000) (Jackson Immunoresearch, West Grove, PA) and then washed three times in PBST for five minutes each. Fluorescent sections were mounted with ProLong Gold antifade reagent with DAPI (Invitrogen). TUNEL staining was performed using DeadEnd™ Fluorometric TUNEL System (Promega, Madison, WI) according to the manufacturer protocol.

Quantification of immunohistochemistry

Tissue sections were analyzed with a Nikon Eclipse E600 microscope (Nikon, Lewisville, TX). Fluorescent images were captured with a Photometric Coolsnap HQ camera and MetaMorph software (Universal Imaging Corporation). Phospho-H3 and TUNEL staining were quantified by manually counting the number of positive cells in five random 400X fields per tumor section. Multiple fluorescent images per sample were captured under identical conditions (room temperature, exposure time, high and low limits, and scaling). The percentage of pixels exceeding the threshold value (background) was calculated automatically by the software (% average intensity). Mean blood vessel counts and area were measured either by blind hand counting or by using Metamorph's "Integrated Morphometry Analysis" tool. Pericyte-associated blood vessels were identified by the co-

localization of MECA-32 (green) and SMA [15]. Vessels positive for SMA appeared yellow and were measured by blind hand counting and taken as a percent of the total number of blood vessels present in each field of view.

REFERENCES

1. Beck AW, Luster TA, Miller AF, et al. Combination of a monoclonal anti-phosphatidylserine antibody with gemcitabine strongly inhibits the growth and metastasis of orthotopic pancreatic tumors in mice. Int J Cancer 2006;118(10):2639-43.
2. Sullivan KM, Bissonnette R, Yanagisawa H, Hussain SN, Davis EC. Fibulin-5 functions as an endogenous angiogenesis inhibitor. Lab Invest 2007;87(8):818-27.
3. Hall AP. Review of the pericyte during angiogenesis and its role in cancer and diabetic retinopathy. Toxicol Pathol 2006;34(6):763-75.
4. Kubota T. Metastatic models of human cancer xenografted in the nude mouse: the importance of orthotopic transplantation. J Cell Biochem 1994;56(1):4-8.
5. Hoffman RM. Orthotopic is orthodox: why are orthotopic-transplant metastatic models different from all other models? J Cell Biochem 1994;56(1):1-3.
6. Brekken RA, Puolakkainen P, Graves DC, Workman G, Lubkin SR, Sage EH. Enhanced growth of tumors in SPARC null mice is associated with changes in the ECM. J Clin Invest 2003;111(4):487-95.
7. Puolakkainen PA, Brekken RA, Muneer S, Sage EH. Enhanced growth of pancreatic tumors in SPARC-null mice is associated with decreased deposition of extracellular matrix and reduced tumor cell apoptosis. Mol Cancer Res 2004;2(4):215-24.
8. Lee MJ, Roy NK, Mogford JE, Schiemann WP, Mustoe TA. Fibulin-5 promotes wound healing in vivo. J Am Coll Surg 2004;199(3):403-10.
9. Albig AR, Schiemann WP. Fibulin-5 antagonizes vascular endothelial growth factor (VEGF) signaling and angiogenic sprouting by endothelial cells. DNA Cell Biol 2004;23(6):367-79.
10. Benjamin LE, Golijanin D, Itin A, Pode D, Keshet E. Selective ablation of immature blood vessels in established human tumors follows vascular endothelial growth factor withdrawal. J Clin Invest 1999;103(2):159-65.
11. Yanagisawa H, Davis EC, Starcher BC, et al. Fibulin-5 is an elastin-binding protein essential for elastic fibre development in vivo. Nature 2002;415(6868):168-71.
12. Arnold SA, Mira E, Muneer S, et al. Forced expression of MMP9 rescues the loss of angiogenesis and abrogates metastasis of pancreatic tumors triggered by the absence of host SPARC. Exp Biol Med (Maywood) 2008.
13. Zheng Q, Davis EC, Richardson JA, et al. Molecular analysis of fibulin-5 function during de novo synthesis of elastic fibers. Mol Cell Biol 2007;27(3):1083-95.

14. Hallmann R, Mayer DN, Berg EL, Broermann R, Butcher EC. Novel mouse endothelial cell surface marker is suppressed during differentiation of the blood brain barrier. Dev Dyn 1995;202(4):325-32.
15. Pou S, Pou WS, Bredt DS, Snyder SH, Rosen GM. Generation of superoxide by purified brain nitric oxide synthase. J Biol Chem 1992;267(34):24173-6.

CHAPTER 2. Exploring mechanisms responsible for decreased tumor angiogenesis and growth

INTRODUCTION

In the absence of Fbln5, tumors are unable to support an efficient blood vascular network and fail to thrive. Tumor survival depends largely on its ability to transform the host ECM into a microenvironment conducive to tumor angiogenesis and growth. Failure to achieve this can result in tumor regression. Our studies indicate that Fbln5 is critical for this transformation and its absence leads to the creation of a microenvironment detrimental to tumor angiogenesis. In an attempt to uncover the exact mechanism(s) by which this occurs, we evaluated specific characteristics of the TME that when altered have been shown to curtail tumor growth and angiogenesis and identified two distinct relevant alterations in tumors from *Fbln5*$^{-/-}$ mice. First, we observed an increase in the expression of MMP-2 and -9. Matrix metalloproteinases (MMPs) are a family of proteolytic enzymes that are secreted by tumor cells and assist in tumor cell invasion by degrading ECM proteins.[1] Although the loss of MMP expression and the synthetic inhibition of MMP activity suppress tumor growth and metastasis, an increase in MMP expression can also suppress tumor growth by indirectly inhibiting angigogenesis.[2-4] For example, cleavage of type IV and type XVIII collagen by MMP-9 releases hidden protein fragments with anti-angiogenic properties such as α3NC1 and endostatin respectively.[5] In a relevant study[6], researchers showed that tumor angiogenesis and growth is attenuated in integrin $\alpha_1$knockout mice due to enhanced expression of MMP-9. In these mice, increased expression of MMP-9 led to elevated levels of the anti-angiogenic peptide angiostatin, a cleavage product of plasminogen.[6] These studies underlie the rationale for further investigating the effect of increased MMP expression in our system.

Secondly, we observed an increase in the level of reactive oxygen species (ROS) within tumors from *Fbln5*$^{-/-}$ mice compared to tumors from *WT* mice. ROS including superoxide radicals ($O_2^{\cdot-}$) and hydrogen peroxide (H_2O_2) are highly reactive molecules produced commonly as by-products of aerobic respiration and the mitochondrial transport chain. ROS were identified originally as host defense molecules produced by neutrophils via NAD(P)H oxidase. However, ROS is now appreciated more for their function as messenger molecules involved in redox signaling. Redox signaling is responsible for the initiation of multiple biological processes in normal cells including angiogenesis.[7] For instance, ROS have been shown to activate pathways such as proliferation, cell adhesion, motility and invasion in endothelial cells. Endothelial cells treated with H_2O_2 produced higher levels of VEGF thereby increasing their proliferation and migration.[8] Furthermore, ROS have been shown to be critical for angiogenesis *in vivo*. For example, neovascularization in response to hindlimb ischemia was impaired significantly in mice lacking gp91phox, a critical component of NAD(P)H oxidases.[9] Although, ROS can be beneficial to cells, high levels result in oxidative stress. Oxidative stress is caused by an imbalance between the production of ROS and a biological system's ability to detoxify the environment. Oxidative stress impairs protein synthesis by oxidizing amino acids, causes deleterious DNA mutations by the oxidation of nucleic acids and ultimately results in apoptosis. To prevent the chronic buildup of ROS, enzymes such as superoxide dismutase (SOD) 1, 2 and 3 and catalases are produced to assist in the breakdown and clearance of ROS and their intermediates from tissues.[7] Endothelial cells, in particular, are sensitive to the level of ROS, and it has been shown that chronic exposure can result in endothelial cell dysfunction and death.[10] Therefore, oxidative stress has been implicated in the development of cardiovascular disease including hypertension and atherosclerosis.[11, 12]

The function of ROS in the pathology of cancer has been under

investigation for decades. Free radicals have been reported to initiate tumor formation by damaging DNA generating cancer-causing mutations.[13] Moreover, ROS can be beneficial to the growing tumor by stimulating tumor cell invasion and angiogenesis.[14] Therefore, antioxidants have been evaluated for cancer prevention and cancer treatment. However, early clinical trials have been unsuccessful and have reported that in some populations antioxidant therapy can result in increased carcinoma risk.[15, 16] On the other hand, an alternative approach to anti-tumor therapy called "oxidation therapy" is proving to be an effective method for controlling tumor growth and spread. Oxidation therapy is designed to increase oxidative stress within tumors and induce ROS-dependent apoptosis of tumors cells either by directly increasing ROS production or by preventing the clearance of ROS by inhibiting antioxidant enzymes. Currently, some of our most effective chemotherapies including cisplatin, mitomycin C and doxorubicin yield anti-cancer effects through this mechanism.[17, 18] In addition, promising reports have shown that enhancing oxidative stress specifically on endothelial cells can control tumor growth and spread by inhibiting angiogenesis.[19] These results suggest a possible explanation for the decreased angiogenesis we observed in *Fbln5*$^{-/-}$ mice.

RESULTS

PART I

Determining the significance of augmented MMP expression

We observed a decrease in tumor angiogenesis and growth in *Fbln5*$^{-/-}$ mice. To delineate the mechanism(s) involved in this tumor phenotype, we evaluated the expression of MMPs in tumors from *Fbln5*$^{-/-}$ and *WT* mice. Initially, expression of MMP-2 and -9 were examined by quantitative PCR (qPCR)

using cDNA generated from mRNA extracted from tumors from *Fbln5*$^{-/-}$ and *WT* mice. MMP-2 and -9 transcripts were increased in tumors from *Fbln5*$^{-/-}$ compared to *WT* mice **(Figure 2.1A).** To confirm our findings, expression was evaluated by immunohistochemistry, and results indicated a significant increase in the expression of both MMP-2 and -9 along with membrane type-1 MMP (MT1-MMP, MMP-14) within the TME of tumors from *Fbln5*$^{-/-}$ compared to *WT* mice (**Figure 2.1B**). Although an increase in expression was observed, we did not detect any differences in the pattern of expression. Similar to tumors from *WT*

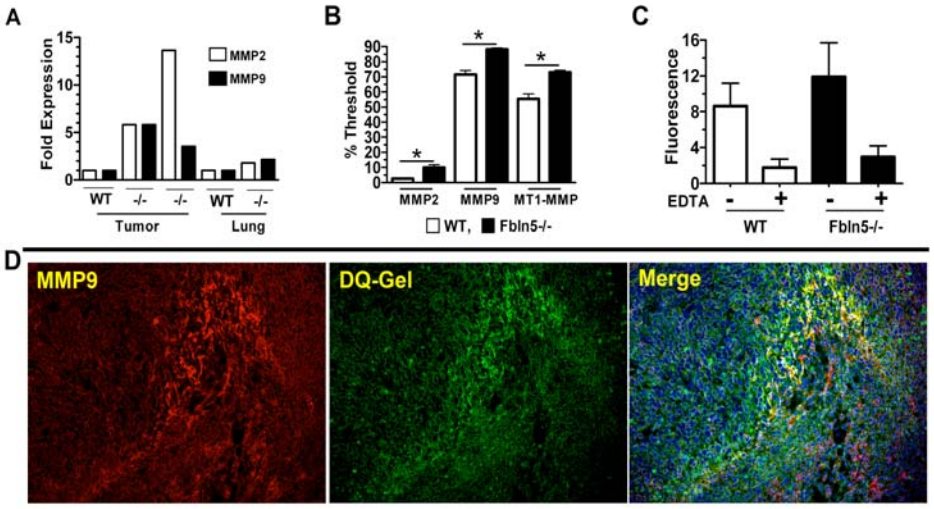

Figure 2.1 Increased MMP expression and activity in tumors from *Fbln5*$^{-/-}$ mice. A) qPCR analysis of MMP-2 and-9 expression using mRNA extracted from tumors from *WT* and *Fbln5*$^{-/-}$ (n=2). Levels were normalized to the Tbp housekeeping gene and to *WT* levels. B) Pan02 tumor sections were stained with antibodies specific for MMP-2, MMP-9, and MT1-MMP and developed with fluorescently labeled secondary antibodies. Fluorescence was quantified using Metamorph software and is presented as percent pixels reaching a threshold value (% threshold). The threshold was set using a negative control primary antibody with subsequent development with the appropriate secondary antibody. *, $p<0.001$ C) MMP activity in fresh frozen sections of tumors harvested from *WT* or *Fbln5*$^{-/-}$ mice was determined by *in situ* zymography. Mean fluorescence from the cleavage of the MMP substrate DQ-gelatin in the presence or absence of EDTA, a MMP inhibitor is displayed. D) Immunohistochemistry for MMP-9 (red) on tumor sections prior to incubation with DQ-gelatin (DQ-gel, green) revealed colocalization of expression with activity. Representative pictures from a Pan02 tumor grown in a *Fbln5*$^{-/-}$ animal is shown. Total magnification, 200X.

animals, expression in tumors from *Fbln5*$^{-/-}$ mice was diffuse throughout the tumor and not localized to specific compartments of the tumor. For example, expression was not localized to the tumor border, which would indicate host expression.

We next set out to determine if the increase in expression culminated in an increase in activity. We performed *in vivo* activity assays, which allowed us to quantitatively measure the level of MMP activity within tissues. Fresh, frozen tumor sections from both *Fbln5*$^{-/-}$ and *WT* mice were treated with a modified MMP substrate, DQ-gelatin. Cleavage of DQ-gelatin by MMPs present within the tumor produced a fluorescent signal that could be reduced by treatment with the calcium-chelator EDTA, a known inhibitor of MMP activity. To further confirm that the fluorescent signal represented MMP activity, we modified the assay by performing immunohistochemistry for MMP-9 prior to the addition of the substrate. We found that the fluorescent signal generated by the cleavage of DQ-gelatin overlayed with areas positive for MMP expression confirming that the signal represented MMP activity. Although we observed a minor increase in MMP activity in tumors from *Fbln5*$^{-/-}$ mice, the increase did not reach statistical significance (**Figure 2.1C**,**D**). These results were recapitulated in *in vitro* experiments where tumor lysates were added to 96-well plates pre-coated with DQ-gelatin. Fluorescent signal measured by a plate reader showed that tumors from *Fbln5*$^{-/-}$ mice did not contain a significant increase in MMP activity compared to tumors from *WT* mice (data not shown). Therefore, we concluded from these experiments that the increase in MMP expression did not correlate with an increase in activity. The reason for this has not been further evaluated but it could be do to an increase in expression of endogenous MMP inhibitors such as the tissue inhibitor of metalloproteinases (TIMPs) family of proteins. TIMP expression needs to be evaluated to investigate this possibility.

Although we did not observe a significant increase in MMP activity in our studies, we continued to investigate the possibility that increased MMPs were affecting tumor angiogenesis in *Fbln5*$^{-/-}$ mice by increasing the level of anti-angiogenic peptides such as α3NC1. Inhibition of angiogenesis by MMPs is mediated through the specific processing of ECM proteins, which result in the generation of anti-angiogenic peptides. In particular, MMP-9 removes the NC1 domain from the α3 chain of Type IV collagen generating a short peptide termed α3NC1 (tumstatin).[20] α3NC1 functions as a powerful angiogenic inhibitor by binding to the vascular integrin $\alpha_v\beta_3$ and inhibiting downstream phosphorylation of focal adhesion kinase (FAK) and PI3-kinase, pathways required for inducing endothelial cell proliferation and migration.[21] Mice deficient in MMP-9 have decreased levels of circulating α3NC1 and increased tumor growth. Treatment with α3NC1 inhibited angiogenesis and reduced tumor growth confirming its relationship to MMP-9 and its anti-tumor effects.[22] Given these reports, we hypothesized that the increased MMP-9 expression observed in tumors from *Fbln5*$^{-/-}$ mice caused an increase in α3NC1 levels resulting in decreased tumor angiogenesis. α3NC1 levels were evaluated in tumor lysates and serum from *Fbln5*$^{-/-}$ and *WT* mice by use of a mouse anti-α3NC1 antibody. **Figure 2.2** shows Western blot results of α3NC1 levels from tumor lysates normalized to the loading control β-actin. α3NC1 levels varied among

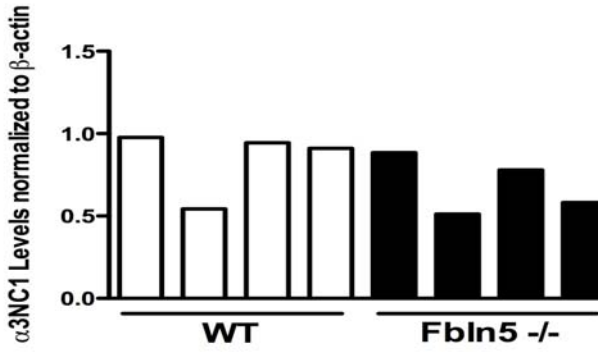

Figure 2.2 Western blot analysis of α3NC1 levels in tumors from WT and *Fbln5*$^{-/-}$ mice. Tumor lysates were ran on an SDS page gel and probed for α3NC1 and β-actin as a loading control. Levels were normalized to β-actin using ImageJ.

tumors but were not increased in tumors from *Fbln5*$^{-/-}$ mice compared to tumors from *WT* animals. Similar results were seen in the serum. These data suggested that although MMP-9 expression was increased, it was not increasing the level of α3NC1 indicating that α3NC1 was not contributing to the decreased angiogenesis observed in tumors from *Fbln5*$^{-/-}$ mice.

Treatment with an MMP inhibitor increases tumor growth in *Fbln5*$^{-/-}$ mice

To further determine if MMPs were affecting tumor growth in *Fbln5*$^{-/-}$ mice, we performed tumor experiments in the presence of Doxyclycline (DOX), a non-specific MMP inhibitor.[23] Pan02HY cells were subcutaneously injected into *Fbln5*$^{-/-}$ and *WT* mice and DOX was administered in the drinking water for the entire length of the experiment. After four weeks, mice were sacrificed and tumors harvested and weighed. As seen previously, tumors in *Fbln5*$^{-/-}$ mice grew slower than tumors in *WT* mice, however, tumor growth in *Fbln5*$^{-/-}$ mice given DOX increased to near *WT* levels (**Figure 2.3A**). We next analyzed angiogenesis in tumors from *Fbln5*$^{-/-}$ mice treated with DOX. Angiogenesis was decreased in tumors from *Fbln5*$^{-/-}$ mice compared to tumors from *WT* mice, but treatment with DOX augmented tumor angiogenesis in *Fbln5*$^{-/-}$ mice (**Figure 2.3B**).

Doxycyline protects endothelial cells from ROS-induced cell death

We have shown above that treatment with DOX can increase tumor angiogenesis and growth in *Fbln5*$^{-/-}$ mice. This data would suggest that the effect of DOX on tumor growth was directly related to its function as an MMP inhibitor, however, because we did not see a significant increase in MMP activity in tumors from *Fbln5*$^{-/-}$ mice we began to speculate that the effect observed by DOX treatment was mediated through a different property of DOX. DOX is a member of the tetracycline antibiotics group commonly used to treat a variety

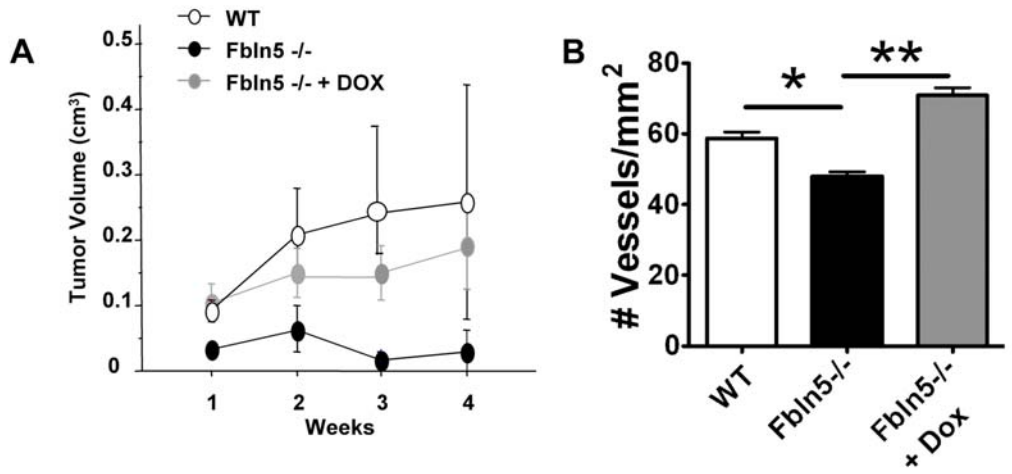

Figure 2.3 DOX increases tumor angiogenesis and growth in *Fbln5*$^{-/-}$ mice. A) Pan02 cells were injected subcutaneously into *WT* (n=12) and *Fbln5*$^{-/-}$ mice (n=16). Doxycycline (0.4 mg/ml) was added to the drinking water of tumor-bearing *WT* (n=4, data not shown) and *Fbln5*$^{-/-}$ (n=9) and tumor volume was monitored. B) Sections of tumors from untreated and doxycycline-treated *WT* and *Fbln5*$^{-/-}$ mice were stained with MECA-32 to determine microvessel density. The number of blood vessels/mm^2 is displayed. Ten pictures (total magnification, 200x) taken of each tumor from *WT* (n=5), *Fbln5*$^{-/-}$ (n=3), and *Fbln5*$^{-/-}$ + DOX (n=3) animals were used for analysis. The results shown are mean +/- SEM. *, p<0.01; **, P<0.001

of infections. Tetracyclines, including DOX, contain antioxidant properties, which aid in their ability to fight infections. [24, 25] Given this knowledge and our observation that ROS levels were increased in tumors from *Fbln5*$^{-/-}$ mice (data discussed in the following section), we speculated that perhaps DOX was acting as an antioxidant in our system. To investigate this further, we first wanted to test the ability of DOX to function as an antioxidant. We performed an *in vitro* cell viability assay and showed that DOX protected endothelial cells from apoptosis brought on by oxidative stress. Murine endothelial cells (bEnd.3) were plated in 96-well plates and treated with the ROS-generating compound paraquat. Treatment with paraquat alone resulted in significant cell death at the 72 hr time point. Co-treatment with DOX partially rescued cell viability (**Figure 2.4**). These results support the antioxidant activity of DOX and turned our focus onto ROS.

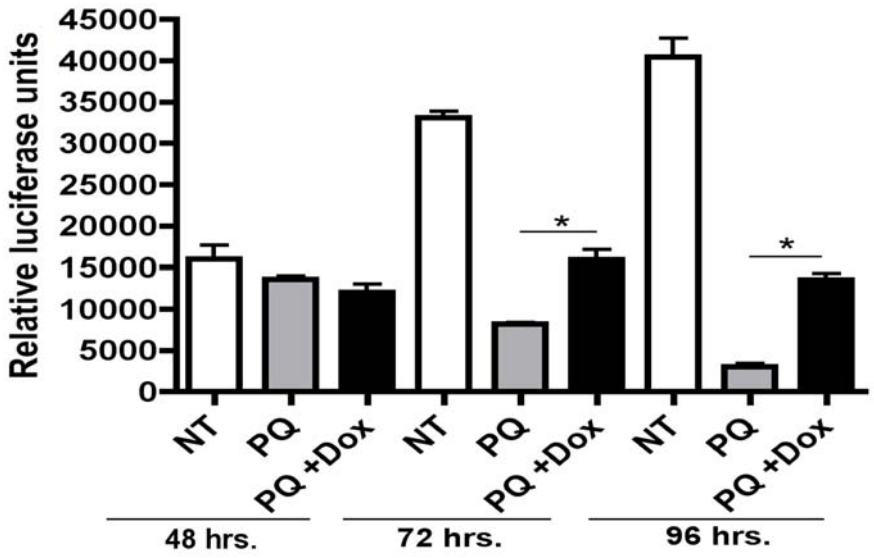

Figure 2.4 DOX protects endothelial cells from ROS-induced cell death. bEnd.3 cells were plated in 96-well plates and treated with paraquat (0.1 mM) in the presence (black bars) or absence doxycycline (gray bars) (Dox, 0.01 mM). Cell viability was determined using a Cell TiterGlo kit 48, 72 and 96 hours after treatment was initiated. The assay was done with three wells per treatment. The results shown are mean +/- SEM. *, $p<0.05$

Part II

Determining the significance of increased ROS

A second potential mechanism responsible for the tumor phenotype in *Fbln5*$^{-/-}$ mice is an alteration in ROS levels. Recently, Nguyen *et al*. [26] reported that Fbln5 interacts with SOD3, a protein involved in the breakdown of superoxides, a commonly occurring ROS. SOD3 is localized to blood vessels were it monitors the level of ROS in the vascular microenvironment to protect endothelial cells from toxic buildup.[27] Fbln5 facilitates the localization of SOD3 to endothelial cells via Fbln5's interaction with integrins such as $\alpha_v\beta_3$. Examination of aortas from *Fbln5*$^{-/-}$ mice revealed an absence of SOD3 expression and a subsequent increase in the level of ROS.[26] Chronic exposure of

ROS to endothelial cells is detrimental and results in apoptosis due to the oxidation and inactivation of essential proteins.[10] Given this finding, we hypothesized that ROS levels would also be increased in tumors from *Fbln5*$^{-/-}$

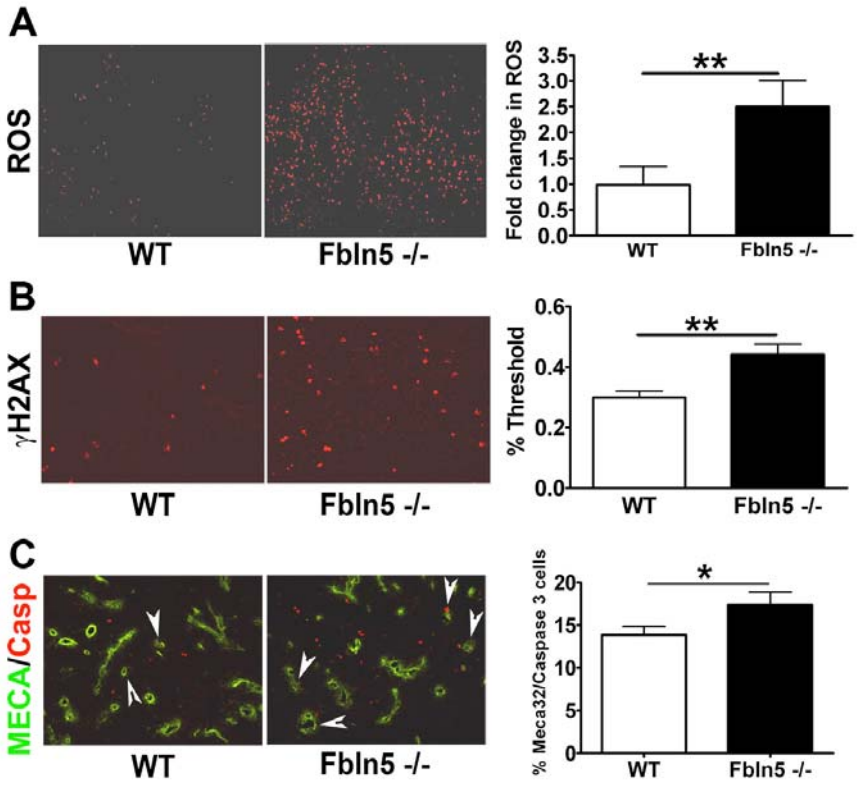

Figure 2.5 Oxidative stress is elevated in tumors grown in *Fbln5*$^{-/-}$ mice. A) Fresh frozen sections of subcutaneous Pan02 tumors from *WT* (n=3) and *Fbln5*$^{-/-}$ (n=3) animals were incubated with dihydroethidium (DHE) for i*n situ* detection of reactive oxygen species (ROS). The resulting DHE-mediated fluorescence was quantified by Metamorph software. A representative image from tumors grown in *WT* and *Fbln5*$^{-/-}$ animals is shown. The results shown are the mean fluorescence intensity (+/- s.e.m.) from at least 5 200x fields from each tumor. B) The presence of DNA damage in frozen sections of subcutaneous Pan02 tumors from *WT* (n=5) and *Fbln5*$^{-/-}$ (n=7) animals was detected by immunohistochemistry with an antibody specific for γH2AX followed by development with a fluorescently-conjugated secondary antibody. A representative image from tumors grown in *WT* and *Fbln5*$^{-/-}$ animals is shown. The results shown are the mean fluorescence intensity (+/- s.e.m.) from at least 5 400x fields from each tumor stained. C) Pan02 tumors from *WT* (n=3) and *Fbln5*$^{-/-}$ (n=3) mice were sectioned and stained with MECA-32 (green) for blood vessel identification and co-localized with anti-cleaved caspase 3 antibody (red) to determine apoptotic endothelial cells. The total number of dying endothelial cells was determined by hand counting and graphed as a percentage of the total number of apoptotic cells. Arrow heads indicate double positive cells. Ten pictures were taken from each tumor section (total magnification, 200x) for analysis. Results shown are +/- s.e.m. *, $p<0.05$; **, $p<0.01$.

mice. We analyzed the level of ROS within fresh, frozen tumor sections by dihydroethidium (DHE) staining. DHE is sequestered in the cytoplasm of cells until its oxidation by ROS, in particular superoxides, where it then intercalates within DNA staining the nucleus a bright fluorescent red. The level of fluorescence directly relates to the level of ROS present within the tissue. Our analysis revealed a significant increase in the level of ROS within tumors from *Fbln5*$^{-/-}$ mice compared to tumors from *WT* mice suggesting a function for Fbln5 in the control of ROS production (**Figure 2.5A**).

A common characteristic of cancer is a persistent state of high oxidative stress within the TME due to the high metabolic rate of tumor cells and the influx of macrophages and neutrophils, which produce ROS as part of the immune response.[28] Knowing this, we hypothesized that the additional increase in ROS due to the loss of Fbln5 would lead to a state of chronic oxidative stress within the tumor microenvironment. Chronic oxidative stress would result in more oxidative damage, therefore, we analyzed the levels of phosphorylated histone H2A (γH2AX), a well-described marker of oxidative damage.[29] Correlating with the increase in ROS, we observed a significant increase in the level of γH2AX in tumors grown in *Fbln5*$^{-/-}$ mice compared to tumors from *WT* mice (**Figure 2.5B**). Low levels of ROS are well tolerated by endothelial cells, however, chronic oxidative stress induces endothelial cell dysfunction and death.[30] To determine if elevated production of ROS in tumors from *Fbln5*$^{-/-}$ mice affected endothelial cell survival, we examined the amount of endothelial cell death in tumors from *WT* and *Fbln5*$^{-/-}$ animals by colocalization of cleaved caspase 3, a marker for apoptosis. We observed a significant increase in the number of apoptotic endothelial cells in tumors from *Fbln5*$^{-/-}$ mice compared to *WT* animals (**Figure 2.5C**). We, therefore, proposed that the decrease in blood vessel density observed

in tumors from *Fbln5*$^{-/-}$ mice was due in part to increased endothelial cell apoptosis caused by oxidative stress and damage.

Loss of Fbln5 does not result in decreased SOD3 expression

We next investigated the involvement of SOD3 in the buildup of ROS within tumors from *Fbln5*$^{-/-}$ mice. We hypothesized that the decrease in angiogenesis was the result of the deleterious buildup of ROS within endothelial cells due to the loss of SOD3 expression. To support our hypothesis, we first evaluated the level of SOD3 within tumor lysates and serum from tumor-bearing mice since SOD3 levels were shown to accumulate in the blood of *Fbln5*$^{-/-}$ mice by western blot.[26] Our analysis revealed no change in SOD3 levels between *Fbln5*$^{-/-}$ and *WT* mice (data not shown). Endothelial cell survival is dependent on the localization of SOD3 to the blood vessel wall to protect against ROS buildup, therefore, we determined if SOD3 localization to blood vessels was altered in

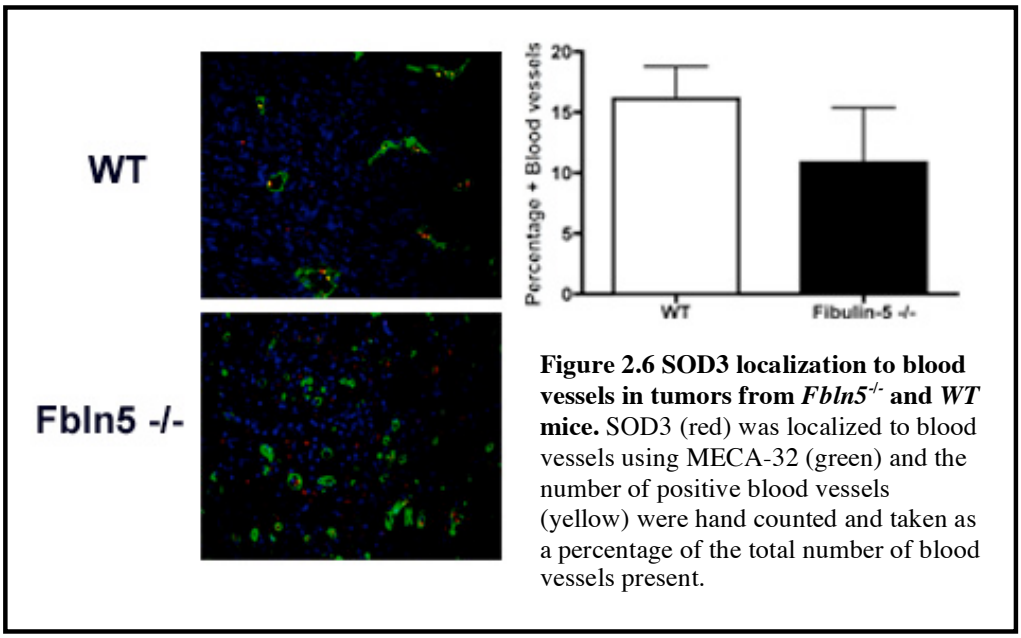

Figure 2.6 SOD3 localization to blood vessels in tumors from *Fbln5*$^{-/-}$ and *WT* mice. SOD3 (red) was localized to blood vessels using MECA-32 (green) and the number of positive blood vessels (yellow) were hand counted and taken as a percentage of the total number of blood vessels present.

tumors from *Fbln5*$^{-/-}$ mice. Tumors were stained with an anti-SOD3 antibody and colocalized to blood vessels using MECA-32. The number of SOD3-positive blood vessels in tumors from *Fbln5*$^{-/-}$ mice was hand counted and compared to tumors from *WT* mice. Our results indicated a modest reduction in the localization of SOD3 to blood vessels in tumors from *Fbln5*$^{-/-}$ mice compared to tumors from *WT* mice **(Figure 2.6).** However, in collaboration with Dr. Tohru Fukai's laboratory at the University of Illinois in Chicago, we analyzed SOD3 activity in tumors from *Fbln5*$^{-/-}$ mice and were unable to detect a decrease in activity compared to tumors from *WT* mice (data not shown). In fact, tumors from *Fbln5*$^{-/-}$ mice contained an increase in SOD3 activity, an effect commonly observed as a result of increased ROS levels. Taken together, these results suggested that the accumulation of ROS was not due to the loss of SOD3 expression and/or activity.

DISCUSSION

In an effort to understand the molecular mechanisms behind the decreased tumor angiogenesis and growth in *Fbln5*$^{-/-}$ mice, we pursued two distinct modifications of the TME identified in tumors from *Fbln5*$^{-/-}$ mice, increased MMP expression and increased ROS levels.

Increased MMP expression does not contribute to tumor phenotype

We observed an increase in the expression of MMP-2, MMP-9 and MT1-MMP in tumors from *Fbln5*$^{-/-}$ mice. However, we did not observe a significant increase in MMP activity. In addition, we did not observe increased levels of α3NC1, an anti-angiogenic peptide generated by the cleavage of Type IV collagen by MMP-9, further indicating that MMP activity is not increased in tumors from *Fbln5*$^{-/-}$ mice.

Our DOX data would suggest that MMP activity was contributing to the tumor phenotype in *Fbln5*$^{-/-}$ mice, however we were unable to examine DOX

tumor tissue for MMP activity therefore we can not say for sure that DOX had its effect on tumor growth by inhibiting MMP activity. In addition, we showed that DOX also functions as an antioxidant and can protect endothelial cells from ROS-induced cell death. Given this information and the fact that we did not see increased MMP activity in tumors from *Fbln5*$^{-/-}$ mice, I speculate that, in our system, the effects of DOX was mediated through its antioxidant properties. These results along with data described later provide further support that increased ROS levels are the major antagonist to tumor angiogenesis and growth in *Fbln5*$^{-/-}$ mice.

Elevated ROS levels caused increased oxidative damage in endothelial cell death

We observed an increase in ROS within tumors from *Fbln5*$^{-/-}$ mice compared to tumors from *WT* mice. Fbln5 was shown to aid in the clearance of ROS by assisting in the localization of SOD3 to blood vessels.[26] Loss of Fbln5 expression elevated ROS levels within aortas of *Fbln5*$^{-/-}$ mice due to the loss of SOD3 expression. [26] However, analysis of SOD3 within tumors from *Fbln5*$^{-/-}$ mice showed that expression and activity were unaffected by the loss of Fbln5. Although, we detected a modest decrease in SOD3 binding to the vasculature, a majority of SOD3 was still localized to vessels. Studies in the aortas of *Fbln5*$^{-/-}$ mice suggest that Fbln5 is the predominant binding partner responsible for anchoring SOD3 to blood vessels however, SOD3 also binds to heparan sulfate proteoglycans (HSPG) expressed on endothelial cell surfaces.[27] The continued expression of SOD3 on the vasculature in the absence of Fbln5 could, therefore, be mediated through HSPG binding. It is possible that tumor cells secrete increased levels of HSPG to promote SOD3 binding in order to control the level of ROS within tumors. This possibility has not been examined but could be determined by examining HSPG expression within tumors and by tumor cells *in*

vitro. Interestingly, we observed an increase in SOD3 activity within tumors from *Fbln5*$^{-/-}$ mice. SOD3 expression is directly related to the level of ROS within tissues and an increase in ROS results in increased levels of SOD3.[27] Therefore, our observation provides further evidence that ROS levels are increased in tumors from *Fbln5*$^{-/-}$ mice.

Our results suggested that SOD3 is not involved in the augmented ROS level and therefore indicates a novel function for Fbln5 in the mediation of ROS production. At physiological levels, ROS promote angiogenesis therefore it is possible that Fbln5 exerts its negative effects on angiogenesis by inhibiting ROS production. The exact mechanism by which Fbln5 inhibits angiogenesis is unknown, but it has been shown that expression of Fbln5 decreases VEGF expression.[14, 31] Interestingly, endothelial cells treated with H_2O_2 produce higher levels of VEGF indicating that ROS promotes angiogenesis, in part, by augmenting VEGF expression.[14] Taken together, one can hypothesize that Fbln5 affects VEGF expression by inhibiting ROS production within endothelial cells. This hypothesis has yet to be validated, but could be determined by reducing the expression of Fbln5 within endothelial cells and determining the effect of VEGF expression with or without antioxidant treatment.

It has also been shown that ROS stimulate expression of MMPs including MMP-2 and -9.[7] Given our data on MMP expression within tumors from *Fbln5*$^{-/-}$ mice, it is reasonable to speculate that the increased level of ROS is responsible for the increase in MMP expression. Preliminary data from Hiromi Yanagisawa's laboratory have shown that *Fbln5*$^{-/-}$ MEFs have increased MMP activity, which can be inhibited by anti-oxidant treatment indicating that Fbln5 functions to control MMP expression by inhibiting ROS generation. To our knowledge, this is the first mechanism described for how Fbln5 regulates MMP expression.

If Fbln5 inhibits angiogenesis by minimizing ROS production, one would expect the loss of Fbln5 *in vivo* to lead to the generation of a pro-angiogenic

environment within tissues. Consistent with other reports, we found this to be true in normal, non-pathological tissues in *Fbln5*$^{-/-}$ mice where an increase in vessel sprouting was observed, however the effect on the TME is much different.[32] Unlike normal tissues, tumors exist in a state of high oxidative stress and we show that the further increase in ROS due to the loss of Fbln5 expression resulted in enhanced oxidative damage within the TME therefore creating an unfavorable environment for angiogenesis. This was confirmed by the observation that endothelial cell death is increased in tumors from *Fbln5*$^{-/-}$ mice compared to tumors from *WT* mice. These data indicate that the effect on angiogenesis due to loss of Fbln5 is entirely context-dependent and is determined by the oxidation state of the surrounding environment.

The results described above indicate a novel function for Fbln5 in controlling ROS production, which when disrupted can negatively impact tumor angiogenesis and growth. These results introduce a potential approach to anti-cancer therapy by which Fbln5 is targeted to modify the oxidative environment within a tumor.

METHODS

qPCR

For analysis of MMP-2 and MMP-9 expression, frozen tumor samples from *WT* and *Fbln5*$^{-/-}$ mice were homogenized in Trizol (Invitrogen, Carlsbad, CA), RNA was purified using RNeasy Mini Kit (Qiagen, Valencia, CA), and 3 μg of RNA was used to generate cDNA using the First Strand cDNA Synthesis Kit (Roche, Indianapolis, IN) as recommended by the manufacturer's protocol. Real Time qPCR was performed using TaqMan Gene Expression Assay (Applied Biosystems, Foster City, CA) and FastStart TaqMan probe (Roche). Primers for MMP-2 and MMP-9 were generated using the Applied Biosystems program. The

assay was performed on a Chromo4™ Four-color Real-Time system (BioRad, Hercules, CA). TATA binding protein (Tbp) was used as a housekeeping gene.

Immunohistochemistry

Examination of MMP-2, MMP-9 and MT1-MMP was performed on tumors fixed in Methyl Carnoy's, embedded in paraffin and sectioned by the Molecular Histopathology Laboratory at UT Southwestern Medical Center (Dallas TX). Fixed tissues were deparaffinized in xylene followed by a graded series of ethanol exchanges and rehydrated in PBS containing 0.2% Tween (PBST). For sections developed with diaminobenzidine (DAB) (Research Genetics, Huntsville, AL), the samples were incubated with a 3% H_2O_2 in methanol solution for thirty minutes at room temperature to block endogenous peroxidases. Sections were washed three times with PBST and incubated for thirty minutes at room temperature in a protein-blocking solution consisting of 20% AquaBlock and DMEM (East Coast Biologics, Inc., North Berwick, ME). Primary antibodies rabbit anti-mouse MMP2 and MMP9 (Chemicon, Temecula, CA) were diluted in blocking solution (15 μg/ml) and applied to the sections overnight at 4^0C. Sections were rinsed in PBST three times for five minutes each then incubated with peroxidase-conjugated secondary antibody for one hour at room temperature. Tissue sections were washed again in PBST three times for five minutes each and incubated with stable DAB for five minutes, counterstained with Meyer's Hematoxylin solution for three minutes, and mounted in Permount (Fisher Scientific, Pittsburgh, PA).

Frozen tumors were sectioned on a cryostat (10 μm) and air-dried overnight. Sections were rehydrated in PBS for five minutes, fixed with acetone for five minutes and incubated for one hour at room temperature with a protein-blocking solution consisting of 20% AquaBlock and DMEM. Sections were

incubated with primary antibodies diluted in 1% BSA/PBS for either one hour at room temperature or overnight at 4°. Primary antibodies used were goat anti-mouse SOD3 (1:50) (Santa Cruz, Santa Cruz, CA), rat anti-mouse MECA-32 (10 μg/ml), rabbit anti-mouse γH2AX (1:250) (NB100-2280, Novus Biologicals, Littleton, CO), rabbit anti-active caspase 3 (1:100) (AB3623, Millipore, Billerica, MA). Sections were washed three times in PBST for five minutes each and incubated for one hour at room temperature with fluorophore-conjugated (fluorescein FITC or Cy3) secondary antibodies in 1% BSA/PBS (1:1000) (Jackson Immunoresearch, West Grove, PA) and then washed three times in PBST for five minutes each. Fluorescent sections were mounted with ProLong Gold antifade reagent with DAPI (Invitrogen).

Quantification of Immunohistochemistry

Tissue sections were analyzed with a Nikon Eclipse E600 microscope (Nikon, Lewisville, TX). Fluorescent images were captured with a Photometric Coolsnap HQ camera and either Metamorph or Elements Imaging software. Multiple fluorescent images per sample were captured under identical conditions (room temperature, exposure time, high and low limits, and scaling). MMP expression and γH2AX levels were measured as the % average intensity which was obtained by taking the percentage of pixels exceeding the threshold value (background) calculated automatically by the software. Blood vessel density was obtained by hand counting by a blinded observer. The percentage of SOD3 localized to blood vessels was obtained by colocalizing MECA-32 staining with SOD3 staining (via the software) and hand counting the number of blood vessels positive for SOD3 staining and dividing that number by the total number of vessels. The percentage of caspase 3 positive endothelial cells were obtained in a similar way by hand

counting the number of MECA-32 positive/ Caspase 3 positive cells and dividing that by the total number of caspase 3 positive cells.

***In vivo* DQ gelatin assay**

To analyze the level of MMP activity in tumors from *WT* and *Fbln5*$^{-/-}$ mice, we performed in situ assays using DQ gelatin (Molecular Probes, Eugene, OR). Immunohistochemistry was first performed on frozen tumor sections as described above with the exception of the fixation step to identify MMP9 localization. After the final washing step, DQ gelatin (1 mg/ml) was diluted 1:10 in PBS and 50 μl was added to the top of each tumor section. For nuclei detection, Hoechst was adding to the DQ/PBS mix at 1 μg/ml. A cover slip was added to the top of each slide and slides were incubated for one hour at room temperature. As control, samples were incubated with EDTA (10 mM/PBS), an MMP inhibitor, for twenty minutes prior to the addition of DQ gelatin.

Western blot analysis

To evaluate α3NC1 levels, tumor lysates were obtained by homogenizing frozen tumors of equal weights in lysis buffer (50mM Tris, pH7.5, NaCl, 0.5M EDTA, pH 8.0, Triton X -100) supplemented with protease inhibitors (Complete Mini tablets, Roche). Equal amounts of each sample were diluted in laemmli sample buffer (Bio-Rad, Hercules, CA) with β -mercaptoethanol (BME) (Sigma-Aldrich, St. Louis, MO). 30 μl were ran on a 7.5% SDS-page gel and transferred to a nitrocellulose membrane. Membranes were blocked in 5% milk/TBST for one hour at room temperature. Membranes were incubated with primary antibodies diluted in 0.1% milk/TBST for either one hour at room temperature or overnight at 4°. Membranes were washed three times in TBST for five minutes each and incubated with HRP-conjugated secondary antibodies diluted in 0.1% milk/TBST

(1:50000). Membranes were again washed three times in TBST for five minutes each and developed using SuperSignal West Dura Extended Duration Substrate (Pierce, Rockford, IL). The primary antibodies used to detect α3NC1 were a generous gift from Dr. Dorin-Bogdan Borza at Vanderbilt and were mouse anti-mouse α3NC1 (8D1) and rat anti-mouse α3NC1 (H31) and rabbit anti-mouse β-actin (A2066, Sigma-Aldrich). To avoid detecting endogenous mouse antibodies with 8D1, we used an mouse TrueBlot™ HRP-conjugated secondary (eBioscience, San Diego, CA) designed not to detect endogenous antibodies.

DOX tumor studies

Subcutaneous tumor experiments in the presence of DOX were performed as previously described (see methods chapter 1). Pan02HY cells ($3x10^6$/100 μl) were injected into the flank region of *WT* and *Fbln5*$^{-/-}$ mice. After injection, the mice were monitored for weight, signs of discomfort or morbidity, and tumor size. Four weeks after injection, mice were euthanized and tumors were excised and weighed. Tumors were frozen in liquid nitrogen or fixed in methyl Carnoy's fixative for histological analysis. Doxycycline (Sigma-Aldrich) was administered in the drinking water at a concentration of 0.4 mg/ml for the full length of the experiment. Tumors were sectioned and analyzed for blood vessel density.

Paraquat cell viability assay

bEnd.3 cells (from Dr. Werner Risau) were maintained in Dulbecco's modified Eagle medium (DMEM) (Invitrogen, Carlsbad, CA) containing 10% fetal bovine serum (FBS) (Gemini Bio-Products, Woodland, CA) and grown in 37°C humidified 5% CO_2 atmosphere. Cells were plated in 96-well plates ($2x10^4$ cells/well) and allowed to adhere overnight. The next day media was removed and replaced with media containing 10% FBS and either paraquat (Sigma-Aldrich)

(0.1 mM) alone or with DOX (0.01 mM). After 48 hrs the media was replaced with fresh media containing paraquat and/or DOX. Cell viability was monitored at 48, 72, and 96 hrs using a CellTiter-Glo Luminescent Cell Viability Assay Kit according to the manufacturer's protocol (Promega).

ROS detection by DHE staining

Frozen tumors were sectioned (10 μm) and allowed to air-dry for thirty minutes. Sections were rehydrated in fifty µl of PBS for five minutes. Fifty μl of 5 μM dihydroethidium (DHE, Molecular Probes) (diluted in PBS) was added to each tumor section, coverslipped, and incubated at 37°C in a humidified incubator for thirty minutes. Nuclear red-fluorescence was visualized and images captured using the Photometric Coolsnap HQ camera. Fluorescence intensity was quantified using Metamorph software as described above.

REFERENCES

1. Liaw L, Crawford HC. Functions of the extracellular matrix and matrix degrading proteases during tumor progression. Braz J Med Biol Res 1999;32(7):805-12.
2. Wojtowicz-Praga SM, Dickson RB, Hawkins MJ. Matrix metalloproteinase inhibitors. Invest New Drugs 1997;15(1):61-75.
3. Balbin M, Fueyo A, Tester AM, et al. Loss of collagenase-2 confers increased skin tumor susceptibility to male mice. Nat Genet 2003;35(3):252-7.
4. McCawley LJ, Crawford HC, King LE, Jr., Mudgett J, Matrisian LM. A protective role for matrix metalloproteinase-3 in squamous cell carcinoma. Cancer Res 2004;64(19):6965-72.
5. Deryugina EI, Quigley JP. Matrix metalloproteinases and tumor metastasis. Cancer Metastasis Rev 2006;25(1):9-34.
6. Pozzi A, Moberg PE, Miles LA, Wagner S, Soloway P, Gardner HA. Elevated matrix metalloprotease and angiostatin levels in integrin alpha 1 knockout mice cause reduced tumor vascularization. Proc Natl Acad Sci U S A 2000;97(5):2202-7.
7. Wu WS. The signaling mechanism of ROS in tumor progression. Cancer Metastasis Rev 2006;25(4):695-705.
8. Chua CC, Hamdy RC, Chua BH. Upregulation of vascular endothelial growth factor by H2O2 in rat heart endothelial cells. Free Radic Biol Med 1998;25(8):891-7.
9. Tojo T, Ushio-Fukai M, Yamaoka-Tojo M, Ikeda S, Patrushev N, Alexander RW. Role of gp91phox (Nox2)-containing NAD(P)H oxidase in angiogenesis in response to hindlimb ischemia. Circulation 2005;111(18):2347-55.
10. Paravicini TM, Touyz RM. Redox signaling in hypertension. Cardiovasc Res 2006;71(2):247-58.
11. Redon J, Oliva MR, Tormos C, et al. Antioxidant activities and oxidative stress byproducts in human hypertension. Hypertension 2003;41(5):1096-101.
12. Vendrov AE, Madamanchi NR, Hakim ZS, Rojas M, Runge MS. Thrombin and NAD(P)H oxidase-mediated regulation of CD44 and BMP4-Id pathway in VSMC, restenosis, and atherosclerosis. Circ Res 2006;98(10):1254-63.
13. Dreher D, Junod AF. Role of oxygen free radicals in cancer development. Eur J Cancer 1996;32A(1):30-8.
14. Ushio-Fukai M, Alexander RW. Reactive oxygen species as mediators of angiogenesis signaling: role of NAD(P)H oxidase. Mol Cell Biochem 2004;264(1-2):85-97.

15. Greenwald P, Anderson D, Nelson SA, Taylor PR. Clinical trials of vitamin and mineral supplements for cancer prevention. Am J Clin Nutr 2007;85(1):314S-7S.
16. Lesperance ML, Olivotto IA, Forde N, et al. Mega-dose vitamins and minerals in the treatment of non-metastatic breast cancer: an historical cohort study. Breast Cancer Res Treat 2002;76(2):137-43.
17. Engel RH, Evens AM. Oxidative stress and apoptosis: a new treatment paradigm in cancer. Front Biosci 2006;11:300-12.
18. Fang J, Nakamura H, Iyer AK. Tumor-targeted induction of oxystress for cancer therapy. J Drug Target 2007;15(7-8):475-86.
19. Marikovsky M. Thiram inhibits angiogenesis and slows the development of experimental tumours in mice. Br J Cancer 2002;86(5):779-87.
20. Maeshima Y, Colorado PC, Torre A, et al. Distinct antitumor properties of a type IV collagen domain derived from basement membrane. J Biol Chem 2000;275(28):21340-8.
21. Maeshima Y, Colorado PC, Kalluri R. Two RGD-independent alpha vbeta 3 integrin binding sites on tumstatin regulate distinct anti-tumor properties. J Biol Chem 2000;275(31):23745-50.
22. Hamano Y, Zeisberg M, Sugimoto H, et al. Physiological levels of tumstatin, a fragment of collagen IV alpha3 chain, are generated by MMP-9 proteolysis and suppress angiogenesis via alphaV beta3 integrin. Cancer Cell 2003;3(6):589-601.
23. Raffetto JD, Khalil RA. Matrix metalloproteinases and their inhibitors in vascular remodeling and vascular disease. Biochem Pharmacol 2008;75(2):346-59.
24. Firatli E, Unal T, Onan U, Sandalli P. Antioxidative activities of some chemotherapeutics. A possible mechanism in reducing gingival inflammation. J Clin Periodontol 1994;21(10):680-3.
25. Halliwell B, Wasil M. Tetracyclines as antioxidants in rheumatoid arthritis: scavenging of hypochlorous acid. J Rheumatol 1988;15(3):530.
26. Nguyen AD, Itoh S, Jeney V, et al. Fibulin-5 is a novel binding protein for extracellular superoxide dismutase. Circ Res 2004;95(11):1067-74.
27. Fukai T, Folz RJ, Landmesser U, Harrison DG. Extracellular superoxide dismutase and cardiovascular disease. Cardiovasc Res 2002;55(2):239-49.
28. Das U. A radical approach to cancer. Med Sci Monit 2002;8(4):RA79-92.
29. Tanaka T, Halicka HD, Huang X, Traganos F, Darzynkiewicz Z. Constitutive histone H2AX phosphorylation and ATM activation, the reporters of DNA damage by endogenous oxidants. Cell Cycle 2006;5(17):1940-5.
30. Touyz RM, Schiffrin EL. Reactive oxygen species in vascular biology: implications in hypertension. Histochem Cell Biol 2004;122(4):339-52.

31. Albig AR, Schiemann WP. Fibulin-5 antagonizes vascular endothelial growth factor (VEGF) signaling and angiogenic sprouting by endothelial cells. DNA Cell Biol 2004;23(6):367-79.
32. Sullivan KM, Bissonnette R, Yanagisawa H, Hussain SN, Davis EC. Fibulin-5 functions as an endogenous angiogenesis inhibitor. Lab Invest 2007;87(8):818-27.

CHAPTER 3. Fbln5 controls integrin-induced ROS production *in vitro*

INTRODUCTION

Since the mid-1980s, redox signaling has become recognized as an important mechanism for signal transduction. ROS including superoxide, nitric oxide, hydroxyl radicals (-OH) and H_2O_2 function as key signaling molecules both intracellularly and in cell-cell communication influencing pathways such as proliferation, differentiation, cytoskeletal rearrangement and apoptosis. ROS are highly reactive oxygen molecules due to the presence of unpaired valence shell electrons that chemically modify DNA and proteins by oxidation of nucleic acids and the amino acid cysteine, respectively. These modifications result in the activation or inactivation of proteins thereby altering downstream signaling. For example, redox signaling is involved in the activation of a series of transcription factors that contain cysteine residues within their DNA binding domains. Oxidation of these residues modifies the structure of the protein allowing it to bind more efficiently to promoter regions and induce expression of target genes.[1-3] In a similar fashion, ROS have also been shown to inactivate kinases and phosphatases, both key enzymes that regulate signaling pathways.[4]

ROS are produced through a variety of mechanisms triggered by environmental stimuli including invading pathogens, cytokines, growth factors, integrins and their ligands. The nitric oxide synthase (NOS) family of proteins including the isoforms endothelial NOS (eNOS) and neuronal NOS (nNOS), which are constitutively expressed on endothelium, platelets, and neurons and inducible NOS (iNOS) whose expression is induced by various cytokines and IFN-γ in immune cells, endothelial cells, fibroblasts and smooth muscle cells are responsible for the production of nitric oxide within tissues.[5] It has also been shown that all three NOS isoforms can participate in superoxide production due to an "uncoupling" event where critical co-factors such as L-arginine and

tetrahydrobiopterin (BH_4) are depleted from the system destabilizing the protein.[6-8] However, mitochondria serve as the major source for intracellular superoxides, which are a natural byproduct of the electron transport chain. Molecular pathways such as tumor necrosis factor α (TNFα) signaling, hypoxia or apoptosis have been shown to modify mitochondrial function promoting the release of superoxides.[9-11] Superoxides are also produced via NAD(P)H oxidases present on the surface of phagocytic cells such as macrophages and neutrophils where it is activated in response to bacterial products. NAD(P)H oxidases have also been identified on non-phagocytic cells including endothelial cells. NAD(P)H oxidase-derived superoxides function in endothelial cell proliferation and migration and are activated in response to growth factors such as VEGF, PDGF and angiopoietin-1. Recently, NAD(P)H oxidase activation has been shown to be dependent on the activation of the small G-proteins Rac1 and Rac2. Rac activation results in its translocation to the membrane where it binds and activates the membrane bound subunit of NAD(P)H oxidase. In support of this, studies using mutant Rac proteins unable to bind oxidases inhibit ROS production.[12] In endothelial cells, activation of this pathway has been linked to VEGF binding to VEGF receptor 2.[13]

Integrin activation has been shown to either enhance or inhibit ROS production in a cell-type dependent manner through mechanisms that largely involve the regulation of Rac1 and Rac2 activity. For example, in fibroblasts, α_5 inetgrin clustering induced mitochondrial superoxide production through a mechanism dependent on Rac1 activation. How Rac1 affects mitochondrial function remains unknown but the increase in ROS production led to NFκB activation and induced MMP-1 expression.[14] Furthermore, via a similar mechanism, $\alpha_2\beta_1$ integrin ligation by Type IV collagen and β_1 integrin activation by fibronectin promoted ROS generation in fibroblasts.[15, 16] On the other hand,

integrin-mediated adherence of neutrophils to ECM proteins suppressed ROS formation by inhibiting the activity of the membrane-associated guanine nucleotide exchange factor, Vav1 which prevented activation of Rac2 and in mesangial cells, activation of $\alpha_1\beta_1$ integrin inhibited NAD(P)H oxidase-mediated ROS production and subsequent collagen deposition by inhibiting EGFR-mediated activation of Rac1.[17, 18]

These studies show that the regulation of ROS is a complex process mediated by a conglomerate of proteins including growth factors and integrins. However, little is known about the function of matricellular proteins in redox signaling. Herein, we describe a novel mechanism by which Fbln5 functions to control β_1 integrin-mediated ROS production by competing with fibronectin.

RESULTS

Fbln5$^{-/-}$ MEFs produce higher levels of ROS than *WT* MEFs

We observed an increase in the level of ROS within tumors from *Fbln5*$^{-/-}$ mice indicating a function for Fbln5 in the control of ROS production. To delineate this mechanism, we performed *in vitro* studies using MEFs harvested from *Fbln5*$^{-/-}$ and *WT* embryos. Infiltrating fibroblasts makeup a large percentage of the cells found in the tumor microenvironment, therefore MEFs provided us with a means of initially investigating the effect of Fbln5 on ROS production in a tumor-relevant cell population.[19] MEFs were grown on fibronectin, gelatin or collagen coated chamber slides or 96-well plates and the level of ROS was evaluated by 2'-7'-dicholordihydrofluorescein diacetate (DCF-DA) staining. DCF-DA is a probe that upon oxidation by ROS emits a fluorescent fluorophore, therefore the level of fluorescence directly relates to the level of ROS within cells. *Fbln5*$^{-/-}$ MEFs produced significantly higher levels of ROS than *WT* MEFs when plated on fibronectin but not on collagen or gelatin (**Figure 3.1A, B**). Thus, cell

association with fibronectin in the absence of Fbln5 was necessary for elevated ROS formation. To determine if the difference in ROS production was

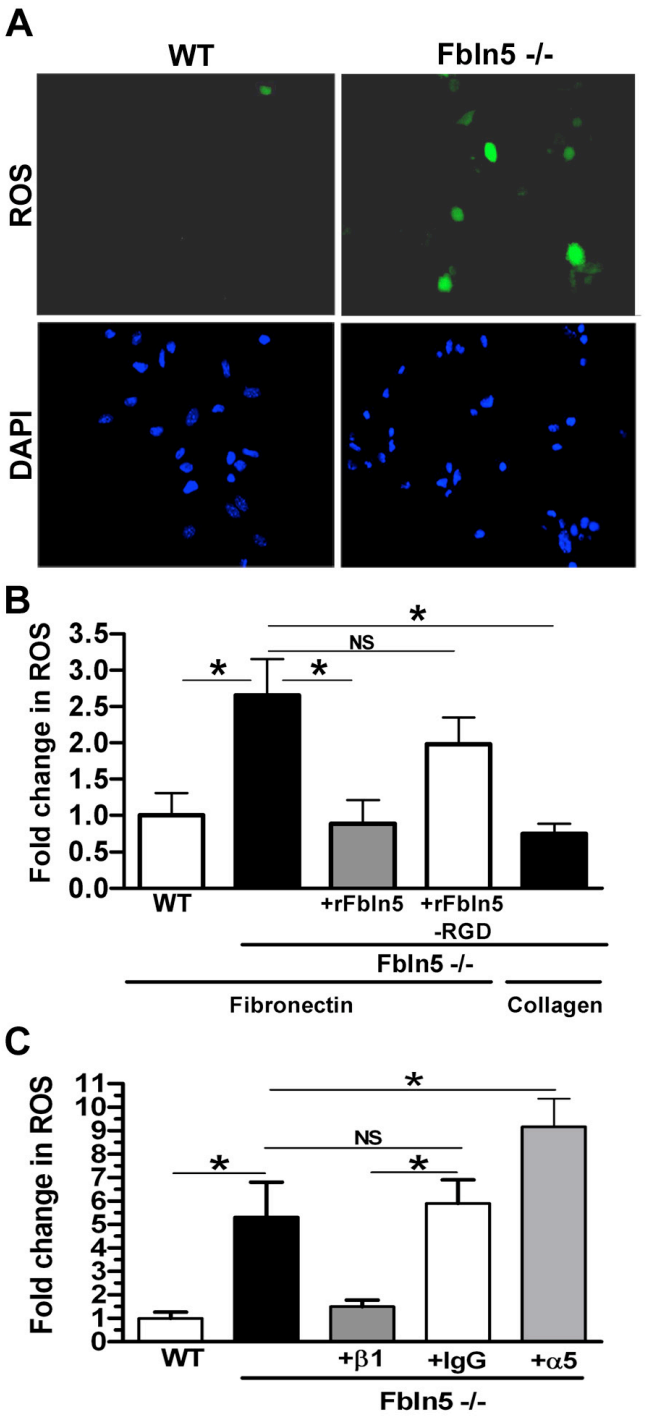

Figure 3.1 *Fbln5*$^{-/-}$ MEFs produced higher levels of ROS in a fibronectin and β1 integrin-dependent fashion. Mouse embryo fibroblasts (MEFs) harvested from *WT* and *Fbln5*$^{-/-}$ mice were grown on fibronectin or collagen. A, B) After 24 hours, the cells were stained with DCF-DA (green) to detect ROS. *Fbln5*$^{-/-}$ MEFs plated on fibronectin expressed higher levels of ROS than *WT* MEFs grown on fibronectin or *Fbln5*$^{-/-}$ MEFs grown on collagen. ROS production by *Fbln5*$^{-/-}$ MEFs was inhibited by addition of recombinant full length Fbln5 but not by mutant Fbln5 where the RGD domain had been deleted. C) ROS production was reduced by blocking β1 activation but was not affected by a control antibody. Treating *Fbln5*$^{-/-}$ MEFs with an α5 integrin activating antibody further increased ROS production. Ten pictures (total magnification, 200x) were taken of each condition and used for analysis. DCF-DA staining was normalized to cell number by DAPI staining. The assay was performed in triplicate. The results shown are mean +/- s.e.m. *p<0.05

due directly to a loss of Fbln5 expression, *Fbln5*$^{-/-}$ MEFs were treated with full-length recombinant Fbln5 protein prior to plating on fibronectin. Treatment with full-length Fbln5 but not with a NH2-terminal truncation mutant that lacks the RGD-integrin binding motif reduced ROS production by *Fbln5*$^{-/-}$ MEFs (**Figure 3.1B**). This result suggested that Fbln5 binding to integrins was necessary to block ROS generation. Lastly, to further confirm a direct function of Fbln5 in regulation of ROS production, Fbln5 expression was knocked down in an independent cell line, NIH 3T3 fibroblasts by shRNA (**Figure 3.2A**). When 3T3 cells treated with Fbln5-specific shRNA were plated on fibronectin, the loss of Fbln5 expression resulted in elevated ROS production compared to control cells (**Figure 3.2B**).

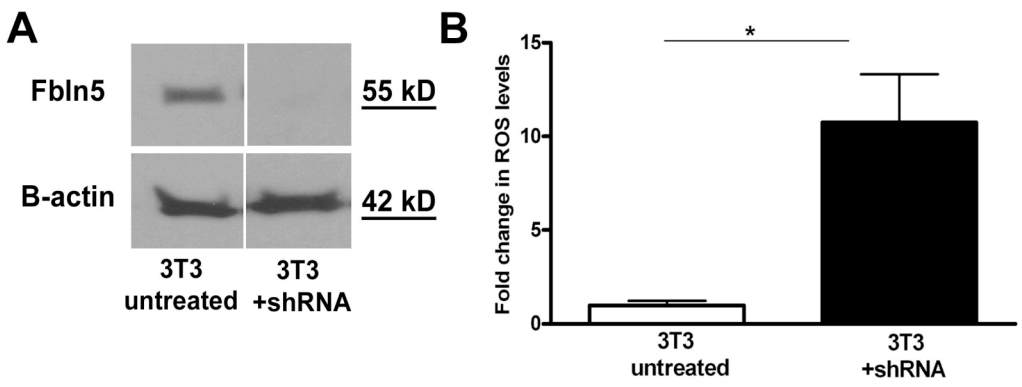

Figure 3.2 Loss of Fbln5 expression in NIH3T3 fibroblasts increases ROS production. A) Western blot analysis showed successful knock down of Fbln5 in NIH3T3 cells treated with Fbln5-specific shRNA. β-actin was used as a loading control. 48hrs. after treatment with shRNA cells were plated on fibronectin and stained with DCF-DA. Loss of Fbln5 increased ROS production compared to untreated cells. Ten pictures were taken of each condition and DCF-DA staining was normalized to cell number by DAPI staining. The assay was performed in duplicate. The results shown are mean +/- s.e.m. *$p<0.05$

$\alpha_5\beta_1$ integrin is the primary fibronectin receptor and it has been shown that binding of this integrin to fibronectin can stimulate downstream signaling leading

to ROS generation.[16, 20] To rule out that increased ROS seen in *Fbln5*$^{-/-}$ MEFs were due to elevated β_1 integrin expression, we examined expression of β_1 integrins by RT-PCR but observed equal expression between *WT* and *Fbln5*$^{-/-}$ MEFs (data not shown). Lomas *et al.* [21] recently provided evidence that Fbln5 competed with fibronectin for β_1 integrin binding. Furthermore, it was shown that binding of Fbln5 to β_1 integrins does not cause activation of the integrin or of downstream signaling pathways.[21] To determine if the effect on ROS formation was dependent on activation of β_1 integrins, we treated *Fbln5*$^{-/-}$ and *WT* MEFs plated on fibronectin with a β_1 function-blocking antibody. Addition of the antibody reduced the level of ROS produced by *Fbln5*$^{-/-}$ MEFs while the control IgG antibody had no effect (**Figure 3.1C**). Finally, to validate our assay, *Fbln5*$^{-/-}$ MEFs were treated with an activating anti-α_5 integrin antibody which has been shown previously to induce ROS production in fibroblasts.[14] As expected, treatment with this antibody further increased ROS production in *Fbln5*$^{-/-}$ MEFs (**Figure 3.1C**).

The above experiments suggested that Fbln5 competes with fibronectin for integrin binding to down-regulate ROS production and in the absence of Fbln5, more β_1 integrins are activated by fibronectin leading to higher levels of ROS. To prove this, we determined the level of β_1 integrin activation in *Fbln5*$^{-/-}$ and *WT* MEFs by analyzing cleavage of the focal adhesion protein, talin. Talin is a 270-kD protein consisting of a N-terminal 47-kD head domain which binds to cytoplasmic tails of β_1 integrins and a ~220-kD C-terminal rod domain critical for linking integrins to the cytoskeleton. Upon β_1 integrin ligation, the talin head domain binds to β_1 integrin tails inducing a conformational change that "activates" the integrin and increases its affinity for the ligand. Via the rod domain, talin binds integrins to actin filaments inducing focal adhesion formation, which is critical for cell adhesion and migration.[22] Cleavage of talin (47-kD head

and 220-kD rod domains) quickly follows integrin activation to promote disassembly of the adhesion complex.[23] *Fbln5*$^{-/-}$ and *WT* MEFs were plated on either fibronectin or collagen for 24 hours. Western blot analysis was performed on cell lysates to evaluate the level of talin cleavage products. *Fbln5*$^{-/-}$ and *WT* MEFs plated on collagen revealed no difference in the level of the 190-kD rod domain indicating equal activation of β_1 integrins in these cells. However, when plated on fibronectin, *Fbln5*$^{-/-}$ MEFs contained higher levels of the 190-kD fragment than *WT* cells. Furthermore, the full-length 270-kD protein could not be detected in *Fbln5*$^{-/-}$ MEFs plated on fibronectin but was present in *WT* cells and *Fbln5*$^{-/-}$ cells treated with a β_1 integrin function-blocking antibody which prevents integrin activation (**Figure 3.3 A,B**). These results indicated that in *Fbln5*$^{-/-}$ cells the loss of Fbln5 expression results in increased activation of β_1 integrins by fibronectin and enhanced cleavage of full-length talin.

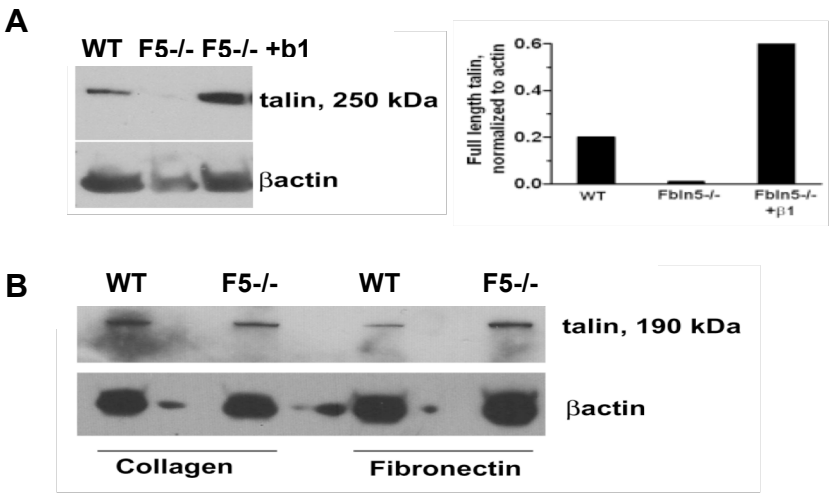

Figure 3.3 Increased β_1 integrin activation results in increased talin cleavage in *Fbln5*$^{-/-}$ MEFs plated on fibronectin. *WT* and *Fbln5*$^{-/-}$ MEFs were plated on collagen and fibronectin for 24hrs. Western blot analysis was performed on cell lysates probing for A) full length talin at 250 kDa. Prior to plating cells were treated with a β_1 integrin function-blocking antibody, which blocked activation of β_1 integrin and resulted in decreased cleavage of talin indicated by the increased levels of full length talin. Results were normalized to β-actin levels. B) The cleavage of talin was increased in *Fbln5*$^{-/-}$ MEFs plated on fibronectin indicated by the increase in the level of the 190 kDa fragment.

We next focused on identifying signaling components downstream of β_1 integrins that are involved in mediating ROS generation. It has been well documented that integrin-induced ROS production is dependent largely on Rac1 activation therefore, we evaluated Rac1 activation in *Fbln5*$^{-/-}$ MEFs. Inactive Rac1 exists in a GDP-bound form and activation to its GTP-bound form requires guanine nucleotide exchange factors (GEFs), which facilitate the exchange of GDP for GTP.[24] The level of Rac1-GTP present within cells can therefore, determine Rac1 activity. We hypothesized that *Fbln5*$^{-/-}$ MEFs plated on fibronectin would have increased levels of Rac1-GTP, however we observed equal levels between *Fbln5*$^{-/-}$ and *WT* cells (**Figure 3.4A**). We also analyzed a direct target of Rac1-GTP, nuclear factor kappa-light-chain-enhancer of activated B cells (NF-κB). It has been shown that activation of Rac1 by α_5 integrin stimulation leads to Rac1-dependent activation of NF-κB.[14] While in an inactivate state, NF-κB is located in the cytosol complexed with the inhibitory protein IκBα. Degradation of IκBα activates NF-κB where it is then translocated into the nucleus and turns on transcription of downstream targets. Activation of NF-κB is most commonly assessed by the level of IκBα present therefore, to determine if there was an increase in NF-κB activity due to

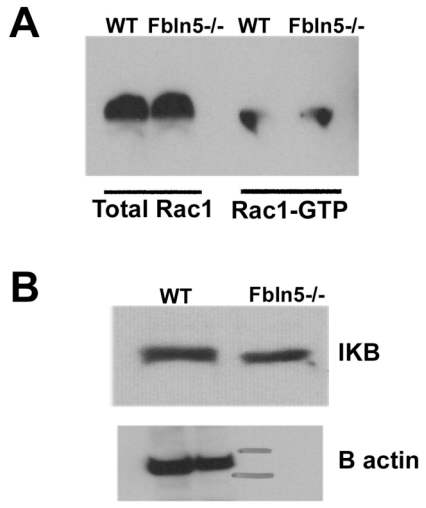

Figure 3.4 Rac1 activity is not increased in *Fbln5*$^{-/-}$ MEFs. A) WT and *Fbln5*$^{-/-}$ MEFs were plated on fibronectin for 4 hours. Cell lysates were mixed with PAK PBD protein beads to pull out Rac1-GTP. Western blots were probed for Rac1-GTP and total Rac1 was used as loading control. B) Cells were plated on fibronectin for 4 hours and cell lysates were analyzed for IκBα levels by western blot. β-actin was used as loading control.

augmented Rac1 activation, we analyzed the level IκBα in *WT* and *Fbln5*$^{-/-}$ MEFs plated on fibronectin. We did not detect an increase in IκBα degradation indicating that NF-κB activation was equal in *WT* and *Fbln5*$^{-/-}$ MEFs (**Figure 3.4B**). From these results, we concluded that Rac1 was not inducing ROS production in *Fbln5*$^{-/-}$ MEFs and suggested a possible uncharacterized mechanism by which integrin activation promotes ROS formation without modifying Rac1 activity.

L-Name reduces ROS production in *Fbln5*$^{-/-}$ MEFs

The three main sources for ROS production within cells are: 1) mitochondria, 2) NAD(P)H oxidases and 3) NOS proteins. To determine which route is activated by β_1 integrin signaling in the absence of Fbln5, we examined ROS production in *Fbln5*$^{-/-}$ MEFs in the presence of inhibitors specific to each of these sources. *Fbln5*$^{-/-}$ and *WT* MEFs were plated on fibronectin in the presence of varying concentrations of either rotenone (mitochondrial ROS inhibitor), apocynin (NAD(P)H oxidase inhibitor), or L-Name (NOS inhibitor) and ROS levels examined by DCF-DA staining. Given that integrin signaling has been shown to directly impact mitochondrial derived and NAD(P)H oxidase derived ROS production, we anticipated that one of these inhibitors would reduce ROS production in *Fbln5*$^{-/-}$ cells, however, ROS production was only inhibited by L-Name (**Figure 3.5 A, B**). These surprising results indicated that nitric oxide was being produced via NOS proteins in *Fbln5*$^{-/-}$ MEFs. To further investigate this finding, we evaluated the level of nitric oxide production in *Fbln5*$^{-/-}$ MEFs plated on fibronectin by performing a Griess assay but was unable to detect elevated levels (data not shown). These results suggested that in the absence of Fbln5 uncoupling of the NOS protein occurs to induce superoxide production instead of nitric oxide.

Loss of Fbln5 expression in endothelial cells enhances ROS production

Results from our tumor studies suggested that the higher level of ROS present within tumors from *Fbln5*$^{-/-}$ mice affected endothelial cell survival. Therefore, we next wanted to determine if Fbln5 controlled ROS generation in endothelial cells by a mechanism similar to that observed in fibroblasts. bEnd.3 cells, a mouse endothelial cell line, were treated with siRNA to knockdown expression of Fbln5. We confirmed by western blot that two siRNAs directed against Fbln5 successfully reduced expression in bEnd.3 cells (**Figure 3.5A**). Expression was not affected by transfection of a scrambled siRNA. After transfection, cells were plated on either fibronectin or collagen coated 96-well plates and stained with DCF-DA. The loss of Fbln5 expression significantly increased ROS formation in endothelial cells plated on fibronectin but not collagen. This was reversed with the addition of the anti-oxidant N-acetyl cysteine (NAC) (**Figure 3.5B**). Treatment with the β_1 integrin function-blocking antibody inhibited the increase in ROS production within these cells (**Figure 3.5C**). These results confirmed that Fbln5 regulates

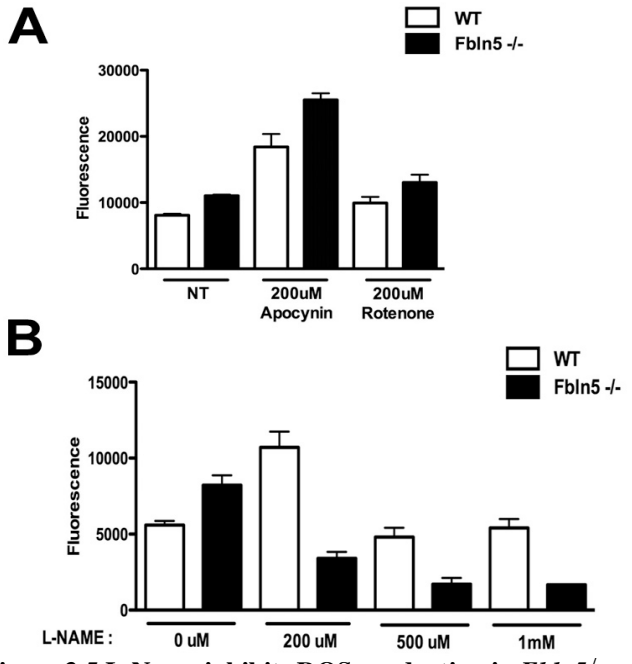

Figure 3.5 L-Name inhibits ROS production in *Fbln5*$^{-/-}$ MEFs. *WT* and *Fbln5*$^{-/-}$ MEFs were treated with varying concentrations of the inhibitors A) apocynin, rotenone, and B) L-Name and plated on fibronectin. One hour after plating, ROS production was detected by DCF-DA staining. Only L-Name treatment reduced ROS production in *Fbln5*$^{-/-}$ MEFs.

integrin-induced ROS production in endothelial cells and provided further support that one possible mechanism for reduced angiogenesis in tumors from *Fbln5*$^{-/-}$ mice was increased ROS generation by endothelial cells. This increase combined with the high level of ROS already present within the tumor could lead to chronic oxidative stress on endothelial cells resulting in reduced tumor angiogenesis.

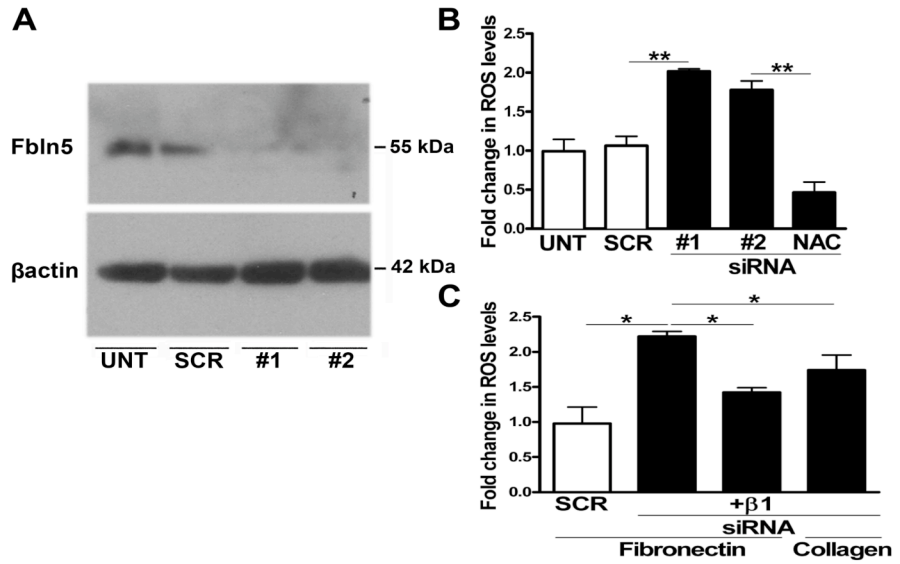

Figure 3.6 Loss of Fbln5 expression in endothelial cells resulted in increased ROS production. A) Treatment of bEnd.3 cells with two different (#1, #2) Fbln5-specific siRNAs successfully knocked down expression of Fbln5. UNT, untreated, SCR, scrambled siRNA. B,C) 24 hours after siRNA treatment, cells were plated on either fibronectin or collagen coated 96-well plates and analyzed for ROS production using DCF-DA. Knocking down Fbln5 expression increased ROS production which could be reduced by treatment with NAC and a β_1 integrin function-blocking

To better determine how the loss of Fbln5 affects ROS production in the endothelial cells, we isolated primary endothelial cells from *Fbln5*$^{-/-}$ and *WT* mice. The lungs and liver are highly vascularized organs, therefore they were used for endothelial cell extraction. Organs were minced and forced through a sterile cell strainer to generate a single cell suspension. Endothelial cells were pulled out of the cell suspension by an immuno-magnetic bead technique. Following isolation, cells were stained with a series of endothelial markers and fibroblasts markers (a

common cell contaminant) to confirm the identity and purity of the isolated cell population. By this technique, we were able to successfully generate primary *Fbln5*$^{-/-}$ and *WT* endothelial cell lines that were then analyzed for ROS production. *Fbln5*$^{-/-}$ and *WT* cells were plated on fibronectin coated 96 well plates and stained with DCF-DA and revealed a significant increase in ROS production within *Fbln5*$^{-/-}$ endothelial cells compared to *WT* cells (**Figure 3.7**). These results validated our findings in bEnd.3 cells and further supported our hypothesis that the loss of Fbln5 expression in tumors from *Fbln5*$^{-/-}$ mice caused a detrimental increase in ROS production within endothelial cells resulting in cell death.

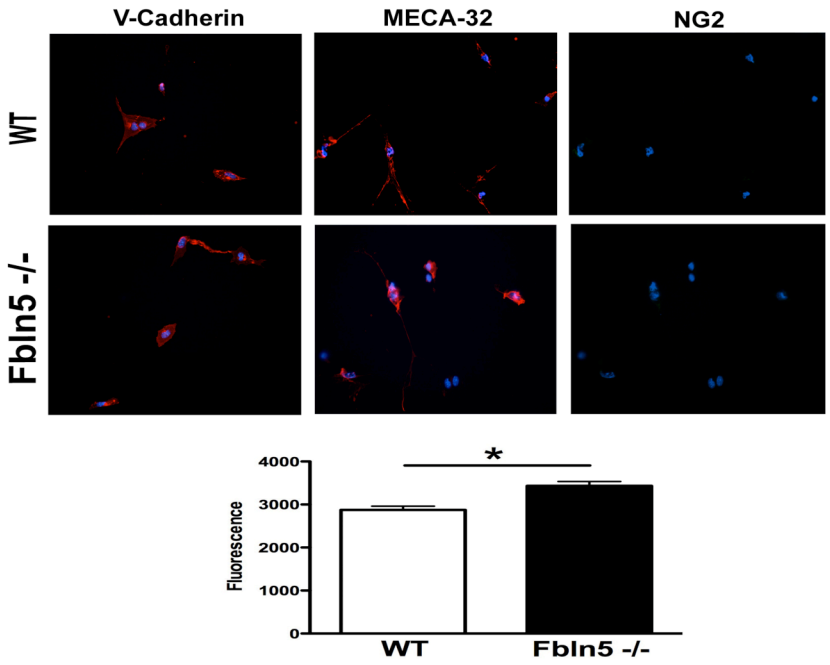

Figure 3.7 Primary *Fbln5*$^{-/-}$ endothelial cells produce higher levels of ROS. Primary endothelial cells isolated from livers of *WT* and *Fbln5*$^{-/-}$ mice were stained with the endothelial cell markers V-cadherin and MECA-32 and with the fibroblast marker NG2. Cells were plated on fibronectin coated 96-well plates and stained for DCF-DA to detect the level of ROS. The results are mean +/- s.e.m. * $p < 0.005$.

DISCUSSION

Our tumor studies in *Fbln5*$^{-/-}$ mice indicated an undescribed function for Fbln5 in the regulation of ROS generation. Through the *in vitro* experiments described above, we delineated a mechanism by which Fbln5 controls integrin-induced ROS generation by interfering with β_1 integrin ligation by fibronectin, a process reported previously to induce ROS formation.[16] Lomas *et al.* [21] reported that Fbln5 competes with fibronectin for β_1 integrins but that binding of Fbln5 to β_1 integrins does not induce activation and therefore inhibits downstream signaling including cell adhesion and migration. We extend these reports by showing that through this mechanism Fbln5 also inhibits fibronectin dependent integrin-induced ROS production.

We showed Fbln5 inhibition of ROS production was substrate dependent because binding of *Fbln5*$^{-/-}$ MEFs to fibronectin but not collagen increased production of ROS. Future experiments should be focused on determining the specificity of this mechanism. Does Fbln5 prevent activation of other integrins in order to limit ROS production? For instance, fibronectin also interacts with integrin $\alpha_v\beta_3$ and, although not reported, activation of this integrin may induce ROS formation.[25] If so, does Fbln5 interfere with fibronectin binding to integrin $\alpha_v\beta_3$ to further regulate ROS generation. Also, multiple ECM substrates bind to cells through β_1 integrins including vitronectin and laminin. It would be interesting to determine if Fbln5 competes with these proteins for integrin binding as well. These questions may be addressed by first analyzing ROS production downstream of integrin activation by the various ligands and then by determining how the addition of exogenous Fbln5 protein modifies the effect. Determining the specificity of this pathway is critical for designing therapeutic strategies that target this pathway. By knowing all possible avenues by which Fbln5 controls

ROS production, one can decide which area to target that will 1) be the easiest and most effective and 2) result in minimal side effects.

We attempted to identify components downstream of β_1 integrin activation by analyzing the activity of Rac1 and the source of ROS production through inhibitor studies. These experiments provided interesting results that suggested a novel Rac1-independent mechanism by which β_1 integrin activation modifies the function of NOS proteins to promote the release of superoxides. Previously, activation of Rac1 or Rac2 has been shown to be a critical step in integrin-mediated ROS formation. Our analysis indicated that Rac1 was not involved in the pathway inhibited by Fbln5 in MEFs. However, Rac1-GTP is transient making timing critical in these experiments. We looked at Rac1 activation four hours (also 24 hours, data not shown) after cells were plated on fibronectin. It could be that these experiments need to be repeated harvesting cells thirty minutes, one hour and two hours after plating. Western blot analysis of active Rac proteins was performed using a Rac1 specific antibody, therefore, we did not evaluate the activity level of Rac2. To completely rule out the involvement of Rac proteins in this pathway, Rac2 activity in *Fbln5*$^{-/-}$ MEFs must be determined. Also, given that pathways mediating ROS production are often cell-type dependent, it is necessary to repeat the Rac activity assays in endothelial cells to determine if a Rac1-independent mechanism similar the one observed in MEFs is occurring in these cells.

In our studies, L-name, an inhibitor of NOS proteins, reduced ROS production indicating that the ROS produced in the absence of Fbln5 were NO. The specific NOS protein involved has not been determined. Although the expression of both eNOS and iNOS is induced upon integrin activation, only iNOS has been shown to be expressed in both fibroblasts and endothelial cells leading one to speculate that it could be the key protein involved in this

pathway.[26-28] siRNA knock down of either iNOS or eNOS could help determine the involvement of these proteins in this pathway. NOS proteins normally produce nitric oxide, but when accessory proteins critical for stabilization are depleted, NOS proteins switch to superoxide production, a term described as "uncoupling".[6-8] This event is relevant to our studies given that we were unable to detect elevated levels of nitric oxide in *Fbln5*$^{-/-}$ MEFs plated on fibronectin. It is possible that β_1 integrin activation in the absence of Fbln5 forces NOS proteins to release superoxides. This idea is supported by the fact that the reagent used to detect ROS, DCF-DA, detects superoxides predominantly. Evaluating co-factor expression such as L-arginine or BH_4 in *Fbln5*$^{-/-}$ MEFs and endothelial cells plated on fibronectin may provide support for this possible mechanism.

Lastly, we determined that the loss of Fbln5 expression in endothelial cells resulted in increased integrin-mediated ROS production when plated on fibronectin. This is a critical finding because it not only supports our hypothesis that endothelial cells within tumors from *Fbln5*$^{-/-}$ mice die do to chronic exposure to ROS (ROS produced intracellularly in combination with the already present high levels of ROS within the TME) but also demonstrates a mechanism by which Fbln5 exerts its effects on endothelial cells and angiogenesis. Fbln5 has been labeled an angiogenic inhibitor due to its ability to impede endothelial cell proliferation and migration, however the molecular mechanisms behind these effects have remained unknown. Here, we have shown that Fbln5 limits the production of ROS, potent inducers of angiogenesis. These results help explain effects of Fbln5 that were previously identified but not well understood. For example, it was reported that Fbln5 reduced VEGF expression thereby inhibiting endothelial cell migration.[28, 29] ROS induces VEGF expression therefore, it is possible that Fbln5 controls VEGF expression and its effects on endothelial cells by abrogating ROS production. Furthermore, since ROS have been shown to induce angiogenesis *in vivo*, we can speculate that the increased vessel density

observed in non-pathological tissues from *Fbln5*$^{-/-}$ mice is due to the enhancement of ROS to pro-angiogenic levels.

These findings provide valuable information regarding the function of Fbln5 in angiogenesis and validate our in vivo observations that tumors from *Fbln5*$^{-/-}$ mice contain augmented ROS levels. Therapeutically, this discovery is critical because it highlights a potential target (interaction with β_1 integrin), which may block the function of Fbln5 and enhance ROS production within tumors.

METHODS

Cell Culture

Mouse embryonic fibroblasts (MEFs) were isolated from *WT* and *Fbln5*$^{-/-}$ E 13.5 embryos. Embryos were removed and washed in sterile PBS. The internal organs were removed by sterile dissection. The remaining embryo was put in a one ml syringe and forced through a 27-gauge needle into a 10 cm tissue culture dish containing DMEM supplemented with 10% FBS and streptomyocin. Cells passage 1-6 were used for experiments. All cells including MEFS, NIH 3T3 cells (from H. Yanagisawa), bEnd.3 cells (from Dr. Werner Risau) and primary endothelial cells were maintained in Dulbecco's modified Eagle medium (DMEM) (Invitrogen, Carlsbad, CA) containing 10% fetal bovine serum (FBS) (Gemini Bio-Products, Woodland, CA). All cells were grown in 37°C humidified 5% CO_2 atmosphere.

ROS detection *in vitro*

To visualize ROS in MEFs and NIH 3T3 cells, cells were grown on slides pre-coated with fibronectin (F1141 Sigma-Aldrich) or collagen Type 1 (354236 BD Biosciences, San Diego, CA) at 5 μg/ml. After 24 hours, media was removed; cells were washed once with warm PBS and incubated with 10 μM 2'-7'-

dicholordihydrofluorescein diacetate (DCF-DA) (D399, Molecular Probes) in warm PBS with 5.5 mM glucose for 10 minutes at 37°C. The DCF-DA was removed and replaced with DMEM with 10% FCS for an additional 10 minutes at 37°C. Cells were again washed with warm PBS, fixed with 10% formalin for 5 minutes, and mounted with ProLong Gold antifade reagent with DAPI (Invitrogen). Cells were analyzed with a Nikon Eclipse E600 microscope (Nikon) and fluorescent images were captured with a Photometric Coolsnap HQ camera and either Metamorph or Elements Imaging software. Multiple fluorescent images per sample were captured under identical conditions (room temperature, exposure time, high and low limits, and scaling). Fluorescence were quantified as the % average intensity, normalized to cell number and calculated as fold change compared to *WT* levels. ROS levels were also detected in cells by use of a fluorometer. MEFs, bEnd.3, or primary endothelial cells ($2x10^4$) were plated on 96-well plates (black plates with clear bottom) pre-coated with either fibronectin or collagen (5 μg/ml) for 2 hours. Cells were allowed to adhere for 1 hour and then media was removed and DCF-DA (100 μM) in PBS and 5.5 mM glucose was added for 1 hour at 37°C. DCF-DA was removed and cells washed once with PBS. Fluorescence was measured with excitation of 480 nm and emission of 520 nm. Cells were treated with either full length recombinant Fbln5, NH2-terminal truncation mutant Fbln5 (10 μg/ml) (generous gift from Elaine C. Davis, McGill University), a control IgG (C44, 10 μg/ml), anti-mouse β_1 integrin blocking antibody (CD29 #555002, BD Biosciences) (10 μg/ml) or anti-mouse α_5 integrin activating antibody (CD49e #103807 Biolegend, San Diego, CA) (10 μg/ml) for 15 minutes at 37°C prior to plating in wells. To block ROS signal N-acetyl cysteine (NAC) (10 mM) was added to the DCF-DA reagent prior to adding to cells. Each experiment was done in triplicate.

shRNA knock down of Fbln5

Mission® shRNA plasmid DNA targeted to Fbln5 was obtained from Sigma-Aldrich, Inc. NIH 3T3 cells ($2x10^5$) were plated in 6-well tissue culture plates and grown to 90% confluency overnight. Cells were transfected using Fugene 6 transfection reagent (Roche Applied Science, Indianapolis, IN) with either twelve μg of shRNA and 36 μl of Fugen 6 or Fugene 6 alone as a control. Forty-eight hours after transfection, cells were re-plated on fibronectin-coated slides for 24 hrs and then loaded with DCF-DA as described above to detect ROS levels. Ten pictures were taken from each condition for analysis. Lysates were made from remaining cells by directly lysing them in laemmli sample buffer (Bio-Rad, Hercules, CA) with BME (Sigma-Aldrich). Samples were ran on a 10% SDS-page gel and transferred to a nitrocellulose membrance. Membranes were blocked in 5% milk/TBST for one hour at room temperature and incubated with the primary antibodies, rabbit anti-mouse Fbln5 antibody (10 μg/ml) (BSYN1923) or anti-mouse β-actin (1:1000) (A2066, Sigma-Aldrich), diluted in 0.1% milk/TBST for either one hour at room temperature or overnight at 4°. Membranes were washed three times in TBST for five minutes each and incubated with anti-rabbit HRP-conjugated secondary antibodies diluted in 0.1% milk/TBST (1:50000). Membranes were again washed three times in TBST for five minutes each and developed using SuperSignal West Dura Extended Duration Substrate (Pierce). β-actin was used a loading control.

Western blot analysis

To analyze cleavage of talin or IκBα levels, MEFs ($3x10^5$) were plated on either fibronectin or collagen (5 μg/ml) coated 6-well plates for 24 hours for talin analysis or 4 hours for IκBα. Cells were harvested and resuspended in laemmli sample buffer (Bio-Rad) with BME (Sigma-Aldrich). Samples were ran on a 10%

SDS-page gel and transferred to a PVDF membrane. Membranes were blocked in 5% milk/TBST for one hour at room temperature and incubated with the primary antibodies: mouse anti-mouse talin (1:500, MAB3264 Chemicon), rabbit anti-mouse IκBα (1:1000, Santa Cruz) diluted in 0.1% milk/TBST for either one hour at room temperature or overnight at 4°. Membranes were washed three times in TBST for five minutes each and incubated with anti-rabbit HRP-conjugated secondary antibodies diluted in 0.1% milk/TBST (1:50000). Membranes were again washed three times in TBST for five minutes each and developed using SuperSignal West Dura Extended Duration Substrate (Pierce). β-actin was used a loading control.

Rac1 assay

To analyze Rac1 activity, MEFs ($3x10^5$) were plated on fibronectin (5 μg/ml) coated 6-well plates for 24 hours. Cells were harvested, washed once in PBS and kept on ice for the entire length of the experiment. Rac1 activity was detected according to the protocol of the Rac Activation Assay Biochem kit (BK035, Cytoskeleton, Denver, CO). Cell lysates were made by resuspending cells in 1X ice cold cell lysis buffer and centrifuged for five minutes at 8,000 rpm to clarify lysates. Lysates were mixed with twenty μl of PAK-PBD beads, which bind to RAC1-GTP, and ten μl of protease inhibitor cocktail for one hour at 4° on a rocker. Beads were pelleted by centrifugation at 5,000 rpm for three minutes, washed with 1X lysis buffer and spinned again. Beads were resuspended in ten μl of laemmli sample buffer (Bio-Rad) with BME (Sigma-Aldrich) and western blot analysis was performed as described above. Primary Rac1-GTP antibody was supplied by the kit.

Inhibitor studies

To determine the effect of various inhibitors on ROS production in *Fbln5*$^{-/-}$ MEFs, the *in vitro* ROS assay modified to the 96-well format was performed as described above. Prior to plating, cells were mixed with varying concentrations of inhibitors for fifteen minutes at 37°. The inhibitors used were apocynin (200 μM, Sigma-Aldrich), rotenone (200 μM, Sigma-Aldrich) and L-Name (200 μM, 500 μM, and 1 mM, Sigma-Aldrich).

siRNA knockdown of Fbln5

bEnd.3 endothelial cells ($3x10^5$)were plated in 6-well plates and allowed to adhere overnight. Cells were transfected with either pre-designed siRNAs directed against Fbln5 or a scrambled sequence (Sigma-Aldrich) using the N-TER™ Nanoparticle siRNA Transfection System (Sigma-Aldrich). 24 hours after transfection, cells were trypsinized and a portion was plated in 96-well plates ($2x10^4$) for ROS detection as described above. The remaining portion of cells was resuspended in laemmli sample buffer (Bio-Rad) with BME (Sigma-Aldrich) for western blot analysis as described above. Primary antibodies used were rabbit anti-mouse Fbln5 antibody (10 μg/ml) (BSYN1923) or anti-mouse β-actin (1:1000) (A2066, Sigma-Aldrich) for loading control.

Primary endothelial cell isolation

Endothelial cells were isolated from the lungs and liver of *WT* and *Fbln5*$^{-/-}$ mice using Dynabeads. The Dynabead protocol was followed to successfully isolate endothelial cells. Lungs and the livers from two WT and two *Fbln5*$^{-/-}$ were removed and washed in cold PBS. Tissues were placed in ten cm dishes containing sterile PBS and sliced in small pieces using sterile razor blades. Tissue pieces were mixed with twenty mls of Type I collagenase buffer (400 mM Hepes) for 3-4 hours with pipetting every hour to aid in digestion. After complete

digestion, the tissue mix was forced through a sterile cell strainer and combined with 10% FBS DMEM to quench collagenase. Cells were pelleted and washed with fresh 10% FBS DMEM. Cells were again pelleted and resuspended in ten mls of Buffer 1 (Dynabeads protocol, 0.1% BSA, 2mM EDTA/PBS at pH 7.4) Cells were counted and made into five ml aliquots of $1x10^7$ cells/ml. Cells were mixed with 500 μl of dynabeads that had been previously incubated in Buffer 1 overnight at 4° with rat anti-mouse CD31 (2 μg/ml, MEC13.3, BD Biosciences). Beads and antibody mix were washed twice with one ml of Buffer 1 prior to adding to cell mixture. Cell/bead mixes were incubated for one hour at 4° on rotator. To remove beads from the cell mix, tubes containing the mix were held up to a magnet causing the dynabeads to stick to the side of the tube. Supernant was removed and beads were washed in one ml of Buffer 1. This step was repeated twice. Finally, beads were resuspended in four mls of complete endothelial cell growth media (ScienCell, Carlsbad, CA) and added to T75 tissue culture flasks pre-coated with 20% FBS/PBS. Cells were grown in 37°C humidified 5% CO_2 atmosphere. Once cells were confluent, they were tryspinized and a portion of the cells was plated on chamber slides precoated with fibronectin (2 μg/ml) for immunocytochemistry. Cells were allowed to adhere overnight and then washed once with PBS, fixed in acetone for five minutes and a blocking solution (20%Aquablock/DMEM) was added for one hour at room temperature. Primary antibodies rabbit anti-mouse V-cadherin (1:50, sc-6458 Santa Cruz), rat anti-mouse MECA-32 (10 μg/ml, Developmental Studies Hybridoma Bank, University of Iowa) and rabbit anti-mouse NG2 (1:50, AB5320 Chemicon) were diluted in 1% BSA/PBS added for one hour at room temperature. Cells were washed three times in PBST for five minutes each and incubated with fluorophore-conjugated (fluorescein FITC or Cy3) secondary antibodies in 1% BSA/PBS (1:1000) (Jackson Immunoresearch) for one hour at room temperature. Cells were again

washed three times in PBST for five minutes each and mounted with ProLong Gold antifade reagent with DAPI (Invitrogen). The remaining cells were plated ($1x10^4$) on fibronectin coated 96-well plates for one hour and the ROS assay was performed as described above.

REFERENCES

1. Aslund F, Zheng M, Beckwith J, Storz G. Regulation of the OxyR transcription factor by hydrogen peroxide and the cellular thiol-disulfide status. Proc Natl Acad Sci U S A 1999;96(11):6161-5.
2. Carriere A, Carmona MC, Fernandez Y, et al. Mitochondrial reactive oxygen species control the transcription factor CHOP-10/GADD153 and adipocyte differentiation: a mechanism for hypoxia-dependent effect. J Biol Chem 2004;279(39):40462-9.
3. Storz G, Polla BS. Transcriptional regulators of oxidative stress-inducible genes in prokaryotes and eukaryotes. Exs 1996;77:239-54.
4. Wu WS. The signaling mechanism of ROS in tumor progression. Cancer Metastasis Rev 2006;25(4):695-705.
5. Aktan F. iNOS-mediated nitric oxide production and its regulation. Life Sci 2004;75(6):639-53.
6. Xia Y, Zweier JL. Superoxide and peroxynitrite generation from inducible nitric oxide synthase in macrophages. Proc Natl Acad Sci U S A 1997;94(13):6954-8.
7. Xia Y, Tsai AL, Berka V, Zweier JL. Superoxide generation from endothelial nitric-oxide synthase. A Ca2+/calmodulin-dependent and tetrahydrobiopterin regulatory process. J Biol Chem 1998;273(40):25804-8.
8. Pou S, Pou WS, Bredt DS, Snyder SH, Rosen GM. Generation of superoxide by purified brain nitric oxide synthase. J Biol Chem 1992;267(34):24173-6.
9. Sanchez-Alcazar JA, Schneider E, Martinez MA, et al. Tumor necrosis factor-alpha increases the steady-state reduction of cytochrome b of the mitochondrial respiratory chain in metabolically inhibited L929 cells. J Biol Chem 2000;275(18):13353-61.
10. Vanden Hoek TL, Shao Z, Li C, Schumacker PT, Becker LB. Mitochondrial electron transport can become a significant source of oxidative injury in cardiomyocytes. J Mol Cell Cardiol 1997;29(9):2441-50.
11. Cai J, Jones DP. Superoxide in apoptosis. Mitochondrial generation triggered by cytochrome c loss. J Biol Chem 1998;273(19):11401-4.
12. Hordijk PL. Regulation of NADPH oxidases: the role of Rac proteins. Circ Res 2006;98(4):453-62.
13. Ushio-Fukai M. Redox signaling in angiogenesis: role of NADPH oxidase. Cardiovasc Res 2006;71(2):226-35.
14. Werner E, Werb Z. Integrins engage mitochondrial function for signal transduction by a mechanism dependent on Rho GTPases. J Cell Biol 2002;158(2):357-68.

15. Honore S, Kovacic H, Pichard V, Briand C, Rognoni JB. Alpha2beta1-integrin signaling by itself controls G1/S transition in a human adenocarcinoma cell line (Caco-2): implication of NADPH oxidase-dependent production of ROS. Exp Cell Res 2003;285(1):59-71.
16. Chiarugi P, Pani G, Giannoni E, et al. Reactive oxygen species as essential mediators of cell adhesion: the oxidative inhibition of a FAK tyrosine phosphatase is required for cell adhesion. J Cell Biol 2003;161(5):933-44.
17. Zhao T, Benard V, Bohl BP, Bokoch GM. The molecular basis for adhesion-mediated suppression of reactive oxygen species generation by human neutrophils. J Clin Invest 2003;112(11):1732-40.
18. Chen X, Abair TD, Ibanez MR, et al. Integrin alpha1beta1 controls reactive oxygen species synthesis by negatively regulating epidermal growth factor receptor-mediated Rac activation. Mol Cell Biol 2007;27(9):3313-26.
19. Kunz-Schughart LA, Knuechel R. Tumor-associated fibroblasts (part I): Active stromal participants in tumor development and progression? Histol Histopathol 2002;17(2):599-621.
20. Umanskiy K, Robinson C, Cave C, et al. NADPH oxidase activation in fibronectin adherent human neutrophils: A potential role for beta1 integrin ligation. Surgery 2003;134(2):378-83.
21. Lomas AC, Mellody KT, Freeman LJ, Bax DV, Shuttleworth CA, Kielty CM. Fibulin-5 binds human smooth-muscle cells through alpha5beta1 and alpha4beta1 integrins, but does not support receptor activation. Biochem J 2007;405(3):417-28.
22. Calderwood DA, Zent R, Grant R, Rees DJ, Hynes RO, Ginsberg MH. The Talin head domain binds to integrin beta subunit cytoplasmic tails and regulates integrin activation. J Biol Chem 1999;274(40):28071-4.
23. Franco SJ, Rodgers MA, Perrin BJ, et al. Calpain-mediated proteolysis of talin regulates adhesion dynamics. Nat Cell Biol 2004;6(10):977-83.
24. Bosco EE, Mulloy JC, Zheng Y. Rac1 GTPase: a "Rac" of all trades. Cell Mol Life Sci 2009;66(3):370-4.
25. Charo IF, Nannizzi L, Smith JW, Cheresh DA. The vitronectin receptor alpha v beta 3 binds fibronectin and acts in concert with alpha 5 beta 1 in promoting cellular attachment and spreading on fibronectin. J Cell Biol 1990;111(6 Pt 1):2795-800.
26. Kroll J, Waltenberger J. VEGF-A induces expression of eNOS and iNOS in endothelial cells via VEGF receptor-2 (KDR). Biochem Biophys Res Commun 1998;252(3):743-6.
27. Gupta SK, Vlahakis NE. Integrin {alpha}9{beta}1 mediates enhanced cell migration through nitric oxide synthase activity regulated by Src tyrosine kinase. J Cell Sci 2009;122(Pt 12):2043-54.

28. Balligand JL, Feron O, Dessy C. eNOS activation by physical forces: from short-term regulation of contraction to chronic remodeling of cardiovascular tissues. Physiol Rev 2009;89(2):481-534.
29. Albig AR, Schiemann WP. Fibulin-5 antagonizes vascular endothelial growth factor (VEGF) signaling and angiogenic sprouting by endothelial cells. DNA Cell Biol 2004;23(6):367-79.

CHAPTER 4. Antioxidant treatment rescues angiogenesis and enhances tumor growth in *Fbln5*$^{-/-}$ mice

INTRODUCTION

ROS has long been associated with cancer but the effects of ROS on tumor growth and progression are complex and at times paradoxical. Initially, ROS induced by environmental stressors such as cigarette smoke and pollutants were shown to assist in carcinoma formation by inducing DNA generating cancer-causing mutations.[1] For instance, multiple cancers develop due to inactivating mutations in the tumor suppressor gene p53 resulting in uncontrolled cell proliferation, a defining characteristic of tumor cells.[2] Mutations due to oxidative damage also occur in the ras family of oncogenes including Kras, a mutation of which is commonly observed in pancreatic carcinomas.[3] It has become clear that ROS also participate in tumor progression. For instance, ROS have been reported to contribute to tumor angiogenesis. VEGF and hypoxia inducible factor-1 (HIF-1) are prominent factors in initiating blood vessel formation and are often found highly expressed within tumors. Recently, expression of these two factors was shown to be induced by ROS generated from ovarian and prostate cancer cells. Inhibiting ROS production within these cells reduced VEGF and HIF-1 levels and resulted in blunted angiogenesis and tumor growth *in vivo* [4]. ROS also contribute to tumor progression by promoting metastasis through MMP secretion and induction of epithelial-mesenchymal transition (EMT). How MMPs promote metastasis is unclear but it is generally thought that MMP-mediated cleavage of ECM proteins results in enhanced migration of tumor cells and liberation of ECM-bound growth factors that stimulate angiogenesis and tumor cell proliferation.[5] Epidermal growth factor (EGF) has been shown to promote tumor invasion by inducing MMP expression and a recent study[6] reported that this effect is ROS dependent. In this study, it was determined that EGF receptor activation

resulted in downstream activation of NAD(P)H oxidase through Rac1. This resulted in increased superoxide production and subsequent MMP expression. Inhibiting ROS production blocked MMP expression and reduced the invasiveness of PANC-1 tumor cells.[6] Furthermore, ROS has been implicated in the induction of EMT, a process where primary epithelial tumor cells take on a more invasive mesenchymal phenotype. ROS have been shown to stimulate several pathways involved in the regulation of EMT. In particular, ROS promotes the expression of Smad and AP-1 through activation of protein kinase C (PKC) and TGF-β. These proteins induce expression of proteins required for EMT.[7]

These reports identify a positive correlation between ROS levels and tumor progression. However, numerous reports are beginning to surface that also suggest a negative role for ROS in tumor progression. This first became evident when antioxidant therapy failed in clinical trials and even promoted tumor growth in certain types of cancer.[8, 9] It is believed that antioxidant therapy was not successful at controlling tumor growth because it blocked apoptosis of tumor cells normally induced by the heightened level of ROS within tumors. It has been reported that tumor cells express higher levels of ROS than normal, non malignant cells.[10] This is believed to be due to the high metabolic rate of tumor cells and to mitochondrial DNA mutations that decrease the efficiency of mitochondria causing them to release more superoxides. Although tumor-derived ROS has beneficial effects for the tumor (promotion of angiogenesis and metastasis), the constant oxidative stress weakens the cell making it susceptible to further increases in ROS. A recent report showed that dietary depletion of the naturally-derived antioxidants, vitamins E and A, reduced tumor growth and metastasis in two mouse transgenic models of brain and breast cancer by augmenting ROS within the tumor. This data provides supportive evidence for the idea that tumor cells are sensitive to increases in ROS.[11] This is the mechanism of action behind many of our most successful chemotherapeutics and a new type of

therapy coined “oxidation therapy”. These drugs work by increasing ROS levels within tumor cells pushing the already stressed cells beyond their breaking point and inducing apoptosis. Tumor cells are not the only cells sensitive to ROS levels within tumors, however. Endothelial cells are also targets of ROS-induced damage and it has been shown that specifically increasing ROS within endothelial cells by inhibiting SOD activity can reduce their survival within the tumor and diminish tumor growth.[12] In support of these findings, our studies suggest that decreased tumor angiogenesis and growth in *Fbln5*$^{-/-}$ mice result from increased ROS generation and oxidative damage, which stem from elevated activation of β_1 integrins. In the following chapter, we describe results from experiments we performed to validate our findings and prove that the underlying cause for decreased tumor growth in *Fbln5*$^{-/-}$ mice is enhanced integrin-induced ROS production.

RESULTS

Tumor angiogenesis and growth are reduced and ROS levels are increased in *Fbln5*$^{RGE/RGE}$ mice

We determined that the binding of Fbln5 to integrins is critical for its regulation of ROS production. To confirm this *in vivo,* we repeated Pan02 tumor studies in transgenic knockin mice containing an altered RGD motif. In these mice, the aspartic acid of the integrin-binding RGD sequence of Fbln5 was changed to glutamic acid rendering the protein unable to bind to integrins. These mice appear normal and do not exhibit any of the defects observed in *Fbln5*$^{-/-}$ mice (H. Yanagisawa, unpublished). Pan02HY cells were injected subcutaneously into *WT, Fbln5*$^{-/-}$, and *Fbln5*$^{RGE/RGE}$ mice and tumor growth was monitored. As observed in *Fbln5*$^{-/-}$ mice, tumors from *Fbln5*$^{RGE/RGE}$ mice grew slower and were smaller than tumors from *WT* animals (**Figure 4.1A**). At the time of

sacrifice, tumors were harvested and the level of ROS was determined by DHE

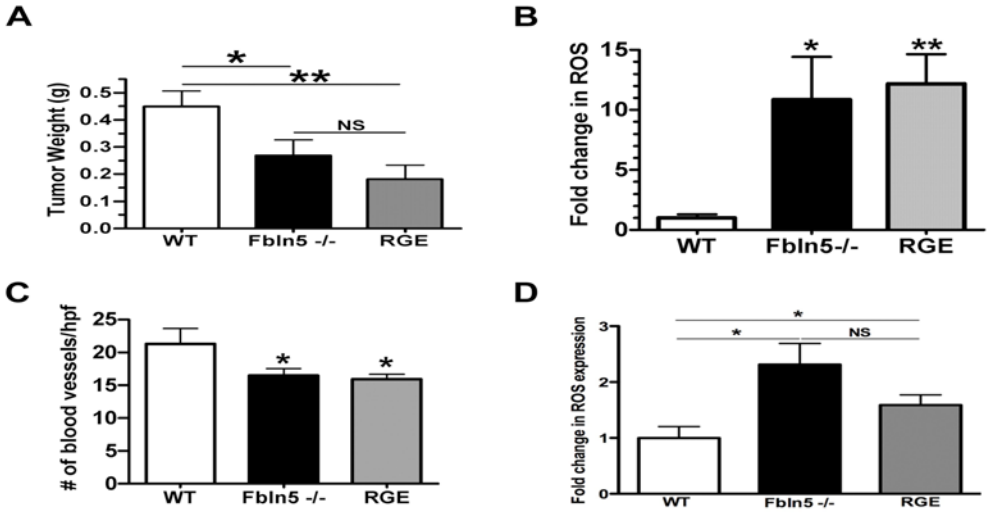

Figure 4.1 Tumor growth is decreased in *Fbln5*$^{RGE/RGE}$ mice. A-C) Pan02 cells were injected subcutaneously into *WT* (n=8), *Fbln5*$^{-/-}$ (n=7), and *Fbln5*$^{RGE/RGE}$ mice (n=8). Final mean (+/-s.e.m) tumor weight at time of harvest 4 weeks post tumor cell injection is displayed. *, p<0.05; **, p<0.01. Sections of tumor tissue from mice of each genotype were stained with B) DHE to assess the level of ROS and with C) MECA-32 to assess blood vessel density. For ROS and blood vessel density analysis a minimum of ten pictures (total magnification, 200x) of three tumors from each group were analyzed. *, p<0.05; **, p<0.01 vs *WT*. D) MEFs were isolated from *Fbln5*$^{RGE/RGE}$ mice, plated on fibronectin and stained with DCF-DA for ROS detection. Similar to *Fbln5*$^{-/-}$ MEFs, *Fbln5*$^{RGE/RGE}$ MEFs produce higher levels of ROS than *WT*. Results shown are +/- s.e.m. *p<0.01

staining. Consistent with results from tumors grown in *Fbln5*$^{-/-}$ animals, tumors from *Fbln5*$^{RGE/RGE}$ mice had significantly higher levels of ROS than tumor from *WT* animals furthering confirming the function of Fbln5 in controlling integrin-induced ROS production (**Figure 4.1B**). These results were validated by *in vitro* experiments showing that MEFs harvested from *Fbln5*$^{RGE/RGE}$ mice produce higher levels of ROS when plated on fibronectin than *WT* MEFs (**Figure 4.1D**).

We next evaluated blood vessel density and observed a significant decrease in angiogenesis in tumors grown in *Fbln5*$^{RGE/RGE}$ mice compared to tumors from *WT* mice (**Figure 4.1C**). Thus, we show in two models (*Fbln5*$^{-/-}$ and *Fbln5*$^{RGE/RGE}$ mice) that the loss of Fbln5 function *in vivo* reduces tumor growth and

angiogenesis and leads to increased ROS production. Results from tumor studies in the *Fbln5*$^{RGE/RGE}$ mice also further validate that integrin binding is critical for Fbln5-mediated control of ROS generation.

Treatment with an antioxidant rescues angiogenesis and restores tumor growth in *Fbln5*$^{RGE/RGE}$ mice

To determine if increased ROS production in tumors from *Fbln5*$^{RGE/RGE}$ mice was a major antagonist of blood vessel development and tumor growth, we performed tumor implantation studies in the presence of the antioxidant NAC. Pan02HY cells were injected subcutaneously into the flank of *WT* and *Fbln5*$^{RGE/RGE}$ mice. Following injection, NAC was added to the drinking water. Tumor volume was monitored over the course of the experiment. As previously

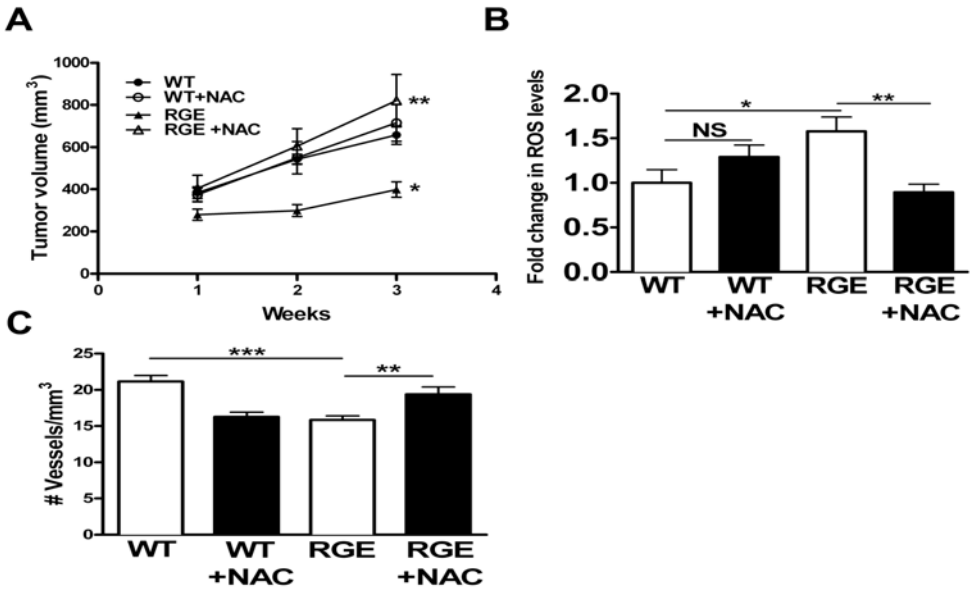

Figure 4.2 Antioxidant treatment restore tumor growth in *Fbln5*$^{RGE/RGE}$ mice. Pan02HY cells were injected subcutaneously into *WT* (n=20) and *Fbln5*$^{RGE/RGE}$ mice (n=21). NAC was added to the drinking water of tumor-bearing *WT* (n=10) and *Fbln5*$^{RGE/RGE}$ (n=11). A) Tumor volume was recored for three weeks.***, p<0.001 vs *Fbln5*$^{RGE/RGE}$ B) Sections of tumors from untreated and NAC-treated *WT* and *Fbln5*$^{RGE/RGE}$ mice were stained with DHE to determine the level of ROS. Ten pictures (total magnification, 200x) taken of each tumor from *WT* (n=5), *WT* +NAC (n=4), *Fbln5*$^{RGE/RGE}$ (n=5), and *Fbln5*$^{RGE/RGE}$ +NAC (n=5) animals were used for analysis. C) Tumor sections were also stained with MECA-32 to analyze vessel density (n=5 for each condition). The number of blood vessels/mm^2 is displayed. The results shown are mean +/- s.e.m. *, p<0.01; **, p<0.005, ***p<0.001.

shown, tumors grew slower in *Fbln5*$^{RGE/RGE}$ mice than tumors in *WT* mice. However, tumor growth rate was restored to *WT* levels in *Fbln5*$^{RGE/RGE}$ mice treated with NAC (**Figure 4.2A**). Tumors stained with DHE demonstrated that treatment with NAC reduced the level of ROS in *Fbln5*$^{RGE/RGE}$ mice (**Figure 4.2B**). To determine if increased tumor growth in *Fbln5*$^{RGE/RGE}$ mice treated with NAC was due to alleviation of the angiogenic defect, we analyzed blood vessel density in tumors from NAC treated and untreated *Fbln5*$^{RGE/RGE}$ mice. The number of MECA-32 positive blood vessels in tumors from *Fbln5*$^{RGE/RGE}$ mice was increased to *WT* levels in the presence of NAC (**Figure 4.2C**). These findings further support our hypothesis that the loss of Fbln5 led to chronic ROS exposure within tumors causing endothelial cell death and reduced tumor growth.

Antioxidant treatment prevents increased angiogenesis in non-tumorigenic tissues in *Fbln5*$^{-/-}$ mice

It was recently shown that angiogenesis in PVA sponges implanted in *Fbln5*$^{-/-}$ mice was increased suggesting that Fbln5 inhibits angiogenesis by an unknown mechanism.[13] Our data suggest that Fbln5 functions to control angiogenesis by regulating integrin-mediated ROS formation. We hypothesized that treating *Fbln5*$^{-/-}$ mice with an antioxidant would prevent increased angiogenesis into implanted tissues. To investigate this, we implanted matrigel plugs into *WT* and *Fbln5*$^{-/-}$ mice treated with NAC and observed the effects on angiogenesis. Matrigel was injected into *WT* and *Fbln5*$^{-/-}$ mice and a portion of the mice were given the antioxidant NAC in the drinking water for the length of the experiment. After two weeks, the plugs were removed and the extent of angiogenesis was analyzed. Visual inspection of the plugs after removal from the animals showed a significant amount of angiogenesis in plugs from *Fbln5*$^{-/-}$ mice.

This was not observed in plugs from *Fbln5*$^{-/-}$ mice treated with NAC (**Figure 4.3A**). Analysis of blood vessel density by MECA-32 staining confirmed a

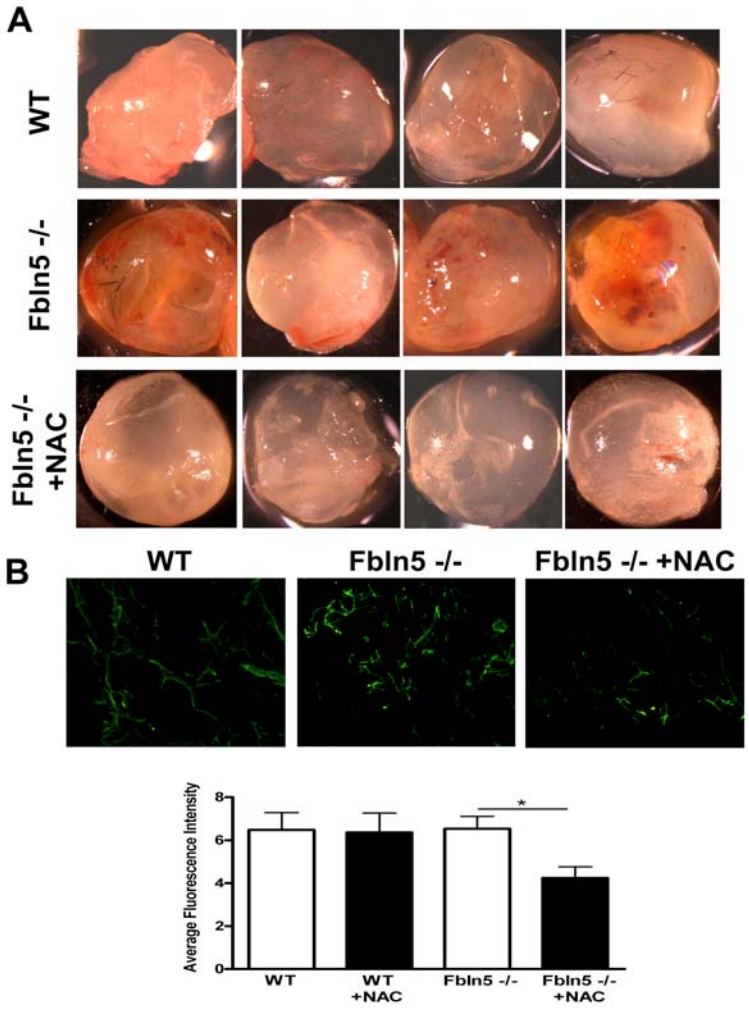

Figure 4.3 ROS is critical for angiogenesis in matrigel plugs implanted into *Fbln5*$^{-/-}$ mice. Matrigel was injected into *WT* (n=10) and *Fbln5*$^{-/-}$ (n=10) mice. Five mice from each group were given NAC (4 mg/ml) in the drinking water. A) Matrigel plugs were harvested from *WT* and *Fbln5*$^{-/-}$ +/- NAC B) Plugs were sectioned and stained with MECA-32 (green) to analyze the level of angiogenesis. Angiogenesis is decreased in *Fbln5*$^{-/-}$ mice upon anti-oxidant treatment. Blood vessel density was not affected in *WT* mice treated with anti-oxidant. Ten pictures were taken (total magnification, 200x) from each plug (5 plugs/condition) for quanitation. The results shown are the mean fluorescence intensity and +/- SEM. *p<0.01

significant decrease in angiogenesis in plugs from *Fbln5*$^{-/-}$ mice treated with NAC compared to untreated *Fbln5*$^{-/-}$ mice (**Figure 4.3B**). Angiogenesis was not affected in plugs from *WT* mice treated with NAC indicating that only angiogenesis in *Fbln5*$^{-/-}$ matrigel plugs is sensitive to antioxidant treatment and that elevated ROS level was responsible, in part, for angiogenesis in matrigel implants in *Fbln5*$^{-/-}$ mice.

From the results described above, we can conclude that Fbln5 inhibits angiogenesis by limiting integrin-induced ROS production. In the context of normal nonpathological tissues, the loss of Fbln5 increases ROS to pro-angiogenic levels and augments blood vessel formation. However, in tumors where high levels of ROS already exist, the increase in ROS due to the loss of Fbln5 deems detrimental to the survival of endothelial cells and results in decreased angiogenesis. **Figure 4.4** is a schematic depicting our current hypothesis for how Fbln5 controls ROS production and how in its absence can inhibit angiogenesis in the TME.

DISCUSSION

We have shown *in vitro* that Fbln5 inhibits integrin-induced ROS production by a mechanism dependent on its ability to bind integrins via the RGD motif. Attenuated tumor angiogenesis and growth in *Fbln5*$^{-/-}$ mice suggested that this function was critical for tumor progression. Loss of Fbln5 *in vivo* led to a chronic buildup of ROS within the TME leading us to hypothesize that this was the underlying cause for decreased endothelial cell survival and tumor growth in *Fbln5*$^{-/-}$ mice. To validate our hypothesis, we performed subcutaneous tumor studies in *Fbln5*$^{RGE/RGE}$ mice. Fbln5 expressed by these mice contains a point mutation in the integrin-binding RGE motif that prevents Fbln5 from interacting

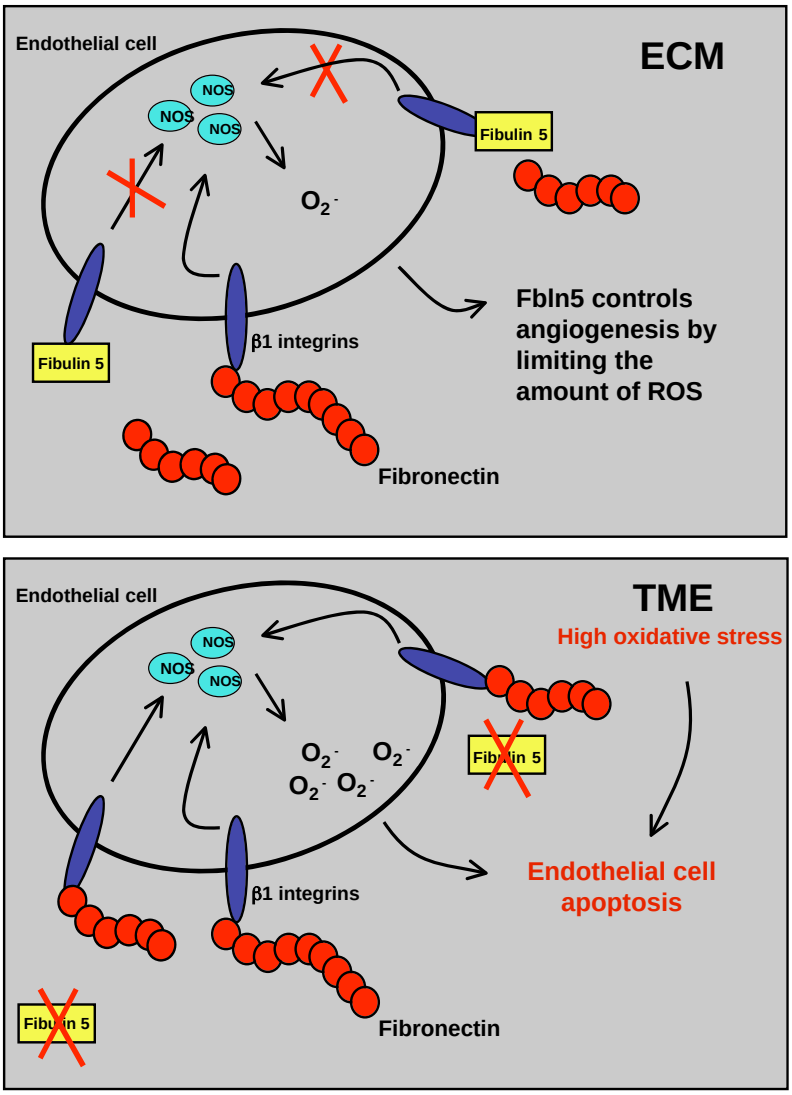

Figure 4.4 Current working model for how Fbln5 controls ROS production and how the loss of Fbln5 affects angiogenesis within the TME. Fbln5 binds to β_1 integrins inhibiting activation by fibronectin and downstream ROS production by NOS proteins. By limiting the amount of ROS present, Fbln5 limits endothelial cell activation and angiogenesis. In the absence of Fbln5, β_1 integrin activation by fibronectin is increased leading to enhanced ROS production. Within the TME, the increase in ROS production combined with the high level of oxidative stress already present results in endothelial cell apoptosis due to chronic oxidative stress and damage. This effect diminishes tumor angiogenesis and suppresses tumor growth.

from interacting with integrins. It is important to note that Fbln5 expression levels are normal in these mice and that this mutation does not disrupt the interaction with tropoelastin (H. Yanagisawa, unpublished data). Use of these mice allowed us to directly test our hypothesis that binding of Fbln5 to integrins is necessary to inhibit ROS production. We observed decreased tumor angiogenesis and growth in *Fbln5*$^{RGE/RGE}$ mice compared to *WT* mice. Tumor growth rate was similar to that observed in *Fbln5*$^{-/-}$ mice. Analysis of ROS levels in tumors from *Fbln5*$^{RGE/RGE}$ mice revealed elevated levels compared to tumors from *WT* mice. These results confirm that Fbln5 binding to integrins is critical for its control of ROS production. Unlike *Fbln5*$^{-/-}$ mice, *Fbln5*$^{RGE/RGE}$ mice do not exhibit elastic fiber defects, loose skin or alveolar defects leading us to speculate that ROS is not involved in the development of these defects.

To provide proof that increased ROS level were killing endothelial cells within the TME of tumors from *Fbln5*$^{-/-}$ and *Fbln5*$^{RGE/RGE}$ mice and inhibiting tumor growth, we performed tumor studies in *Fbln5*$^{RGE/RGE}$ mice in the presence of the antioxidant, NAC. NAC treatment rescued angiogenesis and increased tumor growth. From these results, we can conclude that increased ROS were the main contributors to the tumor phenotype observed in both *Fbln5*$^{-/-}$ and *Fbln5*$^{RGE/RGE}$ mice.

Our above results allowed us to confirm a function for Fbln5 in regulating ROS production. We then hypothesized that it was through this mechanism that Fbln5 was able to control angiogenesis. As detailed in previous chapters, Fbln5 inhibits endothelial cell proliferation and migration and the loss of Fbln5 *in vivo* results in increased blood vessel formation within sponges implanted into *Fbln5*$^{-/-}$ mice [13]. Given that ROS is a potent inducer of angiogenesis, we hypothesized that Fbln5 indirectly inhibits angiogenesis by limiting the amount of ROS available for endothelial stimulation. To test this, we performed implant studies in the presence of NAC with the idea that antioxidant treatment would prevent any

increases in angiogenesis in *Fbln5*$^{-/-}$ mice. Treatment with NAC reduced blood vessel density only in matrigel plugs from *Fbln5*$^{-/-}$ mice and not *WT* mice indicating that ROS were the main angiogenic stimuli in *Fbln5*$^{-/-}$ mice. A caveat to this experiment was that we were unable to observe an increase in angiogenesis in plugs implanted in *Fbln5*$^{-/-}$ mice as observed in similar studies. We contributed this difference to the type of reagent implanted (matrigel vs. PVA sponge). Future experiments should be performed with PVA sponges or a similar material to fully test this hypothesis.

From the results described above, we were able to conclude that 1) Fbln5 inhibits integrin-induced ROS production through a mechanism dependent on its physical interaction with integrins via the RGD motif and 2) that increased ROS level were the main cause for decreased angiogenesis and tumor growth in *Fbln5*$^{-/-}$ mice. These results also provide further support for the development of drugs that alter the oxidative environment within tumors to control tumor growth.

METHODS

Tumor growth in *Fbln5*$^{RGE/RGE}$ mice

Pan02HY cells ($3x10^6$/100 μl) were subcutaneously injected (27 gauge needle) into the shaved flank region of *WT* and *Fbln5*$^{-/-}$ mice. After tumor cell injection, the mice were monitored for weight, signs of discomfort or morbidity, and tumor size. Tumor volume was measured weekly by the use of digital calipers. Tumor volume was calculated using the formula: $(D \times d)^2 \times \pi/6$ (D, largest diameter, d, perpendicular to D). Three weeks after tumor cell injection, mice were euthanized. Subcutaneous tumors were excised, weighed and the tumor samples were frozen in liquid nitrogen for further analysis. NAC (Sigma-Aldrich) was given in the drinking water at 7 mg/ml (pH 7.4) and changed every three days.

ROS detection by DHE staining

Frozen tumors were sectioned (10 μm) and allowed to air-dry for thirty minutes. Sections were rehydrated in fifty µl of PBS for five minutes. Fifty μl of 5 μM dihydroethidium (DHE, Molecular Probes) (diluted in PBS) was added to each tumor section, coverslipped, and incubated at 37°C in a humidified incubator for thirty minutes. Nuclear red-fluorescence was visualized and images captured using the Photometric Coolsnap HQ camera. Fluorescence intensity was quantified using Elements software as described in the methods section of Chapter 2.

Matrigel plug assay

Matrigel (BD Biosciences) (400 µl) was injected into the right and left flanks of *WT* and *Fbln5*$^{-/-}$ mice. NAC (Sigma-Aldrich) was given in the drinking water at 7 mg/ml (pH 7.4) and changed every three days. After two weeks, the mice were sacrificed and the plugs removed for analysis. Plugs were either fixed in 10% formalin or snap-froze in liquid nitrogen for histological analysis.

Analysis of blood vessel density

Frozen tumors or matrigel plugs were sectioned on cryostat (10 µm) and air-dried overnight. Frozen sections were rehydrated in PBS for five minutes and fixed with acetone for five minutes prior to staining. Frozen sections were incubated for one hour at room temperature with a protein-blocking solution consisting of 20% AquaBlock and DMEM (East Coast Biologics). Sections were incubated with primary antibody MECA-32 (10 µg/ml, Developmental Studies Hybridoma Bank, University of Iowa), diluted in 1% BSA/PBS for either one hour at room temperature or overnight at 4°C. Sections were washed three times in PBST for five minutes each and incubated for one hour at room temperature with a

fluorophore-conjugated (fluorescein FITC) secondary antibody in 1% BSA/PBS (1:1000) (Jackson Immunoresearch) and then washed three times in PBST for five minutes each. Fluorescent sections were mounted with ProLong Gold antifade reagent with DAPI (Invitrogen) and quantification was performed by hand counting as described in the methods section of Chapter 1.

REFERENCES

1. Tan D, Goerlitz DS, Dumitrescu RG, et al. Associations between cigarette smoking and mitochondrial DNA abnormalities in buccal cells. Carcinogenesis 2008;29(6):1170-7.
2. Waris G, Ahsan H. Reactive oxygen species: role in the development of cancer and various chronic conditions. J Carcinog 2006;5:14.
3. Riely GJ, Marks J, Pao W. KRAS mutations in non-small cell lung cancer. Proc Am Thorac Soc 2009;6(2):201-5.
4. Xia C, Meng Q, Liu LZ, Rojanasakul Y, Wang XR, Jiang BH. Reactive oxygen species regulate angiogenesis and tumor growth through vascular endothelial growth factor. Cancer Res 2007;67(22):10823-30.
5. Wojtowicz-Praga SM, Dickson RB, Hawkins MJ. Matrix metalloproteinase inhibitors. Invest New Drugs 1997;15(1):61-75.
6. Binker MG, Binker-Cosen AA, Richards D, Oliver B, Cosen-Binker LI. EGF promotes invasion by PANC-1 cells through Rac1/ROS-dependent secretion and activation of MMP-2. Biochem Biophys Res Commun 2009;379(2):445-50.
7. Wu WS. The signaling mechanism of ROS in tumor progression. Cancer Metastasis Rev 2006;25(4):695-705.
8. Greenwald P, Anderson D, Nelson SA, Taylor PR. Clinical trials of vitamin and mineral supplements for cancer prevention. Am J Clin Nutr 2007;85(1):314S-7S.
9. Lesperance ML, Olivotto IA, Forde N, et al. Mega-dose vitamins and minerals in the treatment of non-metastatic breast cancer: an historical cohort study. Breast Cancer Res Treat 2002;76(2):137-43.
10. Trachootham D, Zhou Y, Zhang H, et al. Selective killing of oncogenically transformed cells through a ROS-mediated mechanism by beta-phenylethyl isothiocyanate. Cancer Cell 2006;10(3):241-52.
11. Albright CD, Salganik RI, Van Dyke T. Dietary depletion of vitamin E and vitamin A inhibits mammary tumor growth and metastasis in transgenic mice. J Nutr 2004;134(5):1139-44.
12. Marikovsky M. Thiram inhibits angiogenesis and slows the development of experimental tumours in mice. Br J Cancer 2002;86(5):779-87.
13. Sullivan KM, Bissonnette R, Yanagisawa H, Hussain SN, Davis EC. Fibulin-5 functions as an endogenous angiogenesis inhibitor. Lab Invest 2007;87(8):818-27.
14. Bonomini F, Tengattini S, Fabiano A, Bianchi R, Rezzani R. Atherosclerosis and oxidative stress. Histol Histopathol 2008;23(3):381-90.
15. Touyz RM, Schiffrin EL. Reactive oxygen species in vascular biology: implications in hypertension. Histochem Cell Biol 2004;122(4):339-52.

DISCUSSION

Signal transduction initiated within the TME impacts tumor cell survival. Matricellular proteins govern these signaling pathways and have therefore, been shown to alter tumor outcome. The driving force behind this project was the idea that a better understanding of how matricellular proteins function within the TME may provide new therapeutic targets that effectively control tumor progression. Therefore, the goal of my project was to characterize how the loss of endogenous Fbln5 expression affected pancreatic tumor growth. Fbln5 has been shown to have diverse effects on numerous cellular activities and the context-dependent nature of these effects has made it difficult to decipher a direct mechanism by which Fbln5 functions. While Fbln5 has been shown to influence cellular activities such as proliferation and migration in multiple cell types, it has been its affect on endothelial cells and angiogenesis that has drawn the most attention. Results from both *in vitro* and *in vivo* studies indicate that Fbln5 functions as an angiogenic inhibitor by reducing the proliferation and migration of endothelial cells.[1, 2] In these studies, Fbln5 regulated the expression of several angiogenic proteins including VEGF and angiopoetin-1, -2 and -3 suggesting that the mechanism behind these effects involved gene expression control. Thus far, this has been the only information pertaining to a possible mechanism for Fbln5. The work described here includes the identification of novel function for Fbln5 in the control of integrin-induced ROS production. ROS are potent angiogenic stimuli and are produced by endothelial cells.[3, 4] Therefore, our evidence indicating Fbln5's direct control over ROS production in endothelial cells provides for the first time a specific mechanism for how Fbln5 regulates cellular activities. In addition, we validated the relevance of this finding *in vivo* by showing that the augmented ROS production due to the loss of Fbln5 impacts angiogenesis in a manner dependent on the oxidation status of the surrounding microenvironment.

In non-pathological tissues (matrigel plug) the increase in ROS is critical for angiogenic stimulation but elevated ROS is detrimental to angiogenesis within the TME where the oxidation state is higher. There are two avenues of future interest that stem from this project: 1) the identification of components downstream of β_1 integrin activation that are involved in the generation of ROS and 2) exploring the therapeutic potential of targeting Fbln5.

We have shown that in the absence of Fbln5 there is an increase in β_1 integrin-induced ROS production. Studies have shown that integrin-induced ROS generation is usually mediated through activation of Rac1, which induces superoxide formation via NAD(P)H oxidases or mitochondria.[5] However, our studies indicate that the pathway initiated in the absence of Fbln5 is independent of Rac1. Furthermore, our data suggests that ROS production is mediated through the uncoupling of NOS proteins instead of NAD(P)H oxidases or mitochondria. Therefore, these results hint at a completely novel route for integrin-induced ROS production. Since the results directly downstream of integrin activation are complex and involve multiple proteins, it would be more beneficial for future experiments to be focused on the final endpoint, NOS proteins. Understanding how the activity of NOS proteins are altered in the absence of Fbln5 will allow the identification of components directly involved in the pathway. A thorough understanding of the pathway initiated in the absence of Fbln5 is critical for the development of strategies designed to either enhance or block Fbln5 function for therapeutic purposes.

Mutations in FBLN5 have been associated with the onset of certain human diseases such as macular degeneration and cardiovascular diseases such as atherscelerosis. Our studies offer a possible explanation for how the loss of Fbln5 contributes to the development of these diseases. Heightened ROS levels are involved in the progression of macular degeneration and atherosclerosis therefore,

our findings suggest that the loss of FBLN5 contributes to these diseases by increasing the level of ROS within the effected tissues. Treatment with FBLN5 protein or blocking activity of proteins downstream of β_1 integrin activation could provide a beneficial effect by reducing the level of ROS within effected tissues. This potential mode of therapy could be initially tested in recently generated mouse models of macular degeneration and ApoE-deficient mice, which are highly susceptible to the development of atherosclerosis.[6, 7]

Manipulation of the oxidative environment within the TME has been shown to be effective at controlling tumor growth and progression. A wide variety chemotherapeutics induce apoptosis of tumor cells by augmenting the level of ROS production within tumors.[8] This anti-cancer strategy is the basis for our rationale that blocking the function of Fbln5 is an intriguing idea for cancer therapy.

We have shown that increased ROS production within tumors from *Fbln5*$^{-/-}$ mice enhances oxidative stress on endothelial cells within the TME resulting in apoptosis and reduced angiogenesis and tumor growth. These results could be recapitulated in the clinic by designing a drug that selectively inhibits Fbln5 from binding to β_1 integrins. Since the loss of Fbln5 does not result in complete tumor reduction, we propose that use of a drug targeting Fbln5 would be more effective in combination with other types of cancer therapies.

Targeting Fbln5 as an approach to tumor therapy has several attractive qualities. For example, expression of Fbln5 is minimal in adult tissues. Only during tissue remodeling events does Fbln5 expression increase. This characteristic means that in adult tissues the function of Fbln5 is not required and therefore inhibiting its function for therapeutic purposes may have less systemic side effects. Also, it is clear from the generation of *Fbln5*$^{RGE/RGE}$ mice that blocking Fbln5-integrin interactions is not detrimental to survival of the animal

again suggesting that blocking Fbln5's interaction with integrins for therapeutic purposes may result in few undesired side effects.

The work described herein not only answers numerous questions posed in the literature concerning the mechanism behind Fbln5's effect on angiogenesis but it also provides valuable information pertaining to its effect on cancer progression. As stated previously, the hopes for this project were to provide new targets for cancer therapy. Although much work is to be done to fully evaluate Fbln5's potential as a target for anti-tumor strategies, this work lays the foundation for those studies.

REFERENCES

1. Albig AR, Schiemann WP. Fibulin-5 antagonizes vascular endothelial growth factor (VEGF) signaling and angiogenic sprouting by endothelial cells. DNA Cell Biol 2004;23(6):367-79.
2. Sullivan KM, Bissonnette R, Yanagisawa H, Hussain SN, Davis EC. Fibulin-5 functions as an endogenous angiogenesis inhibitor. Lab Invest 2007;87(8):818-27.
3. Chua CC, Hamdy RC, Chua BH. Upregulation of vascular endothelial growth factor by H2O2 in rat heart endothelial cells. Free Radic Biol Med 1998;25(8):891-7.
4. Tojo T, Ushio-Fukai M, Yamaoka-Tojo M, Ikeda S, Patrushev N, Alexander RW. Role of gp91phox (Nox2)-containing NAD(P)H oxidase in angiogenesis in response to hindlimb ischemia. Circulation 2005;111(18):2347-55.
5. Hordijk PL. Regulation of NADPH oxidases: the role of Rac proteins. Circ Res 2006;98(4):453-62.
6. Elizabeth Rakoczy P, Yu MJ, Nusinowitz S, Chang B, Heckenlively JR. Mouse models of age-related macular degeneration. Exp Eye Res 2006;82(5):741-52.
7. Breslow JL. Mouse models of atherosclerosis. Science 1996;272(5262):685-8.
8. Engel RH, Evens AM. Oxidative stress and apoptosis: a new treatment paradigm in cancer. Front Biosci 2006;11:300-12.

ACKNOWLEDGMENTS

To my mentor Rolf Brekken: The past five years have been an amazing experience. Thank you for your patience and constant support. You have created a wonderful environment to do research in and allowed me to be creative and explore my own ideas. I have learned more from my time in your lab than in any other point in my life. Thank you for your enthusiasm in my project, the freedom to explore, and for caring about me as your student more than anything else. With your guidance, I have become a confident scientist and am inspired to continue working on projects that excite me. I have had so much fun. Thank you for allowing me to be part of something truly great.

To members of the Brekken lab, past and present: It has been a joy getting to know all of you over the years. Thanks for your friendship, for great scientific discussions, and for many, many good laughs. You guys are my family.

To Shelby Chapman: This project would not have been successful without you. Words cannot describe how much I have valued your help over these past five years. You were always willing to do whatever needed to be done. Throughout many longs hours in the mouse room and sacing experiments, we have created a wonderful friendship that I truly cherish. Thanks for everything.

To Hiromi Yanagisawa: Thank you for your collaboration and consistent enthusiasm for my project. It has been great discussing ideas with you and I appreciate all your effort, both financially and intellectually.

To my thesis committee Jim Amatruda, Hiromi Yanagisawa and Eric Olson: First and for most, thank you for being on my committee. In our meetings, you have

challenged me, encouraged me and provided me with insightful advice. I deeply appreciate all your support.

To my parents, sisters and brother: Throughout every step in my life, you have always provided me with faith, support and encouragement. It is because of you that I am here acquiring my Ph.D. My dad has shown me what hard work really means and how rewarding it can be when done right. My mom has shown me that faith will always light your way. Her strength keeps me going. My sister Julie has taught me how to believe in myself. My sister Jennifer has given me more love and encouragement than I could ever give back and my brother Craig has reminded me to laugh along the way. Most importantly, you have all always given me a place to come home.

To my husband's parents, Alvie and Gail: I can't express how much I have appreciated all your support throughout my years in graduate school. Thank you for your constant love and genuine interest in my research.

To my husband and my children: Lyle, I am so fortunate to have someone that truly understands what it is like to be in graduate school. You have always encouraged me to keep going and to always believe in my work. Thank you for all the wonderful advice and great scientific ideas. To my children, in the end, this is all for you. I love you.